LKB1 CONTROLS EXPANSION AND FOLDING OF THE CEREBELLAR CORTEX

By

Kaitlyn Elizabeth Ryan

Dissertation

Submitted to the Faculty of the

Graduate School of Vanderbilt University

in partial fulfillment of the requirements

for the degree of

DOCTOR OF PHILOSOPHY

in

Cell and Developmental Biology

December 2014

Nashville, Tennessee

Committee Members:

Guoqiang Gu, Ph.D.

Bruce D. Carter, Ph.D.

Ian G. Macara, Ph.D.

Matthew J. Tyska, Ph.D.

Chin Chiang, Ph.D.

for my parents and my sister

for my husband and our little red dog

ACKNOWLEDGMENTS

I am grateful and humbled by the support I have received over the years, which has undoubtedly helped me reach this point in my fledgling career as a physician-scientist.

I am grateful to Chin, for welcoming me into his lab and providing sometimes stern but always helpful feedback regarding my decisions and interpretations as a scientist. Chin has helped me focus my attention and energy with lazer-like precision in a way that I simply was unable to do when I joined the lab. Discussing science with Chin is sort of like racing among professional cyclists – it requires unparalleled attention, energy, and assertiveness – all qualities that I lacked before joining his lab and that will undoubtedly serve me as I progress as a physician-scientist. I am confident that I could have not chosen a better lab in which to pursue my PhD.

Members of the Chiang lab, past and present, have been a source of energy, inspiration, and support throughout my graduate career. Ying's enthusiasm, passion, and optimism have motivated me to push forward despite failed hypotheses (something I took very personally when I first started in the lab) and failed experiments. Jon's humor, curiosity, and knowledge of mouse genetics and imaging have served me greatly over the years. Frances' quiet wisdom, sensitivity, and patience—both in and outside of the lab—have helped me stay balanced and committed. Indeed, it was Frances who first mentioned looking to see if changes in the orientation of division were responsible for increased surface area in *Lkb1*^{cko} mice.

I am thankful to Terry Dermody, Larry Swift, and the rest of the Vanderbilt MSTP for taking me in after my first year of medical school. They have cultivated a tremendous program here at Vanderbilt.

I am convinced that I have the best committee in the world. Guoqiang Gu is an incredible scientist and an outstanding chair. The depth and insight of his questions are often so many steps ahead of me that I find myself pondering them for several days after they're posed. There is nothing surface or artificial about Gu; these are not qualities you always find among scientists. Gu's patience and encouragement have allowed me to thrive during my graduate work. Bruce Carter's knowledge, curiosity, and enthusiasm about the nervous system have made him a terrific source of wisdom throughout my time in the lab. As a microscopist and a cell biologist, Matt Tyska has been a valuable resource for my research and for the lab in general. Laurie Lee was a source of support throughout my time in the lab—an excellent scientist and an incredibly caring human being. Finally, Ian Macara's wisdom, insight, and breadth of knowledge have made him an invaluable addition to my committee. Ian's passion and commitment to science inspire me to be a better scientist.

Past and present mentors have shaped my skills as a writer, communicator, and scientist. I am thankful to Karen Shuman for allowing me to spend a summer studying K-Bessell functions after my sophomore year of college. It was that summer I realized I was not going to be a mathematician, a discovery I will be forever grateful for. I am thankful to Victoria Brown, who taught me about women's equality, helped me refined my skills as a writer, and awakened the feminist in me. I am grateful to Charles Sullivan, for mentoring me as I first ventured into the field of developmental biology. I will always think fondly of my time at the NIH working in Dr. Dan Fowler's lab. Shadowing Dan and working in his lab taught me what it means to be a physician-scientist. Jacobo Marriotti was an outstanding mentor during my time in Dan's lab, providing much needed patience and encouragement, not to mention laughter. So much laughter. Finally, I thank

Luc van Kaer and Danyvid Olivares-Villagomez for mentoring me when I first arrived at Vanderbilt and helping me realize the value of a PhD.

I am forever indebted to my parents, Michael and Sally. In addition to their unwavering support, they provided me with invaluable resources when, as a child, a learning disability prevented me from reading at a level comparable to my peers. My father continues to inspire me. My mother's wisdom and sensitivity are a constant source of energy. I have the best sister on earth: brilliant, kind, loving, and the only person I know that will empty a movie theatre because of how loudly she laughs.

Finally, I am thankful to Brian, my husband. For the past 10 years, Brian has been my family, my home, and my support. He has believed in me even when I did not. His love and acceptance are unwavering. Brian's commitment to bettering himself, both personally and professionally, has inspired me to do the same. He has been with me since I began this journey, and it is with hopeful anticipation that I await our future adventures.

TABLE OF CONTENTS

Page

LIST OF TABLES

Table **Page**

LIST OF FIGURES

Figure **Page**

CHAPTER I. GENERAL INTRODUCTION

The Cerebellum: Function, structure, and evolution

Located beneath the cerebral cortex, the cerebellum is a brain region traditionally known for its role in motor control, coordination, and motor learning (Altman and Bayer, 1997). In addition to its motor functions, however, the cerebellum participates extensively in cognition, including emotional control, long-term memory, and language (Leiner et al., 1993; Schmahmann and Caplan, 2006; Yeo, 2004). As such, injury to the cerebellum can cause both motor disabilities as well as difficulties in behavior, memory and speech (Schmahmann and Sherman, 1998). Moreover, a number of neurodevelopmental disorders, including autism spectrum disorder (Fatemi et al., 2012), dyslexia (Stoodley, 2014; Stoodley and Stein, 2011), and attention deficit disorder (Stoodley, 2014) have been linked to the cerebellum, underscoring the importance of the cerebellum in behavior, learning, and attention. Consequently, an improved understanding of cerebellar development may provide insight into the causes and treatment of both cognitive and motor diseases.

The cerebellum contains two principle types of neurons, Purkinje cells and granule cells, as well as a variety of interneurons, including basket cells, stellate cells, Golgi cells, Lugaro cells, and unipolar brush cells (Figure 1.1)(Altman and Bayer, 1997). The mature cerebellar cortex has a uniformly layered architecture (Figure 1.1). The outermost molecular layer is composed primarily of granule cell axons (parallel fibers) and Purkinje cell dendrites; however, basket and stellate cells also reside within the molecular layer. Below the molecular layer lies a monolayer of Purkinje cell bodies interspersed with Bergmann glia, a specialized form of glia in the cerebellum. The

internal granule cell layer, located below the Purkinje cell layer, contains granule cell bodies as well as Golgi, Lugaro, and unipolar brush cells. Granule cells and unipolar brush cells produce the neurotransmitter glutamate and act as excitatory neurons, whereas Purkinje, Golgi, Lugaro, basket, and stellate cells produce the neurotransmitter GABA to elicit an inhibitory response on their targets.

The cerebellar cortex is composed of a central vermis and two lateral hemispheres (Figure 1.1). Perhaps as a result of evolutionary pressures, the lateral hemispheres of the human cerebellum are dramatically enlarged compared to those of other mammals (Altman and Bayer, 1997). Indeed, the shape of the primate cerebellum distinguishes it from the cerebella of other mammals (MacLeod, 2012).

In addition to differences in the overall shape of the cerebellum, evolutionary pressures have caused the primate cerebellum to increase in surface area relative to volume (Sultan, 2002). Whereas the cerebellum remains a relatively constant proportion of total brain volume across mammals (Clark et al., 2001), cerebellar surface area increases in an evolutionarily dependent manner (Sultan, 2002). Surface area expansion is facilitated in part by the formation of fissures, deep folds in the cerebellar surface that separate the cerebellum into lobules (also known as folia) (Figure 1.1). Like surface area, the complexity of foliation appears to scale in an evolutionarily-dependent manner. For example, in birds, the degree of cerebellar foliation correlates with nest complexity, with higher levels of foliation present in birds that construct more elaborate nests (Hall et al., 2013). Additionally, evolutionary pressures have driven the expansion of specific cerebellar lobules. For instance, cerebellar lobules that connect to the prefrontal cortex are enlarged relative to motor cortex-projecting lobules in humans compared to non-human primates (Balsters et al., 2010). Similarly, birds that utilize their beaks such as

parrots and woodpeckers have a specific enlargements in lobes receiving visual and trigeminal inputs, resulting in improved visual acuity and beak dexterity (Sultan, 2005). Together, these findings suggest that changes in cerebellar structure may underlie evolution of the mammalian brain.

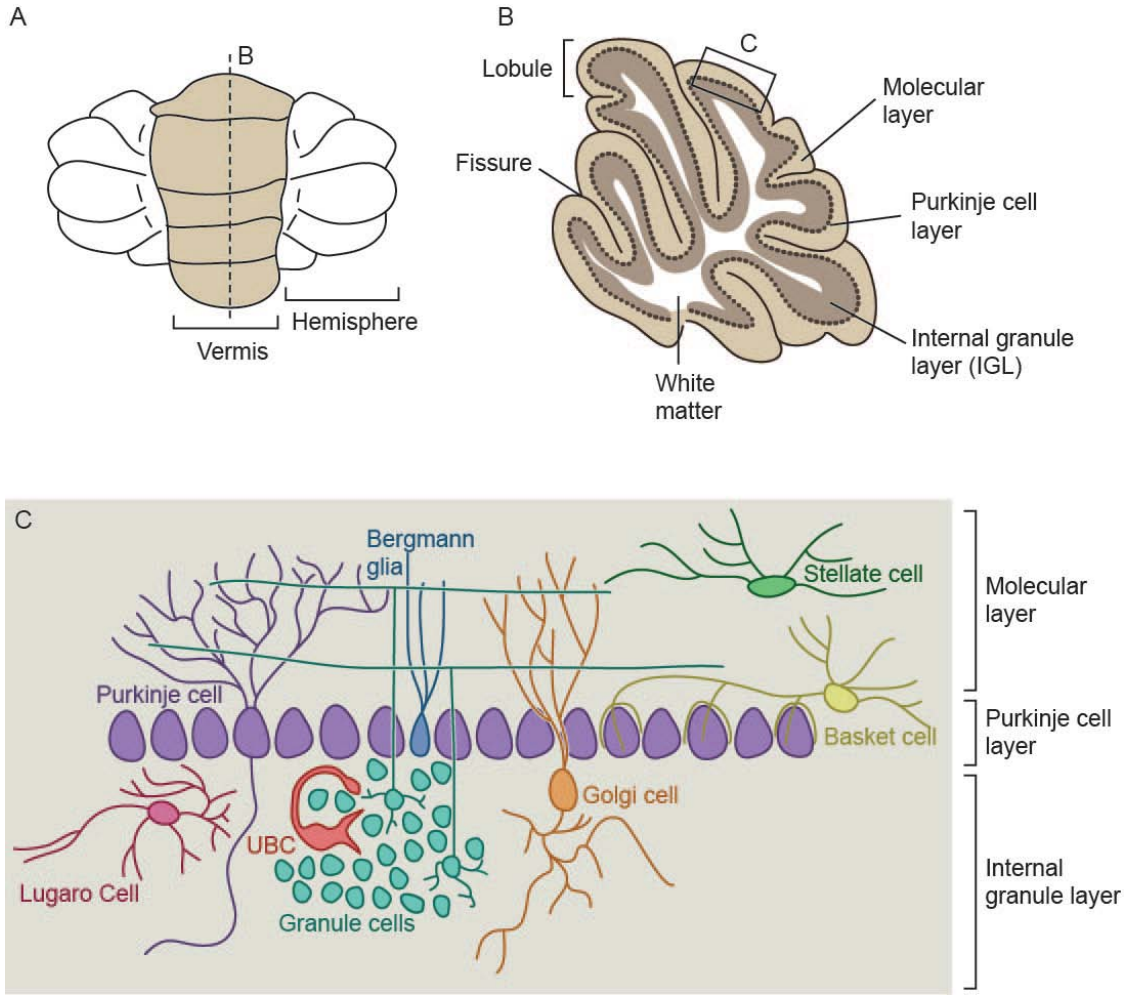

Figure 1.1. Vertebrate cerebellar structure and cell types.
A. Illustration of the adult mouse cerebellum. B. Sagittal section of the mouse cerebellum at the level shown in A. C. Enlargement of the boxed region shown in B illustrating the morphology and location of the various cerebellar subtypes. UBC = unipolar brush cell.

While the cerebellum is not required to initiate movement, it is essential for motor control and dexterity. This is evidenced by the fact that lesions to the cerebellum can cause tremors and unsteadiness (Schmahmann, 2004). Thus, man's improved motor abilities, enabling written forms of communication, tool making, and even the generation of fine arts are perhaps due to the evolution of the cerebellum. As such, understanding how the cerebellum normally develops, particularly with respect to surface area expansion and foliation, could provide insight into evolution of the human brain. *Herein, we propose that surface area expansion in the cerebellum is regulated by the orientation of neural precursor divisions.*

Development of the cerebellum

The cerebellum arises from rhombomere 1, the anterior-most segment of the hindbrain, around embryonic day 9.5 (E9.5) in the mouse (Figure 1.2). A region at the boundary between the midbrain and hindbrain known as the isthmus secretes growth factors, including FGF-8 and Wnt1, which determine the anterior/posterior position of the cerebellum. The isthmus is delineated by the transcription factors Otx2 anteriorly and Gbx2 posteriorly, both of which additionally function to regulate *Fgf8* expression (Wang and Zoghbi, 2001). Isthmus-derived FGF-8 induces the expression of *En1, En2, Pax2* and *Pax5*, all of which are required to delineate rhombomere 1 and establish the cerebellar territory (Joyner et al., 2000). In addition to the isthmus, beginning around E10.5, the roof plate, a specialized group of cells covering the dorsal surface of rhombomere 1, secretes Bmp, Wnt, and retinoic acid to regulate the specification of cerebellar cell types (Figures 1.2, 1.3) (Chizhikov et al., 2006). Between E9.5 and E12.5

the neural tube undergoes at 90 degree rotation that transforms the rostral-caudal axis of the cerebellar anlage into the medio-lateral axis (Figure 1.2) (Sgaier et al., 2005). This rotation forms the wing-like bilateral cerebellar primordial (Sgaier et al., 2005). These bilateral structures ultimately fuse at the midline, establishing the medial vermis and lateral hemispheres of the cerebellum (Millen and Gleeson, 2008).

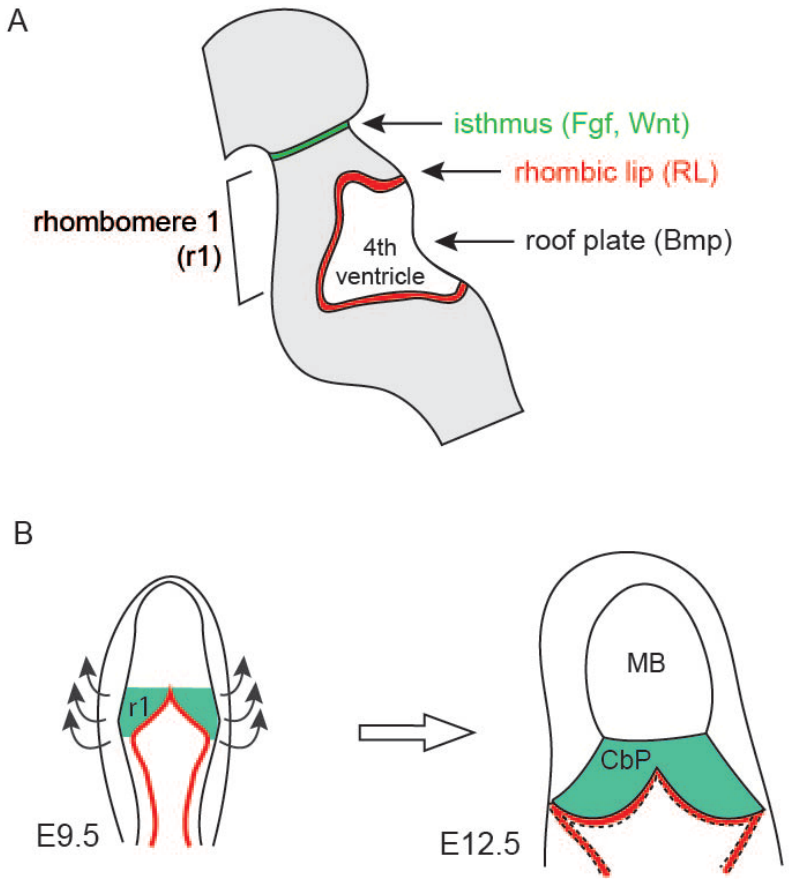

Figure 1.2. Early cerebellar development.
A. View of the early embryo showing the location of the isthmus, a secondary signaling center that patterns the developing hindbrain. The cerebellum is derived from rhombomere 1 (r1). B. The cerebellar primordium undergoes a 90° rotation between E9.5 and E12.5, transforming the rostral-caudal axis into the medio-lateral axis of the cerebellum. Rhombomere 1 is colored in green. MB = midbrain, CbP = cerebellar primordium.

All cerebellar subtypes are generated from two progenitor regions; the ventricular zone (VZ) and the rhombic lip (Figure 1.3). The ventricular zone gives rise to all GABAergic neurons, including Purkinje cells, Golgi, basket, stellate cells and neurons of the cerebellar nuclei (Hoshino et al., 2005; Millen and Gleeson, 2008). The rhombic lip generates granule neurons, the most abundant neuron in the entire mammalian CNS, as

well as a subpopulation of neurons of the cerebellar and precerebellar nuclei (Millen and Gleeson, 2008).

Fate mapping studies in the mouse have demonstrated that VZ progenitors are generated in three sequential and overlapping waves (Morales and Hatten, 2006). The earliest-born VZ-derivatives form the deep cerebellar nuclei (DCN) and emerge from the VZ around E10.25. These cells use radial glial fibers to reach the surface of the cerebellar anlage before ultimately settling below the white matter. A second wave of progenitors emerges between E11 and E14 and ultimately gives rise to Purkinje cells. These Purkinje neuron progenitors express the transcription factors LHX1 and LHX5 and enter the developing cerebellum by way of radial glial fibers (Morales and Hatten, 2006). A final wave of neurogenesis begins after E14.5 and generates progenitors to interneurons of the deep cerebellar nuclei, stellate, basket, Lugaro and Golgi cells (Morales and Hatten, 2006). These neurons migrate along radial glia and settle within the presumptive white matter. Previous work in our lab has demonstrated that Sonic Hedgehog (Shh) signaling is required to generate sufficient number of VZ-derived progenitors, both during embryogenesis and postnatally (Fleming et al., 2013; Huang et al., 2010). In the embryonic cerebellum, the choroid plexus secretes Shh into the cerebral spinal fluid to promote the proliferation of radial glia in the VZ (Huang et al., 2010). Additionally, Purkinje cells produce Shh postnatally, which promotes the proliferation of interneuron progenitors within the postnatal white matter (Fleming et al., 2013).

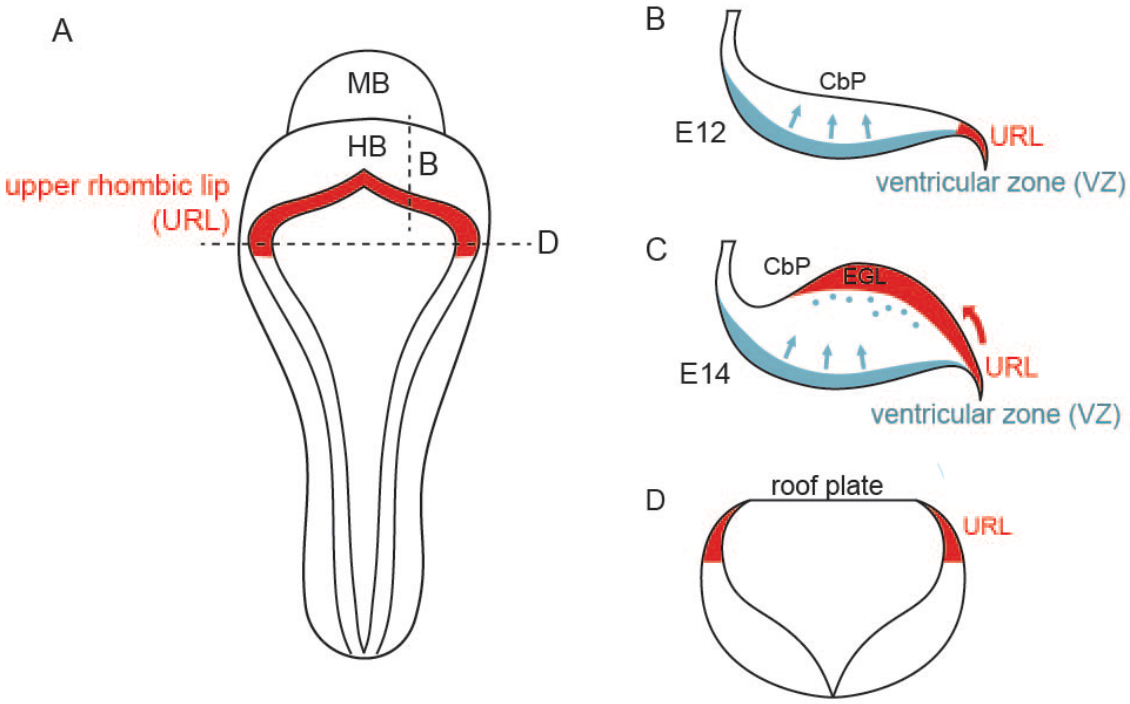

Figure 1.3. All cerebellar subtypes are generated from the rhombic lip and the ventricular zone.
A. The dorsal view of the embryo illustrating the location of the upper rhombic lip. MB = midbrain, HB = hindbrain. B. Sagittal section at the level shown in A to show the location of the ventricular zone and the rhombic lip. Ventricular zone derivatives migrate radially to reach the cerebellar anlage, where as upper rhombic lip derivatives migrate tangentially to cover the cerebellar surface. CbP = cerebellar primordium. C. Slightly later view of the same region shown in B demonstrating the location of the external granule layer (EGL). D. Coronal section through the embryo at the level shown in A to illustrate the location of the rhombic lip and the roof plate.

Around E12.5, a second germinal zone forms in the anterior rhombic lip (Figures 1.2, 1.3). Rhombic lip formation requires signals from the roof plate (Machold and Fishell, 2005), and is molecularly defined by the basic helix-loop-helix transcription factor Mouse atonal homolog 1 (Math1, also known as Atoh1). Our lab (Cheng et al., 2012) and others (Chizhikov et al., 2010) have shown that a subset of rhombic lip cells also expresses Gdf7 and Lmx1a. Beginning around E14, granule cell precursors migrate out of the rhombic lip to cover the cerebellar surface, forming the external granule layer (EGL). Amidst the migration of GCPs, *Math1*-positive cerebellar nuclei progenitors migrate out of the rhombic lip to a position below the forming Purkinje cell monolayer, where they differentiate in the deep cerebellar nuclei (Morales and Hatten, 2006). Additionally, the anterior rhombic lip generates neuronal progenitors that form the lateral pontine nucleus, cochlear nucleus and hindbrain nuclei.

Between mid-embryogenesis and the second postnatal week, the cerebellum undergoes a 1000-fold increase in size and is transformed from a small, ovoid structure into the large, highly foliated organ able to perform motor and cognitive tasks (Goldowitz et al., 1997). The process of cerebellar foliation can be divided into two phases: an embryonic phase, which encompasses cardinal fissure formation, and a postnatal phase, during which time non-cardinal fissures form. Cardinal fissures form around E17 in the mouse and divide the cerebellar surface into five cardinal lobes (Sillitoe and Joyner, 2007). Cardinal fissure formation is at least in part genetically determined, as, for example, mice lacking the *Engrailed* homeobox genes *Engrailed1* or *2* have defects in the placement and depth of cardinal fissures (Cheng et al., 2010). The second phase of foliation begins around birth and is driven largely by the proliferation of GCPs in EGL. Within the EGL, GCPs proliferate in response to Purkinje cell-derived mitogens,

including Shh before exiting the cell cycling and undergoing radial migration along Bergmann glia (Dahmane and Ruiz i Altaba, 1999; Wallace, 1999; Wechsler-Reya and Scott, 1999). Between birth and the second postnatal week, expansion of the EGL leads to the formation of secondary and tertiary fissures, which are thought to arise in response to mechanical forces generated by increasing surface area within the confines of the skull (Altman and Bayer, 1997). As such, disrupting GCP proliferation, either using gamma irradiation or genetic ablation of Shh signaling, leads to a small, hypoplastic cerebellum that lacks secondary and tertiary lobules (Altman and Bayer, 1997; Corrales et al., 2006; Corrales et al., 2004). However, mutations that increase or prolong GCP proliferation lead to a larger cerebellum but do not consistently increase foliation. For example, whereas increased levels of Shh prolongs GCP proliferation and results in a larger cerebellum with 1-2 additional folia (Corrales et al., 2006), loss of the cell cycle inhibitor p27Kip1 extends GCP proliferation and increases cerebellar volume without the formation of additional folds (Miyazawa et al., 2000). These studies suggest that GCP proliferation is necessary, but not always sufficient, to induce cortical folding in the cerebellum. *Aside from GCP proliferation, cellular and genetic mechanisms regulating foliation have not been identified. In Chapter II, we show that loss of the serine-threonine kinase Lkb1 increases cerebellar surface area and foliation by randomizing the orientation of GCP divisions.*

Beginning around birth, a subset of GCPs exits the cell cycle and undergoes radial migration along Bergmann glial fibers to ultimately populate the internal granule layer (IGL). By P21, all GCPs have exited the cell cycle and undergone migration. Granule cell migration has served as a model for studying radial migration for over a century, with some of the earliest histological studies of radial migration being

documented by Ramon y Cajal (Figure 1.4) (Ramon y Cajal, 1911). These seminal studies revealed that granule cell migration is coupled with morphological changes that correspond to granule cell maturation. After exiting the outermost layer of the EGL (oEGL), where proliferation occurs, granule cells in the inner EGL (iEGL) extend two fibers parallel to the cerebellar surface (parallel fibers), forming the granule cell axons. Following parallel fiber extension, the cell soma elaborates a leading process that is thought to guide the cell along Bergmann glial fibers. Upon reaching the IGL, granule cells elaborate multiple claw-like dendrites which synapse on mossy fibers originating from the pre-cerebellar nuclei (Altman and Bayer, 1997).

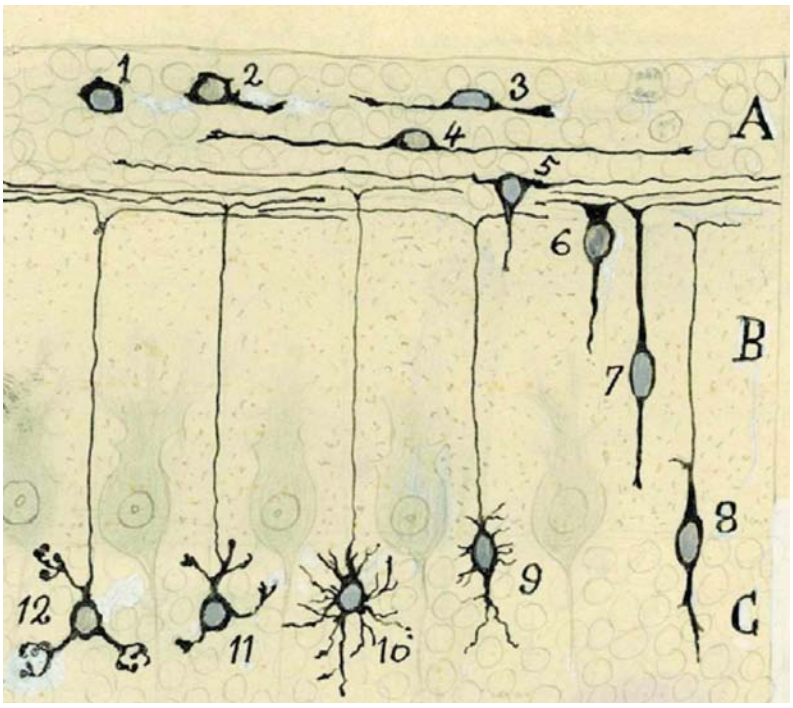

Figure 1.4. Cerebellar granule cell migration and maturation.
Granule cell polarization begins in the middle of the EGL (layer A), with the extension of one (2) and then another (3) process parallel to the pial surface. These processes eventually elongate (4) into parallel fibers. As the maturing granule cells reaches the bottom of the EGL, a leading process extends perpendicular to the pial surface (5). The granule cell migrates inward (6-8). Once the cell has reached the IGL, claw-like dendrites are formed (9-12). (drawing by Ramon y Cahal, 1911)

The cerebellum is an attractive system in which to study radial migration, both because of the abundance of granule cells as well as the ease with which granule cells and Bergman glia can be cultured *in vitro*. Consequently, much of what we know about radial migration stems from studies performed in the cerebellum. Indeed, a least a dozen molecules required for timely and efficient radial migration of GCPs have been identified over the years, including the neurotrophin BDNF, the transmembrane Semaphorin Semaphorin 6A, its receptor Plexin2A, and the cell cycle inhibitor p27Kip1, among others (Chedotal, 2010; Cooper, 2013). Granule cell precursor migration also requires the actin

and tubulin cytoskeletons. In particular, Myosin II in the leading process of migrating GCPs is thought to pull actin fibers forward in the direction of migration. Additionally, the tubulin cytoskeleton is regulated by the polarity protein Par6α, which regulates the assembly of a tubulin cage around the nucleus important for nuclear migration along glial fibers (Solecki et al., 2004; Solecki et al., 2009). *In Chapter III, we show that* Lkb1*, the mammalian homolog of* par-4, *is required for radial migration in the cerebellum.*

Par-4/Liver Kinase B1 (Lkb1)

The *par* genes *par-1* through *par-6* were identified nearly 30 years in a series of genetic screens for mutations disrupting asymmetric cell division in the early *C. elegans* embryo. In worms, *par* mutants have defects in the position of the mitotic spindle or the distribution of cytoplasmic proteins and RNAs (Goldstein and Macara, 2007).

In *par-4* mutant worms, placement of the mitotic spindle is normal, resulting in daughter cells with wild type asymmetry (Kemphues et al., 1988; Morton et al., 1992). However, *par-4* is required for the proper distribution of P granules, ribonucleoprotein (RNP) organelles that normally localize to the posterior pole of the developing embryo (Kemphues et al., 1988; Morton et al., 1992; Watts et al., 2000). Additionally, the asymmetric distribution of par-3 and par-6 is lost in *par-4* mutants (Hung and Kemphues, 1999). Many of the defects in *par-4* mutants are a consequence of defects in the actomyosin cytoskeleton. Following fertilization, contractions of the actomyosin cytoskeleton are critical for the polarizing the embryo (Chartier et al., 2011). Par-4 functions to mobilize a population of myosin II at the cell cortex to regulate polarity and cytoskeletal contractions (Chartier et al., 2011).

Liver kinase B1 (Lkb1; also known as Stk11) is the mammalian homolog of *C. elegans par-4*. In humans, mutations in *Lkb1* lead to Peutz Jeghers Syndrome, an autosomal dominant disorder that is characterized by benign intestinal hamartomas and a predisposition to epithelial-derived cancers (Martin-Belmonte and Perez-Moreno, 2012). In mice, Lkb1 regulates both cell polarity and cell metabolism. Many of Lkb1's metabolic functions are mediated through AMP-activated Kinase (AMPK), which Lkb1 phosphorylates under conditions of energetic stress. AMPK is activated by such phosphorylation, and subsequently downregulates pathways that expend energy while upregulating those that conserve cellular energy stores (Shackelford and Shaw, 2009). In addition to AMPK, Lkb1 phosphorylates 12 other members of the AMPK-related family of kinases. These include the microtubule affinity related kinases (MARKs) 1-4 and SAD family members SAD-A and B, all of which are homologs of *C. elegans* par-1. In vertebrates, the SAD kinases play a critical role in neuronal polarization, where they are essential for axon specification in forebrain neurons (Asada et al., 2007; Barnes et al., 2007). Conversely, MARK2/Par1b plays a central role in establishing hepatocyte polarity both in vivo and in vitro (Lazaro-Dieguez et al., 2013; Slim et al., 2013). A complete list of Lkb1 substrates and their functions in shown in Table 1.1.

In addition to regulating cell polarity and metabolism, Lkb1 suppresses proliferation in a number of tissues, including the gut (Bardeesy et al., 2002; Takeda et al., 2006), lung (Carretero et al., 2007; Ji et al., 2007; Matsumoto et al., 2007; Sanchez-Cespedes, 2007), and epidermis (Gurumurthy et al., 2008). In cultured melanoma and squamous cell carcinoma cell lines, Lkb1 induces p53-dependent and –independent growth arrest, respectively, although the mechanism by which Lkb1 suppresses tumor

formation *in vivo* remains incompletely understood (Baas et al., 2003; Tiainen et al., 2002; Tiainen et al., 1999).

The early embryonic lethality of *Lkb1-/-* mice has necessitated the use of tissue-specific *Lkb1* mutations in order to study Lkb1 function *in vivo* during development. These studies have identified a number of functions for Lkb1 in a wide variety of tissues. In the pancreas, Lkb1 regulates β cell size and polarity through AMPK and MARK2, respectively (Granot et al., 2009). Conversely, loss of *Lkb1* from mammary cells results in a deterioration of the basement membrane, loss of junctional integrity, and aberrant branching of the mammary ductal tree (Partanen et al., 2012). In contrast to mammary tissue, loss of Lkb1 kinase activity in the developing lung lead to decreased, rather than increased, branching (Lo et al., 2012), suggesting that regulation of branching morphogenesis by Lkb1 is tissue-specific. Most recently, Lkb1 was shown to play a critical role in endothelial cells, as endothelial-specific loss of Lkb1 led to hypertension, cardiac hypertrophy, and impaired endothelium-dependent relaxation (Zhang et al., 2014). In the developing forebrain, Lkb1 regulates axonogenesis and may play a role in radial migration (Asada and Sanada, 2010; Asada et al., 2007). *However, the role of Lkb1 in the cerebellum has not been previously explored. Chapters II and III examine the role of Lkb1 in granule cell precursors of the developing cerebellum.*

Table 1.1. Substrates of Lkb1.

Substrate	Other names	Homologs, Paralogs	Function
AMPK (α_1, α_2)			Cell metabolism, mTOR inhibition, cell polarity (particularly in flies)
MARK1	Par1c	Par1, NUAK1	Phosphorylates DCX, MAP2, MAP4 and MAPT/TAU, positive regulator of Wnt signaling, involved in neuronal migration, regulation of Hippo-Yap pathway
MARK2	Par1b, EMK1	Par1, NUAK1	Cell polarity/cell division (hepatocytes), phosphorylates Rab11Fip to control polarity, positively regulates Wnt signaling
MARK3	EMK2, TAK1	Par1, NUAK1	Regulates MAP2 and MAP4 (microtubule stability), regulates some HDACs, regulation of Hippo-Yap pathway
MARK4	PAR1d	Par1	Cilia axoneme extension, regulation of Hippo-Yap pathway
NAUK1		MARK1	P53 binding, serine-threonine kinase activity, cell adhesion via myosin protein phaosphatase, terminal axon branching
NUAK2	SNARK		Cell detachment (via converting F to G actin), tolerance to glucose starvation
BRSK1	SAD-B		Centrosome duplication, neuron polarization, neurotransmitter release
BRSK2	SAD-A		Neuron polarization, cell cycle progression, insulin release, reorganization of actin cytoskeleton
SIK1	SIK		cell cycle regulation, gluconeogenesis, lipogenesis, muscle growth and regulation
SIK2	QIK		Insulin secretion, nuclear export of class II HDACs
SIK3	QSK		Glucose and lipid homeostasis, nuclear export of class II HDACs

CHAPTER II. LKB1 ORIENTS NEURAL PRECURSOR DIVISIONS TO CONTROL EXPANSION AND FOLDING OF THE CEREBELLAR CORTEX

Abstract

Cerebellar growth and foliation require the Hedgehog-driven proliferation of granule cell precursors (GCPs) in the external granule layer (EGL). However, that increased or extended GCP proliferation generally does not elicit ectopic folds suggests that additional cellular mechanisms control cortical expansion and foliation during cerebellar development. Here, we find that genetic loss of the serine-threonine kinase *Liver Kinase B1* (*Lkb1)* in GCPs increased cerebellar cortical size and foliation independent of changes in proliferation or Hedgehog signaling. Our results suggest that Lkb1 regulates cortical expansion and foliation by orienting mitotic GCP divisions perpendicular to the cerebellar surface. Consequently, genetic loss of *Lkb1* from GCPs randomized the orientation of GCP divisions, effectively increasing the proportion of cells dividing parallel to the cerebellar surface. We propose that increased parallel divisions expanded cortical area by positioning GCPs next to, rather than on top of, one another following mitosis. Notably, alterations in the plane of division did not alter GCP differentiation. Additionally, we find that Lkb1 is important for radial migration of post-mitotic GCPs. Cortical expansion, increased foliation, and altered migration were independent of the well-documented Lkb1 substrate AMP-activated Kinase (AMPK). Taken together, our results reveal an important role for Lkb1 during cerebellar development and uncover oriented cell divisions as a previously unappreciated determinant of cerebellar cortical size and folding.

Introduction

The cerebellum integrates sensory and motor information and has recently drawn attention for its extensive involvement in cognition, including emotional control (Tavano and Borgatti, 2010), learning (Bellebaum and Daum, 2011), memory (Rochefort et al., 2011), and decision making (Ito, 2008). Although the importance of the cerebellum during human brain evolution was initially dismissed based on the finding that it occupies a constant proportion of total brain volume (Clark et al., 2001), subsequent analysis revealed that cerebellar surface area—a more accurate measure of processing capacity than volume—increases in an evolutionarily-dependent manner (Sultan, 2002). The capacity of the cerebellum to expand in surface area relative to its volume is facilitated by the presence of deep folds in the cerebellar surface known as fissures that separate the cerebellum into lobules (also known as folia). Like surface area, foliation complexity scales in an evolutionarily-dependent manner (Altman and Bayer, 1997). For example, whereas the central vermis of the mouse cerebellum has 10 lobules, the human vermis has 136 (Altman and Bayer, 1997). Despite the evolutionary import and functional significance of foliation, the cellular cues and genetic programs controlling the expansion and subsequent folding of the cerebellar cortex remain incompletely understood.

Cerebellar foliation occurs in two phases: an embryonic phase, which encompasses cardinal fissure formation, and a postnatal phase, during which time non-cardinal fissures form. Cardinal fissures form around embryonic day 17 (E17) in the mouse and divide the cerebellar surface into five cardinal lobes (Sillitoe and Joyner, 2007). Cardinal fissure formation is at least partially genetically determined, as loss of the Engrailed homeobox genes *En1/2* disrupts placement and depth of cardinal fissures

(Cheng et al., 2010). By contrast, non-cardinal fissures are thought to form in response to mechanical forces; namely, the need to fit the expanding cortical surface within the confines of the skull (Altman and Bayer, 1997).

Expansion of the cerebellar cortex is driven in part by the proliferation of granule cell precursors (GCPs) in the external granule layer (EGL). Between late embryogenesis and the second postnatal week, GCPs in the EGL multiply in response to mitogenic Sonic Hedgehog (Shh) signaling before exiting the cell cycle and migrating radially along Bergmann glia (Dahmane and Ruiz i Altaba, 1999; Wallace, 1999; Wechsler-Reya and Scott, 1999). The importance of the EGL in cortical expansion and foliation is evident from studies showing that reducing GCP proliferation, either using gamma irradiation (Altman and Bayer, 1997) or genetic ablation of Hedgehog (Hh) signaling (Corrales et al., 2006), leads to a small, hypoplastic cerebellum with fewer folds. However, mutations that increase or prolong GCP proliferation do not consistently increase foliation, even when hyperplasia is evident. Although *Shh-P1* transgenic mice, in which Purkinje cell production of Shh is increased, have a larger cerebellum with 1-2 additional folia (Corrales et al., 2006), loss of the cell cycle inhibitor *p27Kip1* extends GCP proliferation and increases cerebellar volume without the formation of additional folds (Miyazawa et al., 2000). Taken together, these studies suggest that GCP proliferation is necessary, but not sufficient, to induce cortical folding in the cerebellum. Thus, one intriguing question regarding cerebellar development is whether factors other than proliferation are important for cortical expansion and foliation.

The position of the mitotic spindle regulates proper patterning in many tissues by controlling daughter cell position (Lu and Johnston, 2013). For example, in the lung, the orientation of cell division determines the relative width and length of tubular epithelium

(Ochoa-Espinosa and Affolter, 2012), while in the developing epidermis, divisions parallel to the epidermal surface expand surface area while perpendicular divisions give rise to stratified dermal layers (Ray and Lechler, 2011). The orientation of cell division can also influence cell fate. For instance, in the developing human neocortex, horizontally dividing basal radial glia give rise to outer radial glia, a distinct progenitor population thought to underlie gyrification of the human cortex (LaMonica et al., 2013). However, whether the plane of cell division regulates cell fate or surface area expansion in the cerebellum has not been explored.

Members of the PAR (PARtitioning defective) family of proteins play an evolutionarily conserved role in cell polarity and cell division. Lkb1 is the vertebrate homolog of *par-4*, a gene originally identified for its role in asymmetric cell division in the early *C. elegans* embryo (Shackelford and Shaw, 2009). With 14 known substrates, Lkb1 controls diverse cellular activities, including cytoskeletal dynamics (Baas et al., 2004; Xu et al., 2010), tight junction formation (Zheng and Cantley, 2007), migration (Marcus and Zhou, 2010), and proliferation (Boudeau et al., 2003). In *Drosophila* neuroblasts, Lkb1 regulates asymmetric cell division by controlling the assembly and stability of the mitotic spindle (Bonaccorsi et al., 2007). However, although a single study found that Lkb1 regulates spindle orientation in cultured epithelial cells (Wei et al., 2012), whether Lkb1 orients vertebrate cell division in vivo remains to be shown. While Lkb1 function has been assessed at later stages of vertebrate neuronal development, including migration (Asada and Sanada, 2010; Asada et al., 2007), axon specification (Barnes et al., 2007; Shelly et al., 2007), and terminal axon branching (Courchet et al., 2013), its role in neural precursors is not known. Moreover, the importance of Lkb1 for cerebellar development has not been explored. Finally, while an initial study

demonstrated that loss of AMP-activated Kinase (AMPK), a key metabolic sensor and the best-studied substrate of Lkb1, led to severe defects in hippocampal and cerebellar development (Dasgupta and Milbrandt, 2009), a subsequent report indicated that AMPK was dispensable for proper brain development (Dzamko et al., 2010), and the role of AMPK in cerebellar development remains unresolved.

We initially became interested in Lkb1 following a recent genetic screen demonstrating that loss of *Lkb1* reduced Hh pathway responsiveness in mouse embryonic fibroblasts (Jacob et al., 2011). To determine if Lkb1 promotes Hh signaling in vivo, we set out to investigate the role of Lkb1 in proliferating GCPs of the cerebellar cortex. To this end, we generated a mouse model of GCP-specific *Lkb1* ablation. Surprisingly, rather than cerebellar hypoplasia, as would be expected if *Lkb1* were important for Hh pathway activation, GCP-specific loss of *Lkb1* resulted in an expanded cerebellar cortex with increased foliation. We propose that loss of *Lkb1* increased cortical size and foliation by altering the axis of GCP divisions while maintaining Hh signal transduction. Thus, our results suggest that Lkb1 regulates cerebellar cortical size by controlling the orientation of GCP divisions.

Experimental Procedures

Mice. All experiments were performed using young neonatal and adult animals (ages P2-P30), according to regulation of the NIH and VUMC Division of Animal Care. *Lkb1fl/fl* mice (Nakada et al., 2010), *Sox2-cre* mice (Hayashi et al., 2002), *AMPKa1fl/fl*, and *AMPKa2fl/fl* mice (Nakada et al., 2010) were obtained from Jackson laboratories. *TSC1fl/fl* mice (Uhlmann et al., 2002) were kindly donated from Kevin Ess (Vanderbilt University). *Math1-cre* mice (Schuller et al., 2007) were kindly donated from David

Rowitch (UCSF). *Lkb1+/-*, *AMPKa1-/-*, and *TSC1+/-* mice were generated by crossing fl/fl animals to *Sox2-cre* females. BrdU (Roche) was dissolved in PBS to a final concentration of 10 mg/ml and administered by intraperitoneal injection.

Quantification.

Area, perimeter, and lobule number. For vermal area and perimeter, at least 3 and up to 10 mid-vermal cross sections were measured in ImageJ and averaged for each mouse, such that each mouse was assigned a single value for area and perimeter. For IGL area, H&E stained sections used to measure the area of IGL in ImageJ. These values were gathered for n=5 control and $Lkb1^{cko}$ mice, and t-tests were performed in Excel. For lobule number, lobules were defined as in (Lancaster et al., 2011), by the separation of individual lobules by molecular layer as well as the presence of white matter. Lobule counts were obtained for n=3 or n=5 animals, and t-tests were performed in Excel.

Proliferation. For P2 and P6 BrdU, sections were stained and a total of 5 regions from each of three sections was imaged using an Olympus fluorescent microscope at 40x magnification. These images were cropped so as to only contain the EGL. Cell Profiler was used to count the total number of Dapi+ cells as well as BrdU+ cells. 3 replicates of each region were averaged. For each mouse, these 5 regions were averaged such that each mouse was assigned a single value representing the % BrdU+ cells. This was done for n=3 mice of each genotype, and t-tests were performed in Excel. For pH3+ counts of the entire cerebellum, the total number of pH3+ cells in the EGL was determined at 20x magnification using a hand tally counter. For each animal, at least 3 and up to 6 sections were analyzed. These numbers were averaged such that each mouse was assigned a single value. T-tests were performed in Excel.

Cilia length. 40x images were taken on an LSM 510. 4 regions for each of n=3 animals were taken. Images were cropped so as to only include the EGL, and Cell Profiler was used to measure cilia length. An average cilia length was obtained for each animal, and these numbers were compared using a Student's paired t-test in Excel.

EGL thickness. Ki67-stained cerebella were scanned through the DHSR. At least 3 sections for each mouse were cropped so as to omit any non-EGL Ki67+ cells (eg, cells of the white matter). The total number of Ki67+ cells per section was determined. EGL length was determined by measuring the perimeter of each section in ImageJ, similar to above measurements of perimeter and area. The number of Ki67+ cells was divided by perimeter length to give the average EGL thickness per section for each of three sections. These numbers were averaged for each mouse, yielding a single value corresponding to each animal. T-tests were performed in Excel for n=3 mice of each genotype.

P27Kip1, Ki67 co-staining and cell cycle exit. Sections were prepared and stained with the appropriate antibodies as described for EGL thickness above. The total number of p27Kip1+, Ki67+, and p27Kip1+ Ki67+ double positive cells was determined across the entire cerebellum for at least 3 sections of each of n=3 animals. Similar analysis was used to count the total number of Brdu+ and Ki67+BrdU+ cells to determine cell cycle exit. oEGL and iEGL area were measured in ImageJ using p27Kip1/Ki67 co-stained sections.

Orientation of cell division. Sections were stained with Aurora B or pH3 for n=3 mice of each genotype (*Lkb1*^{cko} or littermate controls). At least 3 and up to 5 stained sections were imaged at 20x magnification in non-overlapping fields over the entire cerebellum (approximately 12-15 images per section). Angle measurements were taken using the

angle tool in ImageJ. Between 20 and 40 cells were measured for each section depending on stage. The proportion of GCPs dividing parallel (0-30 degrees), perpendicular (60-90 degrees) or tangential (30-60 degrees) was determined for each section. These proportions were averaged such that each mouse was assigned a single set of numbers corresponding to the proportion of GCPs dividing in each orientation, and these numbers were compared using a Student's paired t-test in Excel.

GCP Isolation. GCPs were isolated as previously described (Parathath et al., 2008). Briefly, cerebella were isolated from P4-P6 mice in Hanks buffered saline solution (HBSS) (Gibco) supplemented with glucose. Meninges were removed and cerebella were treated with Trypsin-EDTA. Cerebella were dissociated, large cells were allowed to settle, and GCP-containing supernatants were moved to a fresh tube. For western blotting, cells were spun down and resuspended in RIPA buffer. For RNA extraction, cells were resuspended according to QIAGEN protocols.

Western blotting. Whole cerebella or isolated GCPs were homogenized in RIPA buffer containing protease inhibitors (Roche). Protein concentration was measured using the BCA method, and 20-50 µg protein was separated by SDS-PAGE before being transferred onto nitrocellulose membranes.

RNA Isolation and Reverse Transcription. Total RNA was purified from freshly isolated GCPs using RNAeasy mini kit (QIAGEN) and cell homogenization performed using QIAshredder columns (QIAGEN). cDNAs were synthesized using a high-capacity

cDNA reverse transcription kit (Applied Biosciences). PCR was performed as previously described (Fleming et al., 2013).

Tissue Processing, Immunohistochemistry, and *In Situ* Hybridization. Tissue was collected and processed as described previously (Fleming et al., 2013). Paraffin sections underwent antigen-retrieval using Citrate Buffer pH=6.0. For γ-tubulin staining, frozen sections were dried, post-fixed, washed in PBS and submerged in ice cold acetone before blocking. *In situ* hybridizations were performed as described previously (Li et al., 2006).

Microscopy. Bright-field images were collected on an Olympus BX51 upright microscope or a Leica M165 FC stereoscope. Fluorescent images were taken on a Zeiss LSM510, Leica TSC SP5 Confocal, or Olympus fluorescent microscope with an Optigrid system (Qioptiq Imaging). For automated cell counting of entire postnatal cerebella, slides were scanned on an Ariol SL-50 platform (Leica) through the Vanderbilt DHSR.

Antibodies. The following antibodies were used for immunohistochemistry: p27Kip1 (BD Biosciences, 1:300), Tag1 (Hybridoma Bank, 1:10), γ-tubulin (Sigma, 1:300), BrdU (Hybridoma Bank, 1:100), Ki67 (Thermo Scientific, 1:200), phosphohistone H3 (Upstate, 1:300), p-S6 (Cell Signaling, 1:200), Aurora B (BD Biosciences, 1:300), ARL13B (a kind gift from Jonathan Eggenschwiler, 1:5000), Lkb1 (Santa Cruz, 1:200).

For Western: p-S6 (Cell Signaling, 1:1000), p-ACC (Cell Signaling, 1:1000), ACC (Cell Signaling, 1:1000), S6 (Cell Signaling, 1:1000), Lkb1 (Sigma, 1:3000), α-tubulin

(Hybridoma Bank, 1:10,000), β-Actin (Thermo Scientific, 1:5000), Gli1 (Cell Signaling, 1:1500), p-AMPK (Cell Signaling, 1:1000).

Results

Lkb1 is expressed in neural progenitors

Lkb1 is expressed in developing forebrain progenitors (Barnes et al., 2007); however, its expression in the postnatal cerebellum has not been previously reported. *In situ* hybridization for *Lkb1* at postnatal day 4 (P4) revealed that while *Lkb1* was expressed in all layers of the developing cerebellar cortex, highest levels of expression were seen in the external granule layer (EGL), where Shh-responsive GCPs reside (Figure 2.1A-A'). A similar pattern of *Lkb1* expression was observed at P6 (data not shown).

We also sought to determine the distribution of Lkb1 protein in the developing cerebellum. The EGL can be divided into two regions – an outer layer (oEGL) containing proliferating GCPs, and an inner layer (iEGL) which contains post-mitotic GCPs that have not yet undergone radial migration along Bergmann glia. At P7, Lkb1 protein was localized to the cytoplasm and cell cortex of GCPs throughout the EGL, suggesting that Lkb1 may function in both proliferating and post-mitotic GCPs (Figure 2.1B-B').

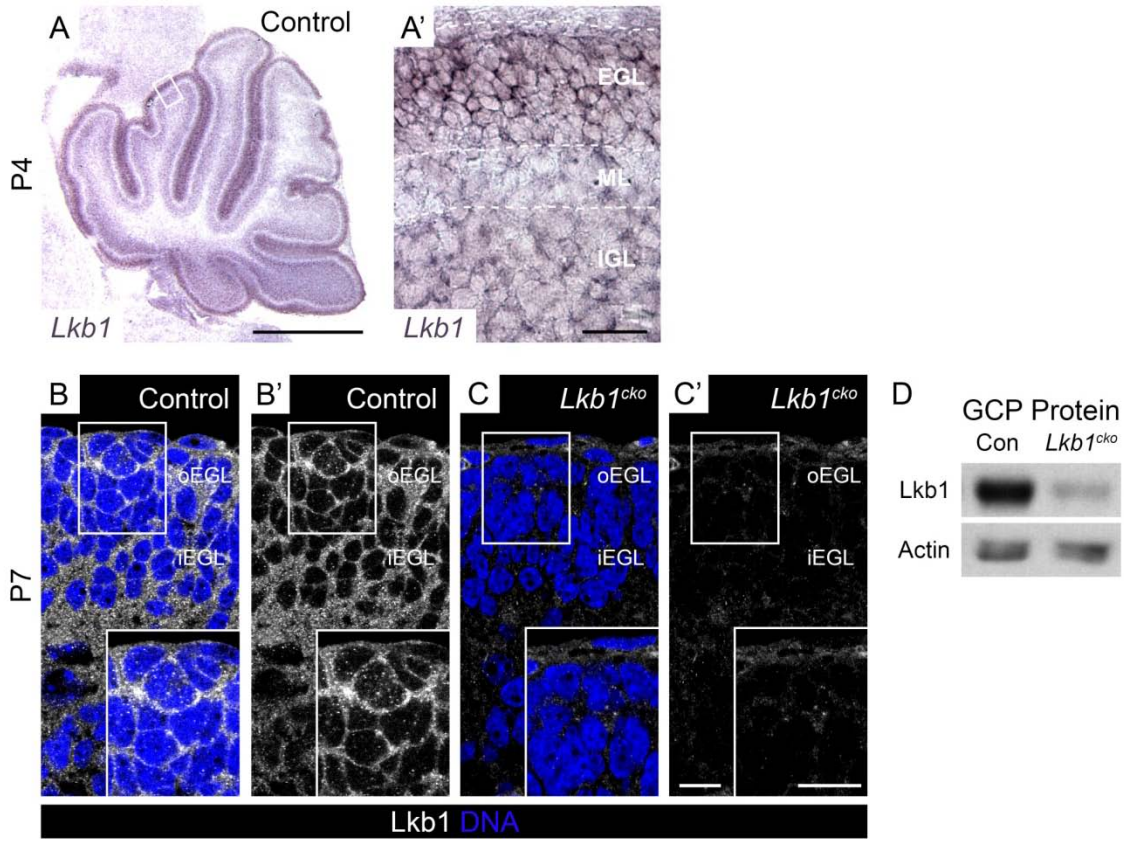

Figure 2.1. *Lkb1* in situ hybridization at postnatal day 4 (P4).
A-A'. Lkb1 is expressed in all cortical layers but is highest in the external granule layer (EGL). B-C. Immunohistochemistry for Lkb1 (white) and TO-PRO 3 (blue) at postnatal day 7 (P7). Lkb1 localizes to the cytoplasm and cell cortex of GCPs in the EGL of control cerebella (B-B') but is absent in $Lkb1^{cko}$ cerebella (C-C'). D. Western blotting for Lkb1 reveals a significant reduction in Lkb1 protein levels in $Lkb1^{cko}$ GCPs compared to controls. Actin was used as loading control. Scalebars: A = 500 µm, A' = 50 µm, C-D = 10 µm. Con = control, EGL = external granule layer, oEGL = outer EGL, iEGL = inner EGL, ML = molecular layer, IGL = internal granule layer.

Loss of *Lkb1* from GCPs increases cortical size and foliation

Mice null for *Lkb1* die between E8 and E11 due to vascular defects (Wang and Zoghbi, 2001). In order to study the function of Lkb1 in the cerebellum, which develops postnatally, we generated *Math1-cre; Lkb1*$^{fl/-}$ mice (hereafter referred to as *Lkb1*^{cko}). Expression of the *Math1* transcription factor is restricted to cerebellar GCPs and deep cerebellar nuclei (Ben-Arie et al., 1997; Machold and Fishell, 2005; Wang et al., 2005). Immunostaining of *Lkb1*^{cko} cerebella revealed a near complete loss of Lkb1 expression throughout the EGL (Figure 2.1C). Additionally, Western blotting of GCPs isolated from early postnatal *Lkb1*^{cko} cerebella revealed a ~90% reduction in Lkb1 protein relative to control GCPs (Figure 2.1D). However, consistent with previous reports of reduced *Math1-cre* activity in the posterior cerebellum (Pan et al., 2009a), recombination efficiency was reduced in lobes IX and X, leading to higher levels of Lkb1 protein relative to other regions of the EGL (data not shown).

Lkb1-/- MEFs have reduced levels of Hh responsiveness (Jacob et al., 2011). Given that Hh signaling is critical for GCP proliferation (Dahmane and Ruiz i Altaba, 1999; Wallace, 1999; Wechsler-Reya and Scott, 1999), we anticipated that *Lkb1*^{cko} cerebella would be smaller than control littermates. Surprisingly, we noted that *Lkb1*^{cko} cerebella were considerably more foliated than littermate controls at adult stages (Figure 2.2A-B); a phenotype that is more consistent with increased Hh pathway activity than its loss. However, folia pattern and number were similar among *Math1-cre; Lkb1*$^{fl/+}$, *Lkb1*$^{+/-}$, *Lkb1*$^{fl/+}$, and *Lkb1*$^{fl/-}$ littermates; thus, the term “control” is used to collectively describe littermates of any of these genotypes.

Figure 2.2. Granule cell precursor-specific loss of *Lkb1* results in increased foliation and cortical expansion.

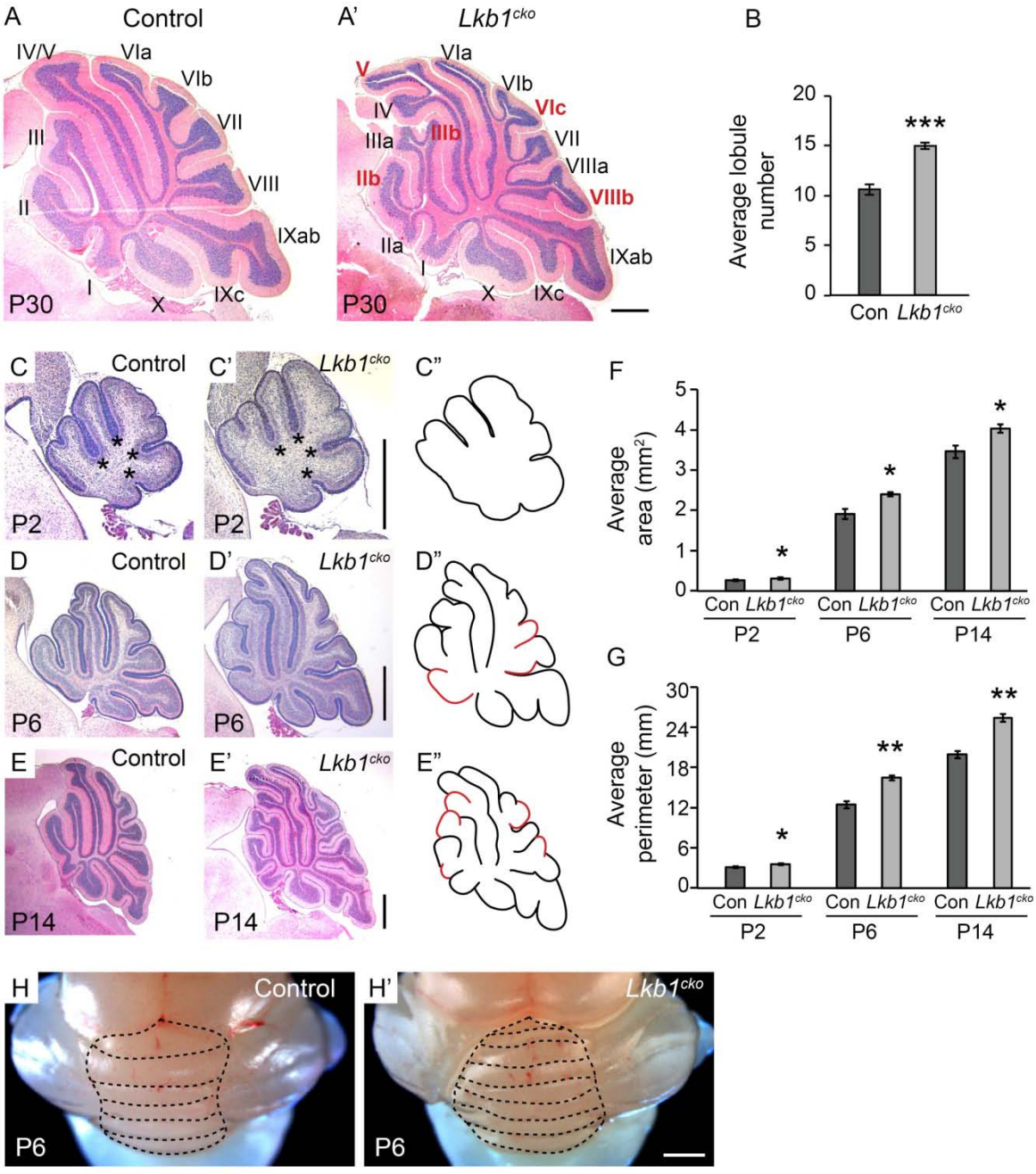

Figure 2.2. Granule cell precursor-specific loss of Lkb1 results in increased foliation and cortical expansion.

A-A'. Hematoxylin and eosin staining of control (A) and $Lkb1^{cko}$ (A') cerebella at P30. Roman numerals denote lobule numbers. Red roman numerals indicate lobules present in $Lkb1^{cko}$ that are absent in the control. B. Average lobule number of control and $Lkb1^{cko}$ cerebella. C-E. Hematoxylin and eosin staining of mid-vermal cerebellar cross-sections at the indicated stages. Lobules present in $Lkb1^{cko}$ not present in the control are highlighted in red in C"-E". Asterisks in C-C' indicate cardinal fissure location. F. Average cross-sectional area of mid-vermal cerebellar sections at the indicated stages. G. Average cross-sectional perimeter measurements of mid-vermal cerebellar cross sections at the indicated stages. H-H'. Whole mount images of P6 control (H) and $Lkb1^{cko}$ (H') cerebella. Dashed lines delineate folia. N=5 for all analyses. *, $p<0.05$, **, $p<0.005$, ***, $p<0.0005$, Student's paired t-test. Scalebar 500 μm for all images. Con = control.

To determine when *Lkb1*^{cko} first exhibited enhanced foliation, we collected cerebella sequentially during the first two postnatal weeks (Figure 2.2; Figure 2.3). The initial stages of cerebellar patterning, including cardinal fissure formation, were normal in *Lkb1*^{cko} cerebella at P2, the earliest stage we examined (Figure 2.2C-C", asterisks denote principal fissures). However, *Lkb1*^{cko} cerebella appeared visibly larger than controls at both P2 (Figure 2.2C-C', F) and P4 (Figure 2.3). Indeed, mid-sagittal cross sectional area was larger in *Lkb1*^{cko} cerebella relative to controls (0.31 +/- 0.029 mm^2 in *Lkb1*^{cko} vs. 0.27 +/- 0.27 mm^2 in controls; Figure 2.2F). Additionally, mid-sagittal EGL perimeter was longer in P2 *Lkb1*^{cko} cerebella (3.5 +/- 0.16 mm in *Lkb1*^{cko} vs. 3.12 +/- 0.16 mm in controls; Figure 2.2G), suggesting that cerebellar surface area was increased. Thus, cortical expansion and increased cross sectional area preceded supernumerary folia in *Lkb1*^{cko}.

Lkb1^{cko} first displayed increased foliation at P6, with multiple lobules not present in controls (Figure 2.2D-D", H-H'). Additionally, mid-sagittal area (2.34 +/- 0.05 mm^2 in *Lkb1*^{cko} vs. 1.92 +/- 0.12 mm^2 in controls) and perimeter (16.5 +/- 0.36 mm in *Lkb1*^{cko} vs. 12.48 +/- 0.52 mm in controls) were larger in P6 *Lkb1*^{cko} relative to controls, indicating an increase in both cerebellar volume and surface area (Figure 2.2F-G). Consistent with increased volume, *Lkb1*^{cko} cerebella were often adhered to the overlying skull, making them difficult to dissect. By P11, dramatic differences in the shape and pattern of *Lkb1*^{cko} cerebella were apparent (Figure 2.3). At P14, when foliation patterns are established (Sudarov and Joyner, 2007), *Lkb1*^{cko} were larger (area: 4.03 +/- 0.10 mm^2 in *Lkb1*^{cko} vs. 3.46 +/- 0.15 mm^2 in controls; Figure 2.2F), had a longer perimeter (25.45 +/- 0.56 mm in *Lkb1*^{cko} vs. 19.95 +/- 0.57 mm in controls; Figure 2.2G), and were considerably more

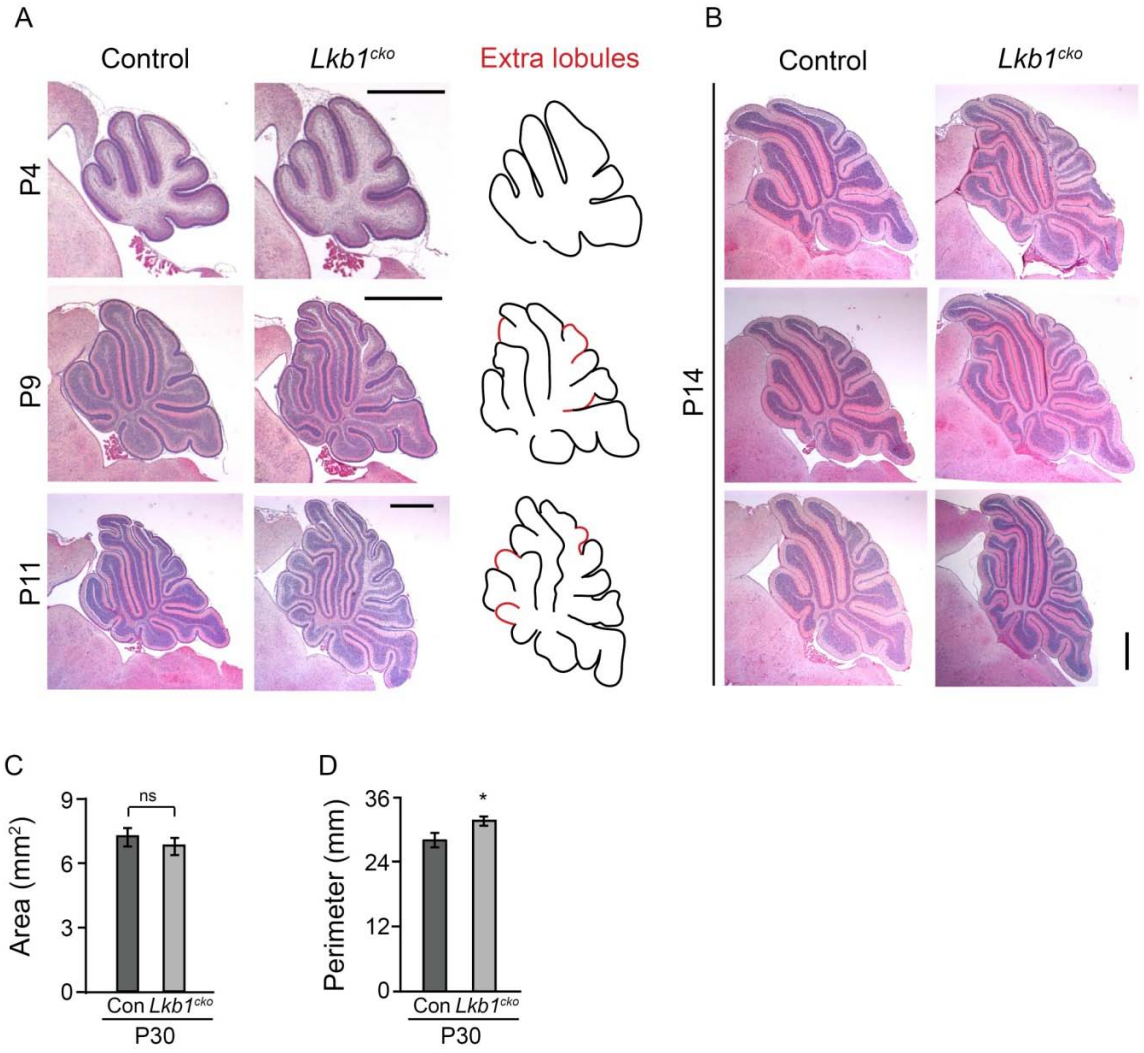

Figure 2.3. Histological analysis of *Lkb1^{cko}* cerebella at additional stages.
A.Hematoxylin and eosin staining of control and Lkb1^{cko} mid-vermal cross-sections at the indicated stages. Scalebar 500 µm. B. H and E staining of 3 control and 3 Lkb1^{cko} cerebella at P14. C. Quantification of cross-sectional area reveals that there is no difference at P30. D. Quantification of cross-sectional perimeter demonstrates that Lkb1^{cko} display cortical expansion at P30. N=4, *, $p<0.05$, Student's paired t-test. Con = control.

Foliated than controls (Figure 2.2E-E", Figure 2.3). However, although P30 *Lkb1*^{cko} cerebella were more foliated than littermate controls (Figure 2.2A-A') and had a larger cross sectional perimeter (31.5 +/- 0.81 mm in *Lkb1*^{cko} vs. 27.89 +/- 1.35 mm in controls; Figure 2.3), cross sectional area was not increased (Figure 2.3).

The central cerebellar vermis of most inbred mouse strains contains between 9 and 11 lobules and sublobules (hereafter referred to collectively as lobules). Whereas the mixed strain control mice used in our studies had an average of 10.5 lobules, *Lkb1*^{cko} had an average of 15 lobules, corresponding to a ~40% increase in foliation (Figure 2.2B). The placement of additional lobules was surprisingly consistent: lobes II, III, Ivb and VIII were consistently split, and lobe I occasionally formed two lobules (Figure 2.2A-A', E-E' and Figure 2.3; see Table 2.1 for detailed analysis). Additionally, whereas lobes IV and V were usually fused in controls, lobes IV and V were distinct in the majority of *Lkb1*^{cko} (Figure 2.2A-A', E-E', Figure 2.3 and Table 2.1). Other morphological changes were also evident in *Lkb1*^{cko}: whereas the interface of lobes V and IV was normally straight in controls, this fissure often had an undulated, rippled appearance in *Lkb1*^{cko} (Figure 2.2A', E' and Figure 2.3). Notably, throughout our analysis, lobes IX and X appeared normal in *Lkb1*^{cko}, consistent with reduced recombination efficiency of *Math1-cre* in these regions (Pan et al., 2009a).

Table 2.1. Location and number of sublobules by lobe in control and *Lkb1^{cko}* cerebella.
The number of sublobules (1, 2, or 3) per lobe was determined in n=10 control and Lkb1^{cko} animals P14 and older. Merged lobes (I/II and IV/V) are labeled as such.

		Number of Sublobules							
		Merged		1		2		3	
		Control	*Lkb1^{cko}*	Control	*Lkb1^{cko}*	Control	*Lkb1^{cko}*	Control	*Lkb1^{cko}*
Lobe	I	5	1	5	7	0	2	0	0
	II			5	2	0	6	0	1
	III	--	--	10	3	0	5	0	2
	IV	8	1	2	9	0	0	0	0
	V			2	9	0	0	0	0
	VI	--	--	4	0	6	0	0	10
	VII	--	--	10	9	0	1	0	0
	VIII	--	--	10	1	0	9	0	0
	IX	--	--	0	0	10	8	0	2
	X	--	--	10	10	0	0	0	0

Loss of Lkb1 does not increase Hedgehog signaling

Given that cardinal lobes formed normally in *Lkb1^{cko}* (Figure 2.2C-C'), we focused our attention on the development of secondary and tertiary lobules, which are thought to form in response to expansion of the EGL within the confines of the skull (Altman and Bayer, 1997). Shh drives GCP proliferation, which is critical for expansion of the EGL. Moreover, the only existing mouse mutant with increased foliation harbors a transgenic *Shh-P1* allele that increases Shh production in Purkinje cells (Corrales et al., 2006). The transcription factor Gli1 is a transcriptional target of Hh signaling, and Gli1 mRNA and protein levels are an established readout for pathway activity (Appendix I) (Ryan and Chiang, 2012). To determine if Hh signaling was increased in *Lkb1^{cko}* GCPs,

we measured Gli1 mRNA and protein in freshly isolated GCPs. Gli1 antibody specificity was verified using cerebellar lysate collected from *Gli1-/-* mice (Figure 2.5). However, neither *in situ* hybridization, nor RT-PCR, nor Western blot showed a significant difference in levels of Gli1 mRNA or protein in $Lkb1^{cko}$ GCPs compared to control (Figure 2.4). Together, these data indicate that *Lkb1* does not regulate cortical expansion or foliation by increasing Hedgehog pathway activity.

Lkb1-/- MEFs have a shorter primary cilium, the microtubule-based organelle that is essential for Hedgehog signaling (Jacob et al., 2011). However, loss of *Lkb1* did not alter primary cilia length in GCPs (Figure 2.5). Thus, unlike MEFs, GCPs do not require *Lkb1* to maintain Hh signaling or cilia length.

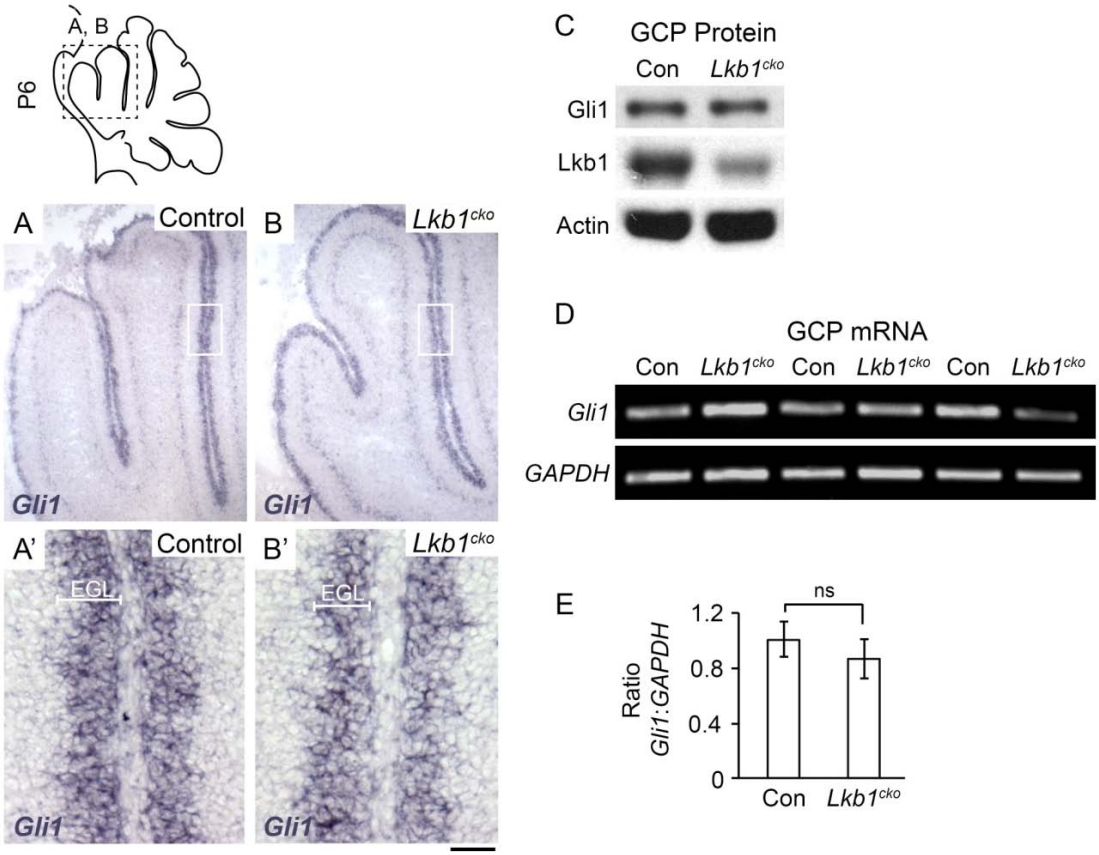

Figure 2.4. Hedgehog signaling is unchanged in *Lkb1^{cko}* cerebella.
A-B. In situ hybridization for Hedgehog target gene Gli1 in postnatal day 6 control (A-A') and Lkb1^{cko} (B-B') cerebella. C. Western blot for Gli1 in isolated granule cell precursors derived from control and Lkb1^{cko} cerebella. Lkb1 and Actin were used as controls to verify knockdown and loading, respectively. D. RT-PCR for Gli1 expression in GCPs isolated from control and Lkb1^{cko} cerebella. GAPDH was used as a loading control. E. Quantification of levels of Gli1 mRNA relative to GAPDH in control and Lkb1^{cko} GCPs. n=3, no significant difference, Student's paired t-test. Scalebar 50 µm. Con = control, EGL = external granule layer.

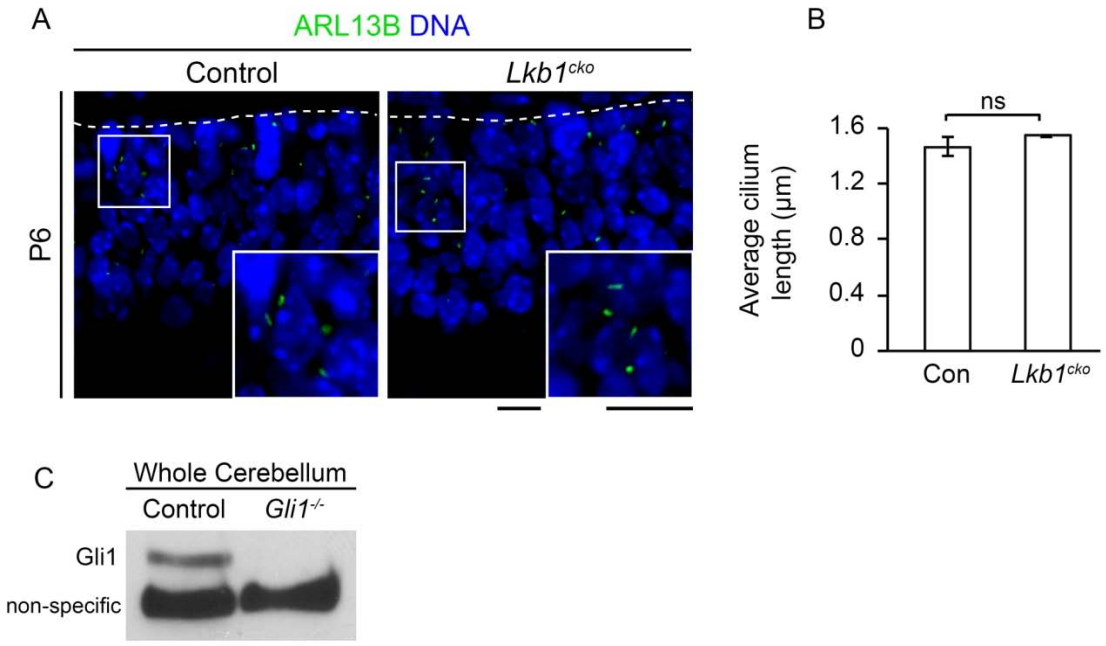

Figure 2.5. Cilia length is not altered in GCPs lacking *Lkb1*.
A. Representative staining for cilia marker ARL13B and DNA in P6 control (left) and Lkb1^{cko} (right) cerebella. Dashed line denotes pial surface. Scalebar 10 µm. B. Quantification of average cilium length using ARL13B staining at P6. C. Western blot for Gli1 on early postnatal cerebellar lysates derived from control and Gli1-/- cerebella. Note the lower background band that is present in both samples. N=3, ns, Student's paired t-test. Con = Control, EGL = external granule layer.

Loss of *Lkb1* does not increase GCP proliferation

Lkb1 functions as a tumor suppressor in the lung, pancreas, and gut (Ollila and Makela, 2011) and *Lkb1* overexpression inhibits proliferation in vitro (Tiainen et al., 1999). Moreover, although Hh signaling is required for GCP proliferation, we speculated that loss of *Lkb1* might stimulate Hh-independent GCP proliferation, perhaps by activating Notch signaling (Solecki et al., 2001), increasing IGF signaling (Parathath et al., 2008) or inhibiting Wnt signaling (Anne et al., 2013).

To determine if cortical expansion and extra folia in *Lkb1*^{cko} were due to increased GCP proliferation, we used short-term (1 hour) labeling with the thymidine analog BrdU to measure the proportion of dividing GCPs at both P2, when changes in foliation were not yet evident, and P6, around the onset of altered foliation in *Lkb1*^{cko}. However, the proportion of BrdU+ GCPs, determined using the automated cell counting software Cell Profiler, was unchanged in *Lkb1*^{cko} compared to controls at both P2 and P6 (Figure 2.6A-C). Given that EGL length was increased in *Lkb1*^{cko} (Figure 2.2), we speculated that the total number of mitotic cells might be higher, even if the proportion of dividing cells was not. However, the total number of mitotic (agnific-histone H3+) GCPs in the EGL did not differ between *Lkb1*^{cko} and littermate controls at P2 or P6 (Figure 2.6D). Together, these data suggested cortical expansion and increased foliation in *Lkb1*^{cko} were not due to increased GCP proliferation.

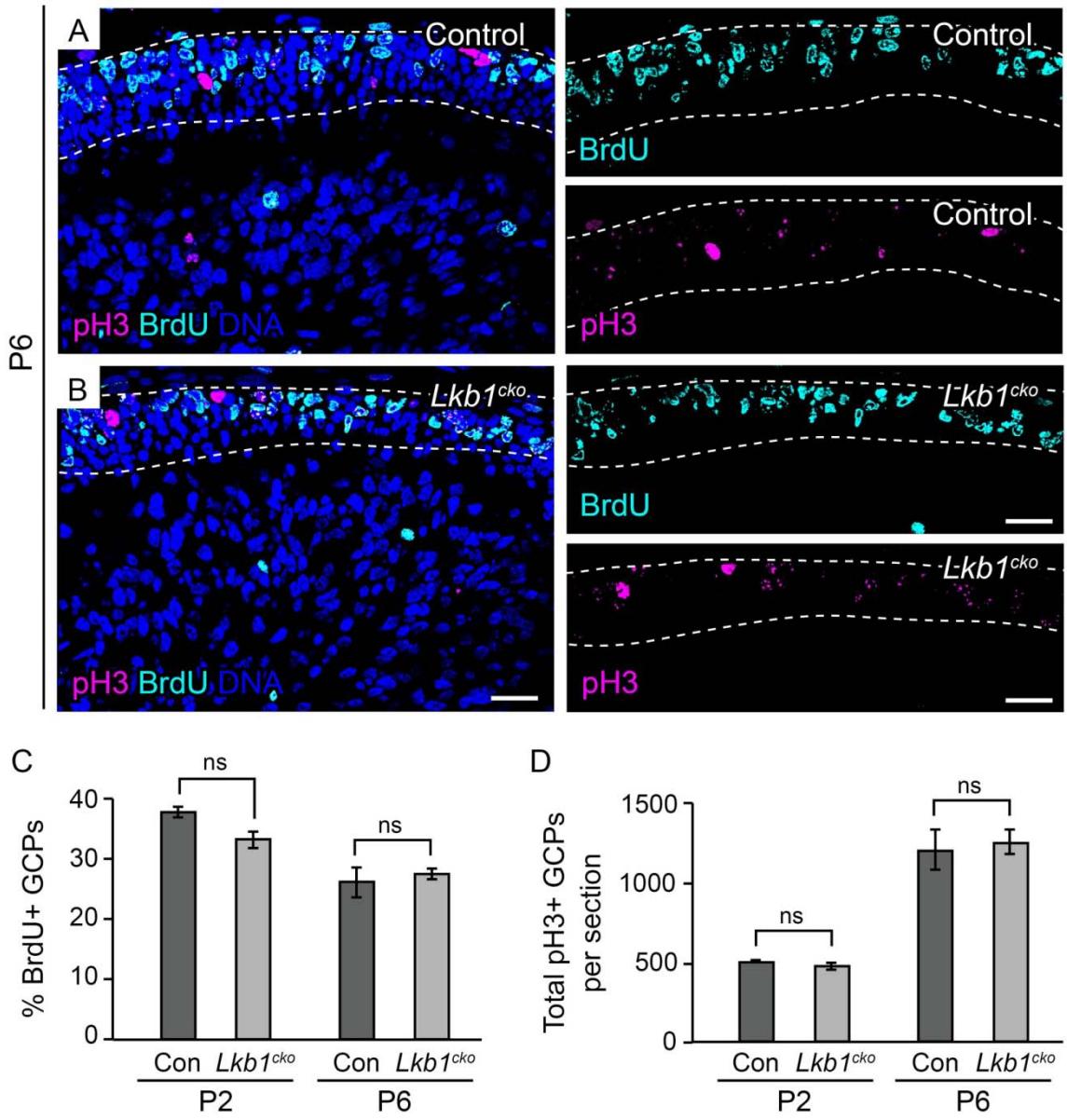

Figure 2.6. Proliferation is not altered in *Lkb1^{cko}* cerebella.
A-B. Immunostaining of P6 control (A) and Lkb1^{cko} (B) for □agnific-histone H3 (pH3) and BrdU one hour after BrdU injection. Dashed lines delimit the EGL. DNA was counterstained with TO-PRO 3. C. Quantification of the percentage of BrdU+ cells in the EGL of control and Lkb1^{cko} cerebella at P2 and P6. D. Quantification of the total number of pH3+ cells per mid-vermal cross section of control and Lkb1^{cko} cerebella at the indicated stages. For all analyses n=3, no significant difference, Student's paired t-test. Scalebar 20 µm. Con = control.

GCPs proliferate in outer EGL (oEGL) before entering the inner EGL (iEGL) where they begin to differentiate. To determine if loss of *Lkb1* altered GCP differentiation, P7 sections were co-labeled with Ki67 and the cell cycle inhibitor p27Kip1 to label the oEGL and iEGL, respectively. However, no difference in the proportion of proliferating or differentiating GCPs was apparent in the $Lkb1^{cko}$ EGL (Figure 2.7). Moreover, neither oEGL nor iEGL area was altered in $Lkb1^{cko}$ relative to controls, indicating that the number of proliferating and differentiating GCPs was unchanged (Figure 2.7). Additionally, both control and *Lkb1*-deficient GCPs were equally able to exit the cell cycle, as determined by measuring the proportion of cycling cells (BrdU+Ki67+/BrdU+) 24 hours after BrdU injection (Figure 2.8). Consistent with the finding loss of *Lkb1* did not alter GCP proliferation or differentiation (Figure 2.7), IGL area was comparable between adult P30 $Lkb1^{cko}$ and control cerebella, indicating that granule cell number was unchanged in $Lkb1^{cko}$ (Figure 2.9).

Figure 2.7. Loss of *Lkb1* does not alter GCP differentiation.

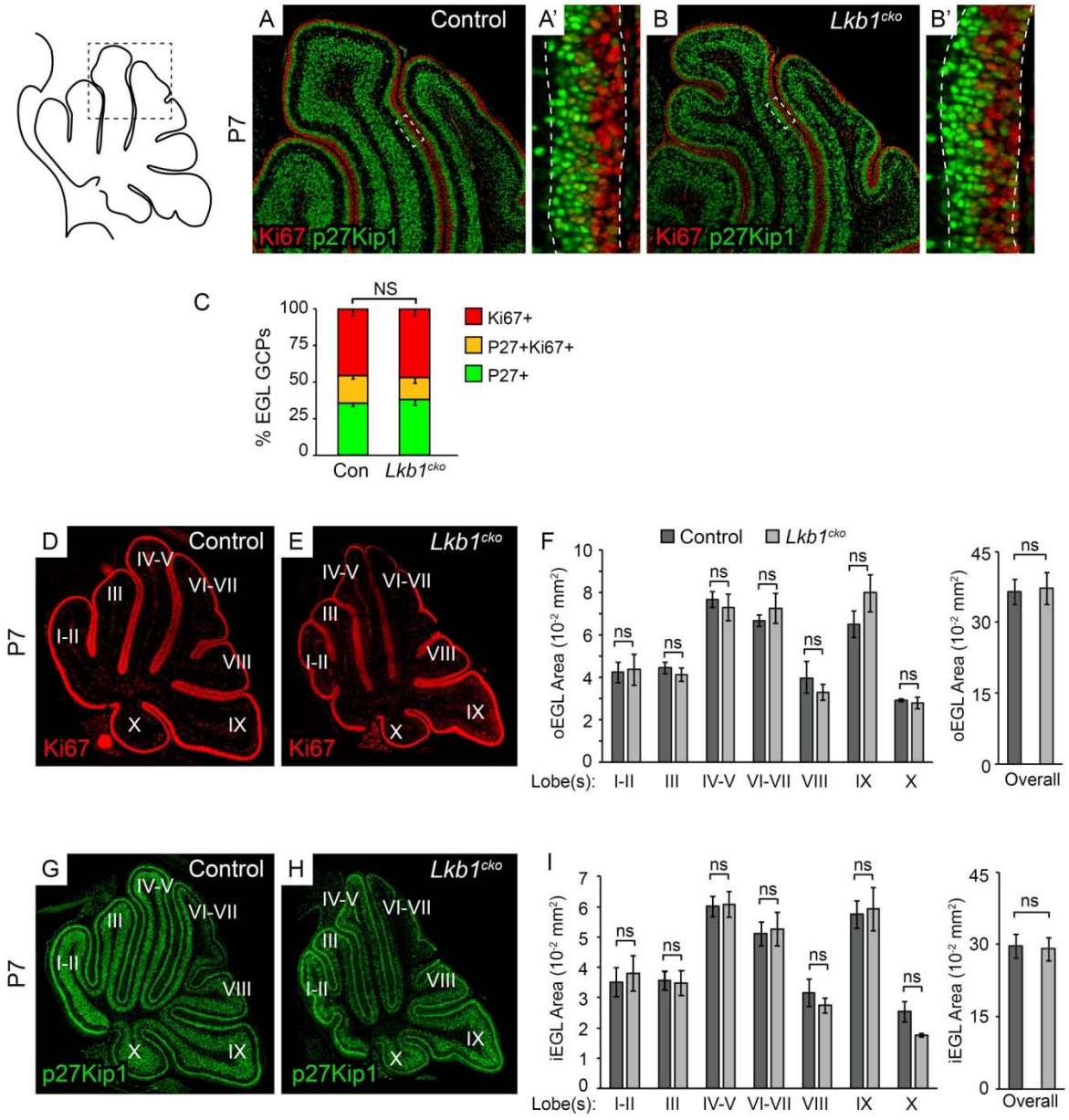

Figure 2.7. Loss of *Lkb1* does not alter GCP differentiation.
A-B. Ki67/p27Kip1 co-staining of P7 control (A) and Lkb1^{cko} (B) cerebella. Ki67 labels proliferating cells in the outer EGL (oEGL), while p27Kip1 marks differentiating cells in the inner EGL (iEGL). C. Quantification of the proportion of proliferative (p27Kip1-, Ki67+), differentiating (Ki67-, p27Kip1+) or double-positive (Ki67+, p27Kip1+) GCPs in the EGL of control and Lkb1^{cko} cerebella. Note: images shown are representative images; quantification was done over the entire cerebellum using automated cell counting in Cell Profiler. D-E. Representative images of P7 Ki67 staining of control and Lkb1^{cko} cerebella to mark the outer EGL. F. Quantification of Ki67+ outer EGL area revealed oEGL area was not significantly different between control and Lkb1^{cko} cerebella, either when measured by lobe (left) or across the entire cerebellum (right). G-H. p27Kip1 staining of P7 control and Lkb1^{cko} cerebella to mark the iEGL. I. Quantification of p27Kip1+ inner EGL area revealed iEGL area was not significantly different between control and Lkb1^{cko} cerebella, either when measured by lobe (left) or across the entire cerebellum (right). For all analysis, n=3, p=ns, Student's paired t-test.

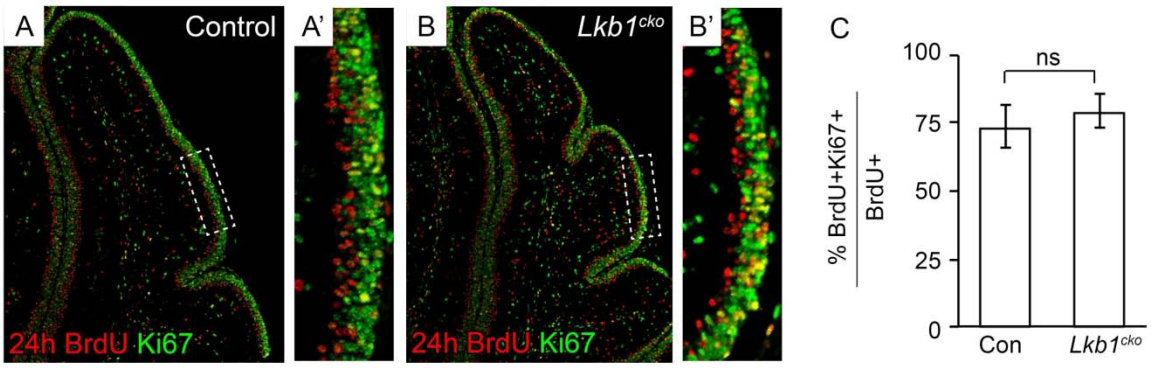

Figure 2.8. Loss of *Lkb1* does not alter GCP cell cycle exit.
A-B. Ki67-BrdU double labeling of control (A-A') and Lkb1^{cko} (B-B') cerebella at P7, 24 hours after BrdU injection. C. Quantification of the proportion of labeled cells that remained in the cell cycle (BrdU+Ki67+/BrdU+) 24 hours after BrdU injection. N=3, p=ns, Student's paired t-test. Note: images shown are representative images; quantification was done over the entire cerebellum using automated cell counting in Cell Profiler.

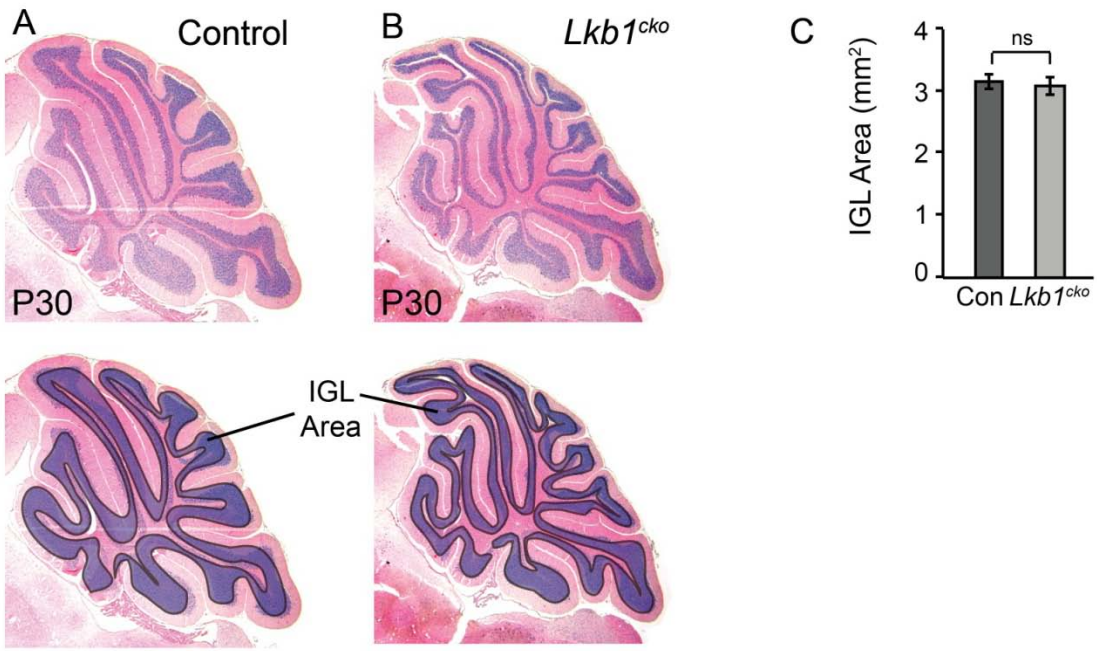

Figure 2.9. IGL area does not differ between control and *Lkb1^{cko}* cerebella at P30. A-B Representative mid-sagittal cross-sections of P30 control and Lkb1^{cko} cerebella. Lower panels illustrate how IGL area was measured. C. Quantification of mid-sagittal IGL area reveals that there is no significant difference at P30. N=4, *, $p<0.05$, Student's paired t-test. Con = control.

Lkb1^{cko} cerebella have a thinner outer EGL

Given that *Lkb1^{cko}* cerebella were larger at P6 (Figure 2.2) but did not harbor an increased number of proliferating GCPs (Figure 2.6, Figure 2.7), we wondered if the oEGL was thinner *Lkb1^{cko}* cerebella. In other words, if GCP proliferation was equivalent in control and *Lkb1^{cko}* mice, but GCPs were distributed over a larger area in *Lkb1^{cko}*, we would expect the oEGL to be thinner in *Lkb1^{cko}*. Indeed, Ki67 staining of P7 sections revealed that many regions of the oEGL appeared thinner in *Lkb1^{cko}* compared to controls (Figure 2.10). To account for variability in EGL thickness, average oEGL

thickness was determined by dividing the total number of Ki67+ GCPs by the length of the EGL. Indeed, the average number of Ki67+ GCPs per mm of EGL was significantly reduced in *Lkb1*^{cko} (538.7 +/- 15 cells/mm in control vs. 436.9 cells/mm in *Lkb1*^{cko}; Figure 2.10C). Thus, loss of *Lkb1* from GCPs leads to a thinner oEGL.

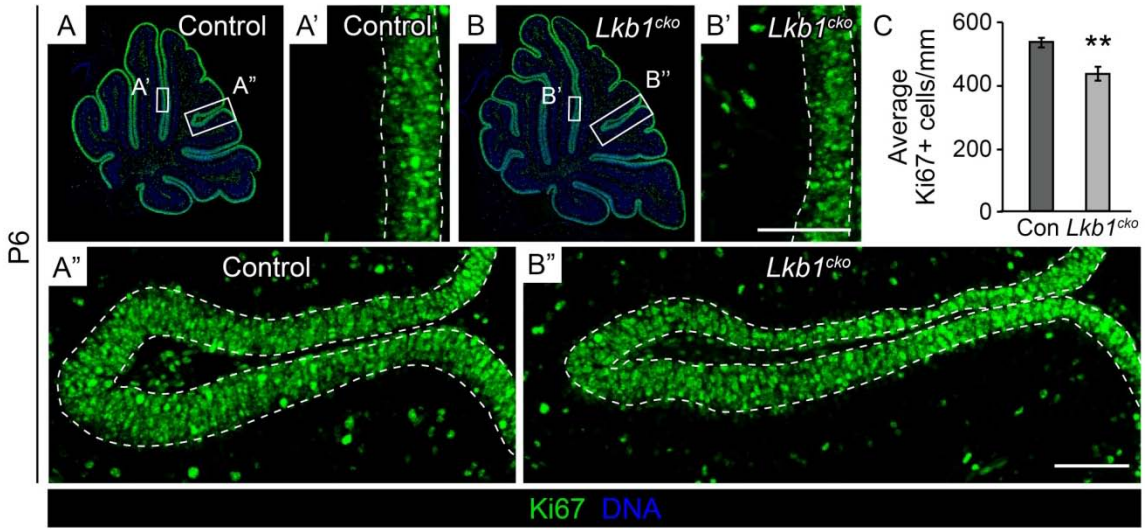

Figure 2.10. Loss of *Lkb1* from granule cell precursors results in a thinner outer EGL.
A-B. Representative Ki67-stained P6 control (A) and Lkb1^{cko} (B) cerebella. Dashed lines in A'-A" and B'-B" delimit outer EGL, where proliferative cells reside. Lkb1^{cko} have a visibly thinner layer of proliferative (Ki67+) GCPs than do littermate controls (compare A' to B', A'' to B''). C. Quantification of outer EGL thickness using Ki67+ cells per mm EGL. n=3, $p<0.001$, Student's paired t-test. Scalebar 50 µm. Con = control.

Lkb1 regulates the orientation of GCP divisions

The plane of cell division regulates surface area expansion and organ shape in a number of tissues, including the lung and epidermis (Ochoa-Espinosa and Affolter, 2012; Poulson and Lechler, 2010; Ray and Lechler, 2011). To determine if cortical expansion and increased foliation in *Lkb1*^{cko} were due to perturbations in spindle orientation, P2 control and *Lkb1*^{cko} cerebella were labeled with □agnific-histone H3 and Aurora B kinase to label mitotic DNA and spindle-associated microtubules, respectively (Figure 2.11A-B). These markers, together with a nuclear dye, were used to determine the plane of division relative to the cerebellar (pial) surface. While the majority of control GCPs divided perpendicularly, with an angle of division close to 0°, the distribution of division angles was nearly random in *Lkb1*^{cko} GCPs (Figure 2.11).

To further quantify changes in division orientation, the proportion of GCPs dividing perpendicular (0-30°), parallel (60-90°), or tangential (30-60°) to the cerebellar surface (Figure 2.11H) was determined across the entire EGL of P2 control and *Lkb1*^{cko} cerebella using Aurora B staining (Figure 2.11I). While the majority of control GCPs divided perpendicular to the cerebellar surface, the orientation of GCP division was randomly distributed in *Lkb1*^{cko} cerebella (control: 65%, 20% and 15%; *Lkb1*^{cko}: 36%, 23% and 42% for perpendicular, tangential and parallel divisions, Figure 2.11I). Consequently, *Lkb1*^{cko} had significantly more parallel divisions than controls and significantly fewer perpendicular GCP divisions (Figure 2.11I). Similar changes in division plane were observed when pH3 was used to determine the plane of division (data not shown).

To determine if changes in division plane persisted at P6, when foliation defects first arose but prior to the completion of foliation, P6 control and *Lkb1*^{cko} cerebella were

co-stained with pH3 and γ-tubulin to label mitotic DNA and centrosomes, respectively, or stained with Aurora B (Figure 2.11D-G). Similar to P2, the majority of control GCPs divided perpendicularly at P6, while *Lkb1*^{cko} had significantly more parallel divisions and significantly fewer perpendicular divisions (control: 52%, 24%, and 24%; *Lkb1*^{cko}: 33%, 25%, and 42% for perpendicular, tangential, and parallel divisions) (Figure 2.11I). However, at P11, when foliation patterns are largely established, no difference in division orientation between control and *Lkb1*^{cko} GCPs was observed (Figure 2.12). Together, these data indicate that *Lkb1* regulates the plane of GCP division when foliation patterns are being established.

Figure 2.11. Loss of *Lkb1* randomizes the plane of GCP division.

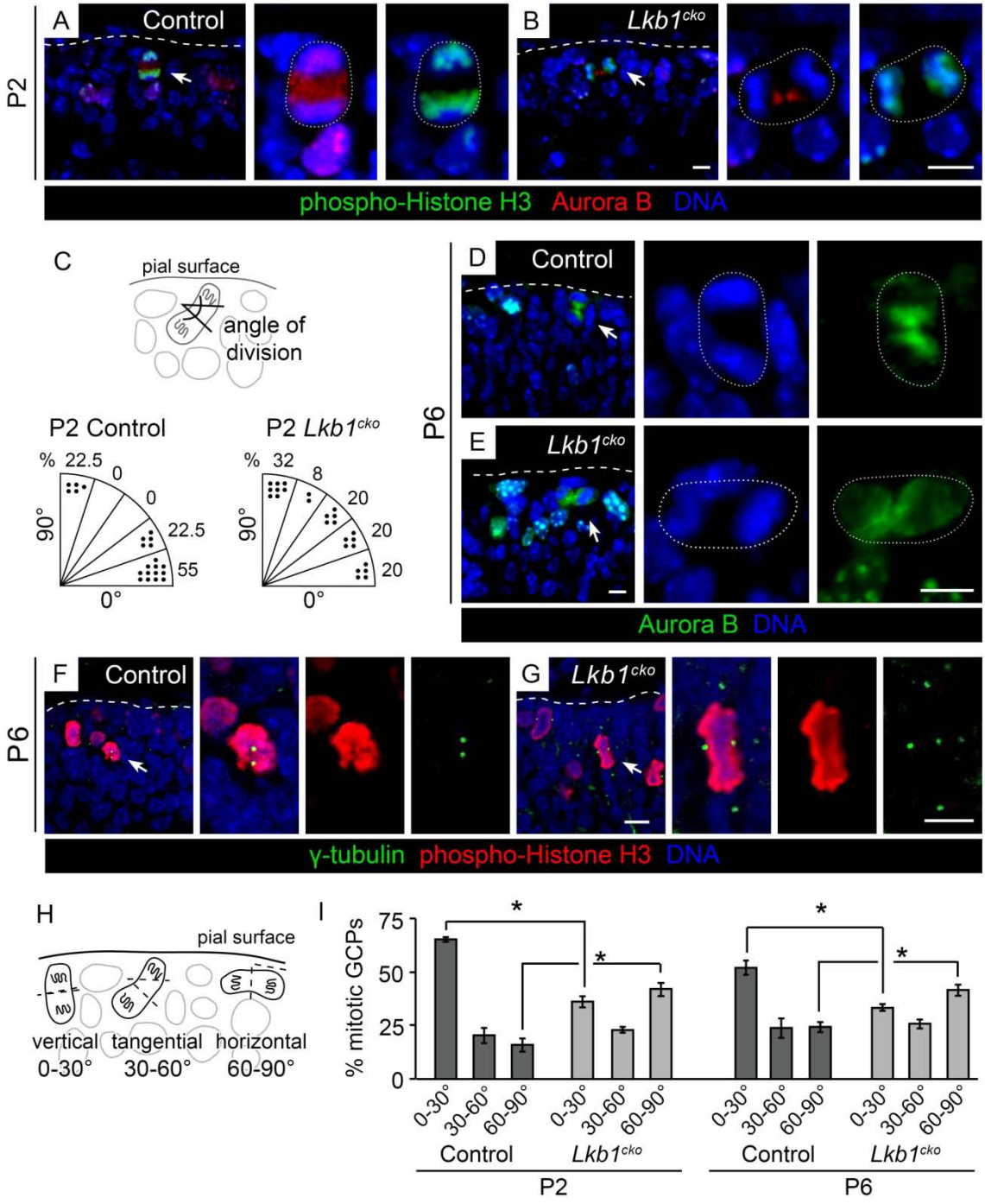

Figure 2.11. Loss of *Lkb1* randomizes the plane of GCP division.
A-B. Aurora B, □agnific-histone H3, and Dapi co-staining at postnatal day 2 (P2) labels mitotic DNA, spindle-associated microtubules and DNA, respectively. Dashed line denotes pial surface. Arrows indicate cells enlarged and encircled with dotted lines in neighboring panels. C. Distribution of GCP division angles at P2. Staining in A and B was used to determine the angle of cell division relative to the pial surface (see diagram). Whereas most control GCPs divided vertically (near 0º), the plane of Lkb1cko GCP divisions were distributed among each of five subdivisions. D-E. Aurora B was used to label spindle-associated microtubules of dividing cells in of control (D) and Lkb1cko (E) cerebella at P6. Sections were co-stained with Dapi to mark DNA. Dashed line follows pial surface. Arrows indicate cells enlarged and encircled with dotted lines in neighboring panels. F-G. Staining of P6 control (F) and Lkb1cko (G) cerebella for pH3 and γ-tubulin to mark mitotic DNA and centrosomes, respectively. Dashed lines denote pial surface. Arrows indicate cells enlarged in adjacent panels. H. Orientations of GCP divisions relative to cell surface. I. Quantification of GCP division orientation for control and Lkb1cko GCPs at indicated stages based on the diagram shown in H. n=3, *, $p<0.05$, Student's paired t-test. Scalebar 5 µm.

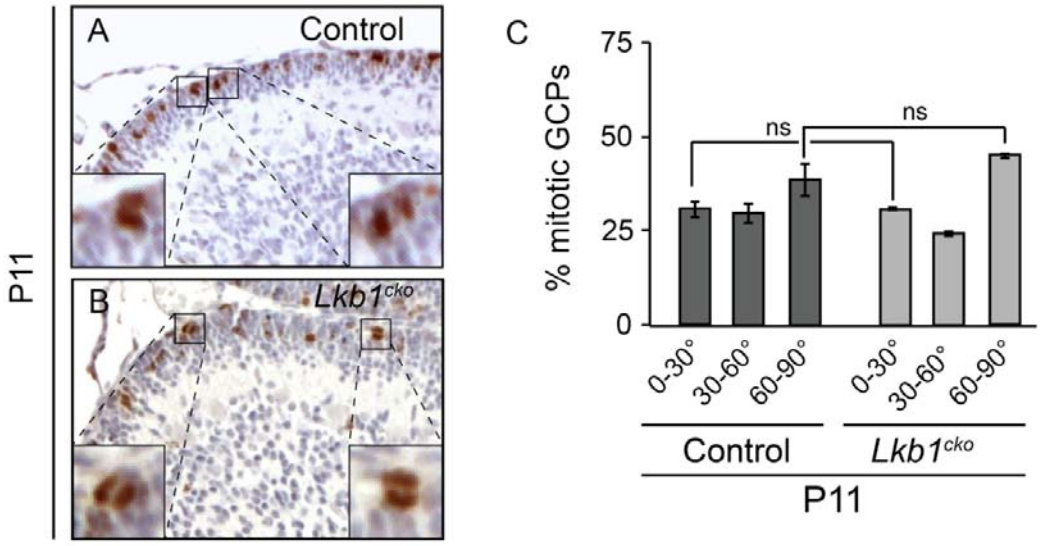

Figure 2.12. Orientation of GCP division at P11 is not altered in *Lkb1^{cko}* cerebella.
A-B. Representative staining of control (A) and Lkb1^{cko} (B) cerebella for □agnific-histone H3 (pH3) at P11 to mark mitotic cells. C. Quantification of the orientation of division for n=3 control and Lkb1^{cko} cerebella at P11 reveals no significant difference in the orientation of cell division relative to the cerebellar surface. N=3, p=ns, Student's paired t-test.

Lkb1 regulates foliation independent of mTOR and AMPK

Under conditions of energetic stress, Lkb1 activates the catalytic α subunits of AMPK via phosphorylation (Shackelford and Shaw, 2009). Activated AMPK inhibits processes that expend energy, including fatty acid synthesis and mTORC1 signaling, a key pathway involved in translation and cell growth (Shackelford and Shaw, 2009). AMPK inhibits mTOR signaling through phosphorylation of the TSC1/TSC2 complex. Accordingly, loss of *Lkb1, AMPK*, *TSC1*, or *TSC2* leads to hyperactivation of mTORC1 signaling (Huang and Manning, 2008). Aberrant mTORC1 activity has been linked to cerebellar abnormalities, as mice harboring a dominant-negative *TSC2* allele exhibit ectopic granule cells and increased GCP proliferation (Bhatia et al., 2009).

Staining of P6 cerebella for □agnific-S6 ribosomal protein, an established readout for mTORC1 pathway activation (Carson et al., 2012), revealed mTORC1 pathway upregulation in $Lkb1^{cko}$ (Figure 2.13A-B). Increased p-S6 levels in $Lkb1^{cko}$ were seen by Western blot (Figure 2.13C). Increased mTORC1 signaling in $Lkb1^{cko}$ likely resulted from reduced AMPK activity, as both AMPK phosphorylation and phosphorylation of the AMPK substrate acetyl co-A carboxylase (ACC) were reduced in $Lkb1^{cko}$ GCPs (Figure 2.13D). Together, these data suggest that loss of *Lkb1* reduced AMPK activity and increased mTOR signaling in GCPs.

To determine if the defects in foliation in $Lkb1^{cko}$ resulted from mTOR pathway upregulation, we generated *Math1-cre*; $TSC1^{flox/-}$ mice (hereafter referred to as $TSC1^{cko}$). Western blotting of GCPs and immunostaining P8 cerebella for p-S6 revealed increased mTOR signaling in $TSC1^{cko}$ (Figure 2.13E-G, Figure 2.14). However, foliation patterns were normal in $TSC1^{cko}$ mutants at P14 and P60 (Figure 2.13, Figure 2.14). Notably, in contrast *TSC2* dominant-negative mice (Bhatia et al., 2009), we did not observe

changes in cerebellar morphology or ectopic granule cell clusters in adult *TSC1*^{cko} (Figure 2.13). Together, these data indicated that mTORC1 signaling was not responsible for increased foliation in *Lkb1*^{cko}.

Figure 2.13. Increased foliation and altered migration in *Lkb1^{cko}* cerebella are mTOR- and AMPK-independent.

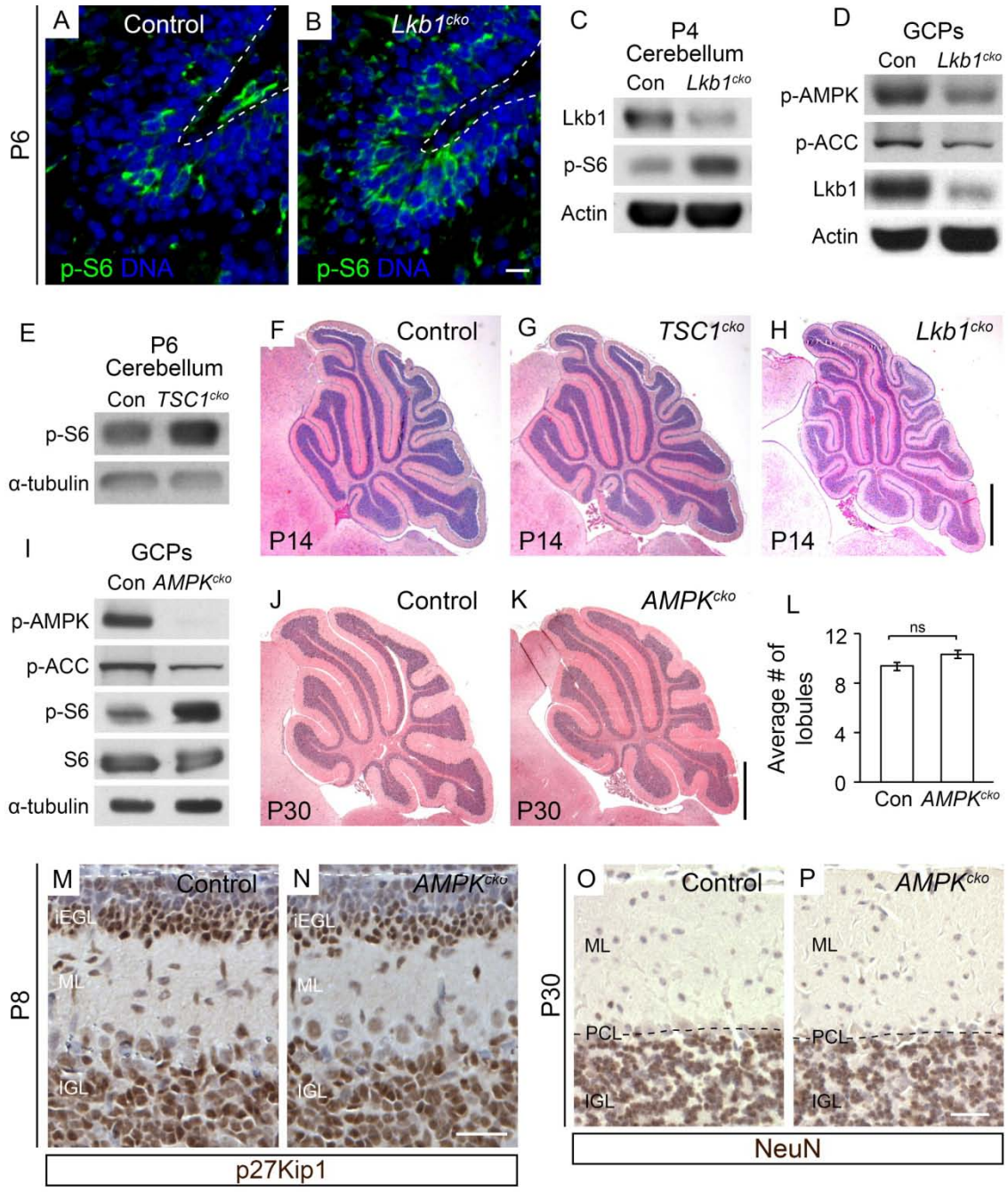

Figure 2.13. Increased foliation and altered migration in *Lkb1^{cko}* cerebella are mTOR- and AMPK-independent.

A-B. Representative staining for the mTOR target phosphorylated S6 ribosomal protein (p-S6) in control (A) and Lkb1^{cko} (B) cerebella at P6. Scalebar 10 µm. C. Western blotting of whole postnatal day 4 cerebella reveals that p-S6 is increased in Lkb1^{cko}. Blotting for Lkb1 and Actin was used to verify knockdown and loading, respectively. D. Western blotting of GCPs isolated from control or Lkb1^{cko} cerebella indicates that AMPK phosphorylation (Thr172) is reduced in the absence of Lkb1. Phosphorylation (Ser79) of Acetyl-CoA Carboxylase (ACC), a direct target of AMPK, is also lower in Lkb1^{cko} GCPs. Lkb1 and Actin were used to verify knockdown and loading, respectively. E. Western blot for p-S6 in control and Math1-cre; TSC1$^{fl/-}$ (TSC1^{cko}) cerebella reveals that loss of TSC1 leads to increased mTOR signaling activity. F-H. Hematoxylin and eosin staining of mid-vermal cross sections of P14 control (F), TSC1^{cko} (G), and Lkb1^{cko} (H) cerebella. Scalebar 500 µm. I. Western blot for AMPK substrates and mTOR activity in control and Math1-cre; AMPKa1$^{-/-}$; AMPKa2$^{fl/fl}$ (AMPK^{cko}) GCPs. p-AMPK and α-tubulin serve as controls for knockdown and loading, respectively. J-K. Hematoxylin and eosin staining of control (J) and AMPK^{cko} (K) mid-vermal sections at P30. Scalebar 500 µm. L. Quantification of lobule number at P30 for control and AMPK^{cko}. n=3, no significant difference, Student's paired t-test. M-N. Representative staining for p27Kip1, a marker of post-mitotic granule cells, in control (M) and AMPK^{cko} (N) cerebella at P8 indicates that migration is not altered in the absence of catalytic AMPK signaling. Dashed line denotes pial surface. Scalebar 50 µm. O-P. Representative Neuron-specific nuclear protein (NeuN) staining of control (O) and AMPK^{cko} (P) cerebella at P30. Dashed line demarcates Purkinje cell layer. All granule cells appear to have migrated past the Purkinje cell layer in AMPK^{cko}. Scalebar 50 µm. iEGL = inner external granule layer, ML = molecular layer, PCL = Purkinje cell layer, IGL = internal granule layer. Con = control.

AMPK signaling has previously been shown to play a critical role in cerebellar development (Dasgupta and Milbrandt, 2009). Additionally, phosphorylated AMPK localizes to centrosomes during mitosis in cultured mammalian cells (Vazquez-Martin et al., 2009). Indeed, p-AMPK co-localized with the centrosome marker γ-tubulin in GCPs of the oEGL and diffusely labeled the iEGL (Figure 2.15). However, the persistence of centrosome-associated p-AMPK in *Lkb1*^{cko} suggested that phosphorylation of centrosome-associated AMPK was Lkb1-independent (Figure 2.15). Nonetheless, we generated a conditional knockout for the two catalytic subunits of AMPK (*Math1-cre; AMPKα1*$^{-/-}$*; AMPKα2*$^{fl/fl}$ mice; *AMPK*^{cko}). Western blotting revealed a significant reduction in both p-AMPK and p-ACC in *AMPK*^{cko} GCPs, indicating AMPK signaling was reduced (Figure 2.13I). Histological staining revealed that *AMPK*^{cko} cerebella appeared grossly normal and did not exhibit changes in foliation (Figure 2.13K-L). Thus, although AMPK is a substrate of Lkb1 in GCPs, altered AMPK signaling is not responsible for defects in foliation observed in *Lkb1*^{cko} cerebella.

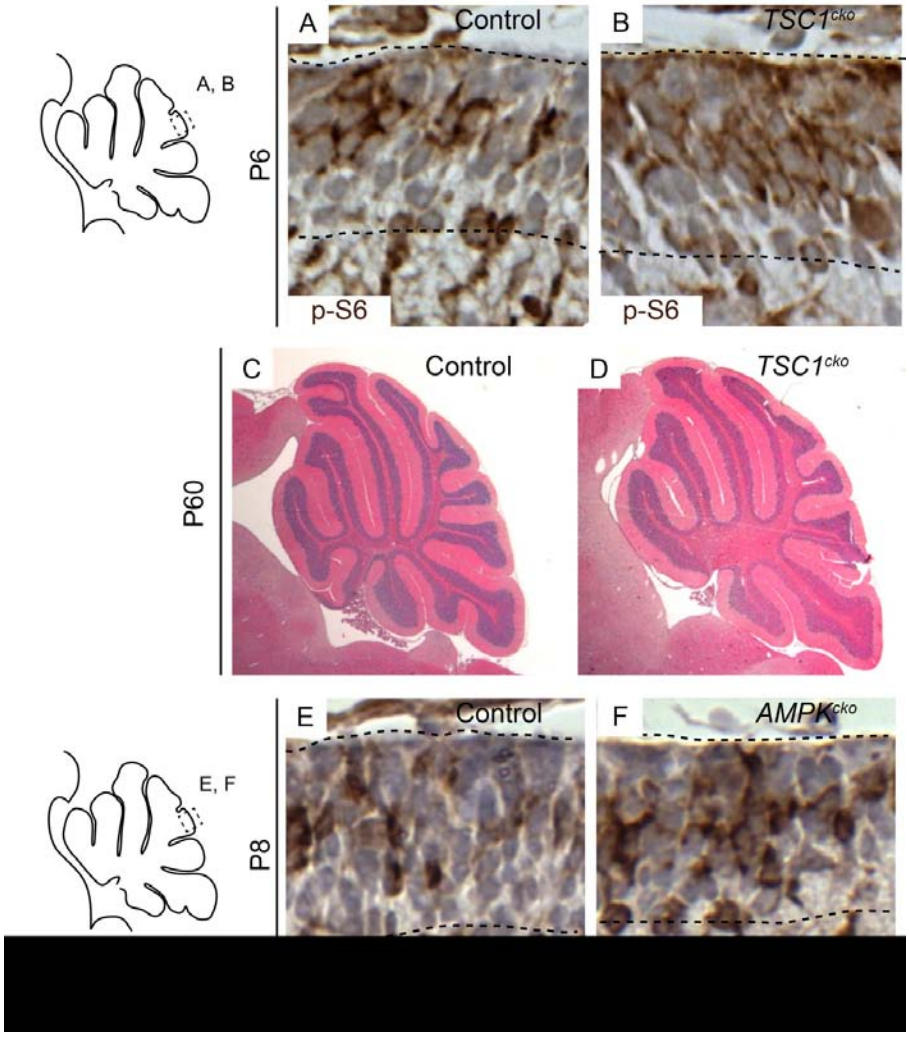

Figure 2.14. Additional images and □agnific-S6 ribosomal protein staining of *TSC1^{cko}* and *AMPK^{cko}*.

A-B. Phosphorylated s6 (p-S6) ribosomal protein staining of P6 control (A) and TSC1^{cko} (B) cerebella reveals that p-S6 is upregulated in TSC1^{cko}. C-D. Hematoxylin and eosin staining of P60 control and TSC1^{cko} cerebella reveals that TSC1^{cko} cerebella develop normally. E-F. p-S6 staining of P8 control (E) and AMPK^{cko} (F) cerebella reveals that p-S6 is upregulated in AMPK^{cko}. Dashed lines denote EGL boundaries.

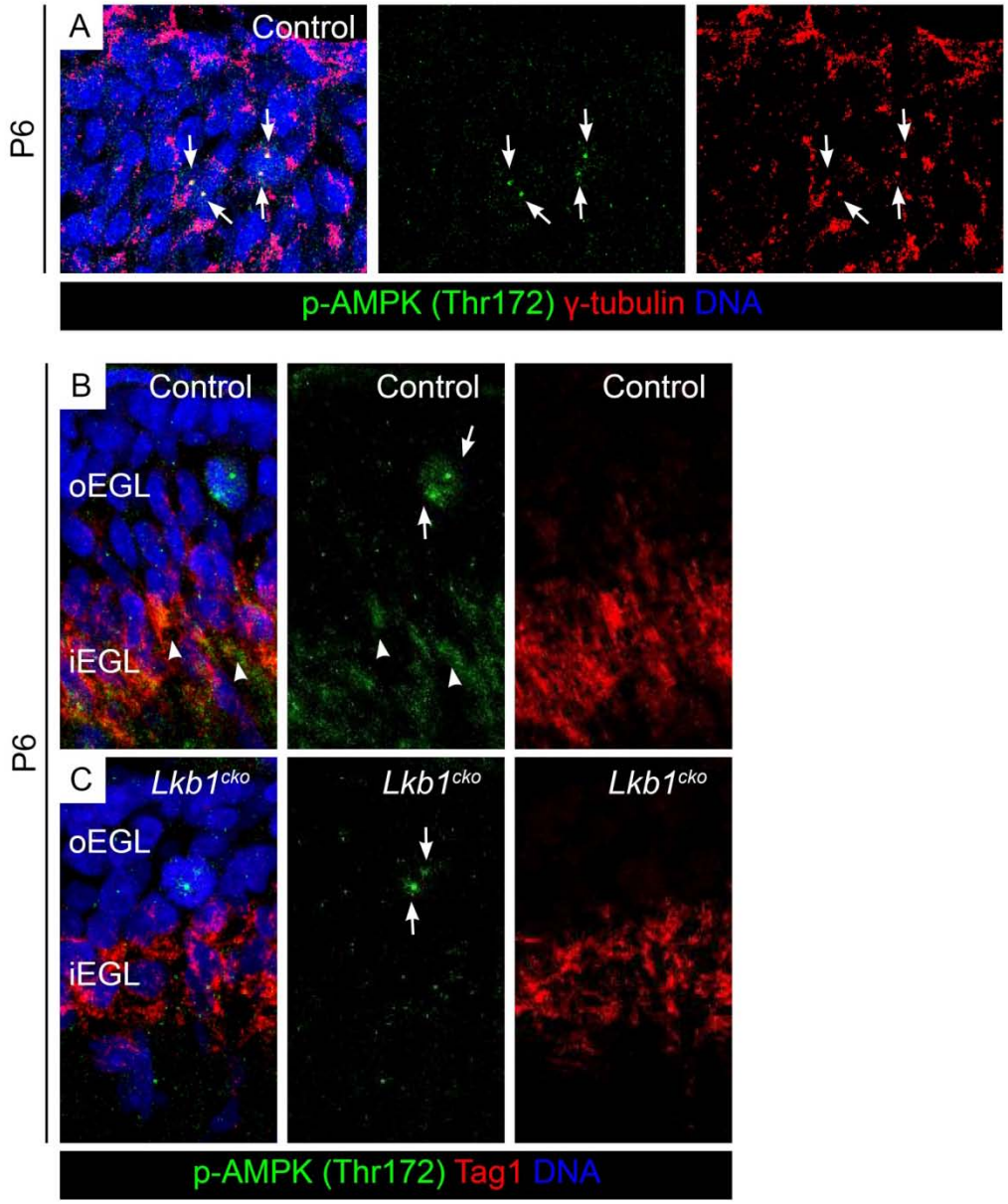

Figure 2.15. Phosphorylated AMPK (Thr172) staining of control and *Lkb1^{cko}*.
A. p-AMPK/γ-tubulin co-staining reveals that p-AMPK localizes to centrosomes of dividing GCPs. B-C. p-AMPK/tag1 co-staining of control (B) and Lkb1^{cko} (C) cerebella at P6 reveals that although centrosome-localized p-AMPK staining is maintained in the absence of Lkb1, inner-EGL localized p-AMPK staining is lost. For all images, arrows indicate centrosomes, arrowheads indicate inner EGL staining. oEGL = outer EGL, iEGL = inner EGL.

Discussion

Our data suggest that Lkb1 regulates cortical size and foliation in the developing cerebellum by controlling the orientation of mitotic neural precursor divisions. Whereas the majority of control GCPs divided perpendicular to the cerebellar surface, loss of *Lkb1* randomized the orientation of GCP divisions, increasing the proportion of cells dividing parallel to the cerebellar surface. We propose that increased parallel divisions in *Lkb1*^{cko} expanded cerebellar cortical area by positioning daughter cells next to one another, similar to surface area expansion in the developing epidermis (Figure 2.16) (Ray and Lechler, 2011). Accordingly, we find that the outer EGL, where proliferative GCPs reside, is larger and thinner in *Lkb1*^{cko} compared to controls. Indeed, expansion of the EGL in *Lkb1*^{cko} is likely responsible for increasing cerebellar size at developmental stages (P2-P14). However, perhaps due to ossification of the overlying skull and/or the inward migration of GCPs, this difference in cerebellar size does not persist at adult (P30) stages. Nonetheless, cortical expansion resulted in a significant increase in foliation: *Lkb1*^{cko} mice had on average 4.5 additional lobules than controls, a nearly 40% increase in foliation. To our knowledge, this is the first example of a mutation that increases foliation in the absence of altered GCP proliferative capacity. As such, we propose that oriented cell divisions serve as a novel mechanism for controlling surface area and folding in the cerebellum.

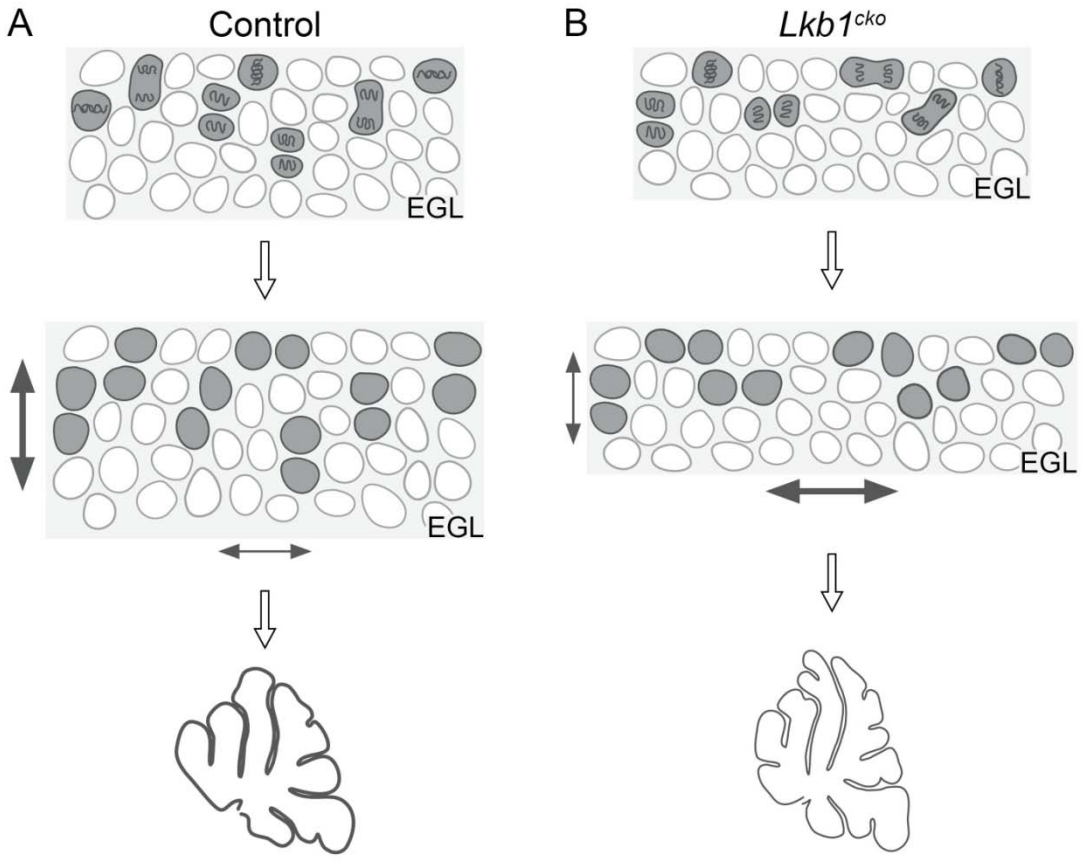

Figure 2.16. Model for cortical expansion and increased foliation in *Lkb1^{cko}*.
A. In the control postnatal cerebellum EGL thickness is maintained by predominantly vertical divisions, which result in daughter cells positioned on top of one another. B. In the Lkb1^{cko} cerebellum, perturbations in the orientation of GCP divisions leads to a substantial increase in horizontally dividing GCPs, resulting in a thinner EGL that is expanded in size.

Surprisingly, we find that Lkb1 controls cerebellar foliation independently of its well-studied downstream target AMPK. AMPK is a heterotrimeric complex consisting of α, β, and γ subunits, all of which are thought to be required for catalytic activity (Hardie, 2004). In contrast to a previous study demonstrating that genome-wide loss of AMPKβ1 using a gene-trap approach led to cerebellar hypoplasia, reduced granule cell number, and disorganized laminar architecture (Dasgupta and Milbrandt, 2009), we find that the cerebellum develops normally in mice harboring GCP-specific deletion of AMPKα1 and AMPKα2. The neuronal defects described in gene-trap-generated AMPKβ1 mutants may be attributed to toxicity from the formation of a C-terminally truncated AMPKβ1 fused to β-galactosidase, as others (Williams et al., 2011) have suggested, given that loss of AMPKβ1 by conventional methods of gene targeting does not disrupt cerebellar development (Dzamko et al., 2010). However, it remains a possibility that proper cerebellar patterning and growth requires AMPK signaling in cells outside of the granule cell lineage.

Of the remaining 12 known substrates of Lkb1, we speculate that the microtubule affinity related kinase (MARK) Par1b may regulate GCP spindle orientation downstream of Lkb1. Par1b regulates neuronal migration in the neocortex (Sapir et al., 2008) and controls spindle orientation in cultured epithelial and hepatic cells by determining the localization of the G-protein regulator LGN, a key determinant of spindle orientation (Lazaro-Dieguez et al., 2013; Slim et al., 2013). Alternatively, Lkb1 may control GCP polarity through regulation of the actin cytoskeleton, as it does in other cell types (Xu et al., 2010; Zhang et al., 2008). Interestingly, Lkb1 was recently shown to regulate epithelial cell polarity under different confinement conditions by controlling cortical actin contractility (Rodriguez-Fraticelli et al., 2012). In particular, while cells grown at low

confinement oriented their nuclei away from the central lumen, loss of Lkb1 caused nuclei to move toward the lumen, similar to cells grown at high confinement (Rodriguez-Fraticelli et al., 2012). It is possible that Lkb1 functions in a similar manner in the cerebellum – sensing space constraints and orienting divisions accordingly to limit cortical expansion and ensure that the cerebellum does not grow beyond the size of its "container".

We find that most GCPs divide perpendicular to the cerebellar surface, which could hypothetically promote cell cycle exit and differentiation by positioning one daughter cell in iEGL, where a host of differentiation-promoting factors reside (Choi et al., 2005; Xenaki et al., 2011). If this were the case, reducing perpendicular divisions would reduce GCP cell cycle exit, increase the proportion of proliferating cells, and decrease the proportion of differentiating GCPs. However, although loss of *Lkb1* decreased the proportion of perpendicular divisions, neither cell cycle exit nor differentiation were altered in *Lkb1*^{cko} cerebella, suggesting that the plane of cell division, at least to the extent that it is controlled by Lkb1, does not regulate asymmetric cell division or cell fate in the EGL. Rather, our data indicate that Lkb1 functions chiefly to control the size and pattern of the cerebellar cortex, likely by orienting GCP divisions.

Cortical folding, whether gyrification in the neocortex or foliation in the cerebellum, is a complex process involving cell proliferation, migration, differentiation and neuronal connectivity (Sun and Hevner, 2014). In the gyrencephalic neocortex of humans and some mammals, cortical folding has been attributed to outer radial glial (oRG), a population of radial glia that are largely absent in mice and other smooth-brained (lissencephalic) species (Borrell and Gotz, 2014). In the cerebellum, cortical folding has been attributed to the postnatal expansion the EGL, and differences in the

degree of cerebellar foliation have historically been credited to differences in GCP number or to a protracted period of GCP proliferation and maturation (Altman and Bayer, 1997; Sillitoe and Joyner, 2007). However, not all mutations that increase GCP proliferation or number are sufficient to increase foliation, even when the overall size and surface area of the cerebellum are larger (Miyazawa et al., 2000; Tanori et al., 2010). The non-linear relationship between GCP number and foliation might be rooted in the need to maintain an optimal EGL thickness in order for folding to occur. Indeed, many mutations that increase GCP proliferation lead to EGL hyperplasia as well as loss of foliation (Cheng et al., 2012; Dey et al., 2012; Miyazawa et al., 2000; Schwartz et al., 1997). Perhaps the most dramatic example of EGL hyperplasia is seen in mouse models of medulloblastoma, in which foliation is lost or completely absent (Cheng et al., 2012; Dey et al., 2012). A thicker EGL may therefore inhibit folding by increasing surface tension and the force required to deform the cerebellar surface, the first described step in fissure formation (Sudarov and Joyner, 2007). By contrast, when *Lkb1* is deleted from GCPs, proliferation is unaffected, but increased parallel divisions cause the EGL to expand, becoming thinner and more receptive to folding.

Emerging evidence suggests that the neocortex and cerebellum likely co-evolved, as neocortical and cerebellar surface area are tightly correlated (Sultan, 2002), and pre-frontal projecting cerebellar lobules are significantly larger than motor cortex-projecting lobules in humans when compared to other primates (Balsters et al., 2010). Interestingly, a recent study of the developing human neocortex demonstrated that horizontally-oriented radial glia divisions give rise to oRG, which are believed to be responsible for increased gyrification in the human neocortex (LaMonica et al., 2013). We find that changes in the orientation of GCP division increased cortical area and

folding in the cerebellum, suggesting that regulation of mitotic spindle orientation may serve as a unifying mechanism for increasing cortical area and folding throughout the brain.

Acknowledgements

We are grateful to Kevin Ess and Eric Armour for providing the *TSC1*$^{flox/flox}$ mice and to David Rowitch for providing the *Math1-cre* mice. We are also grateful to Yongliang Huo for his assistance with Lkb1 immunohistochemistry. We thank Joe Roland of the Digital Histology Shared Resource for his assistance with Cell Profiler, and Sean Schaffer at the Vanderbilt University Cell Imaging Shared Resource for use of the confocal microscope. We are grateful to Laura Lee and Ian Macara for their careful reading and assistance preparing the manuscript. This work was supported by American Heart Association (AHA) pre-doctoral fellowship (K.E.R.), Vanderbilt-Ingram Cancer Center Support Grant P30 CA068485 (C.C.), and National Institutes of Health NS 042205 (C.C.).

CHAPTER III. LKB1 REGULATES RADIAL MIGRATION OF GRANULE CELLS IN THE DEVELOPING CEREBELLUM

Introduction

Cell migration is a tightly regulated component of proper development throughout the embryo. In the developing nervous system, neuronal migrations are broadly characterized as either tangential or radial. Tangential migrations occur in a direction perpendicular to radial glial fibers, whereas radial migrations occur parallel to radial glia and utilizes a glial scaffold for guidance and support. Radial migration is seen broadly during CNS development, both in the developing forebrain during neocortical layer formation, as well in the pre- and postnatal cerebellum. In the embryonic cerebellum, *Ptfa1*-expressing ventricular zone-derivatives, including Purkinje cell progenitors and interneuron progenitors, migrate along radial glia to reach their destination within the cerebellar anlage (Morales and Hatten, 2006). Postnatally, granule cell precursors (GCPs) migrate along Bergmann glia, a specialized subtype of cerebellar glia that expresses many radial glial markers, to reach the internal granule layer (IGL). The abundance of GCPs in the developing cerebellum and the capacity to culture cerebellar cell types in a variety of ways (eg, glial-GCP co-cultures and slice cultures) make the cerebellum a particularly attractive model in which to study radial migration. As such, much of what we know about radial migration stems from studies in the cerebellum.

The maturation of cerebellar GCPs occurs in an outward-to-inward fashion. The most immature GCPs proliferate in a Shh-dependent fashion in the outer EGL (oEGL). Eventually, in response to as-yet determined intrinsic and/or extrinsic factors, GCPs exit the cell cycle and move into the inner EGL (iEGL). Within the iEGL, GCPs elaborate two

short fibers parallel to the pial surface, aptly named parallel fibers, which function as granule cell axons. Parallel fiber formation is coupled to centrosome position, with the centrosome determining the site of parallel fiber formation (Renaud et al., 2008). Amidst parallel fiber formation, GCPs migrate tangentially within the iEGL; however, the function of such tangential migration is not well understood (Komuro et al., 2001). After parallel fibers have formed, the GCP begins to elaborate a third process in the direction orthogonal to the pial surface, which acts as a leading process to direct the GCP along Bergman glial fibers to the IGL (Komuro et al., 2001). Again, the centrosome determines the location of the developing leading process (Renaud et al., 2008). The leading process is thought to guide the maturing GCP down Bergman glia to ultimately reach the internal granule layer (IGL).

Determinants of GCP radial migration can be broadly classified into three categories: 1) adhesion molecules such as Astrotactin and JAM-C; 2) cytoskeletal and polarity proteins including Pard3, Par6α, Semaphorin-6A, Plexin-2B, and the actomyosin cytoskeleton; and 3) neurotrophic growth factors such as BDNF and its receptor TrkB. Although there is significant cross-talk between molecules in each of these categories, a complete picture of how granule cell migration is regulated in vivo is still being painted.

The cell adhesion molecules Astrotactin 1 (Astn1) was among the first molecules identified to regulate granule cell migration (Edmondson et al., 1988; Fishell and Hatten, 1991; Stitt and Hatten, 1990). Recently, a second astrotactin, Astn2, was identified as a mediator of granule cell migration in the cerebellum (Wilson et al., 2010). Astn2 regulates Astn1 surface levels in a dynein-dependent manner, suggesting that Astn1 trafficking may be important during neuronal migration (Wilson et al., 2010). Indeed, live imaging of venus-tagged Astn1 and Astn2 revealed that Astn-based adhesions are

highly dynamic, requiring clathrin-mediated endocytosis for their removal from the cell surface, which permits the migrating granule cell to glide forward along the glial fiber (Wilson et al., 2010). Like Astn1, the adhesion protein JAM-C is also required for granule cell migration. Cell surface levels of JAM-C are modulated by the polarity protein Pard3 (Famulski et al., 2010). Pard3 levels are low within the outer EGL due to SIAH-mediated ubiquitylation; however, in the inner EGL, Pard3 levels increase, permitting JAM-C levels to accumulate on the surface of granule cells. Consequently, loss of SIAH or Pard3 overexpression increases GCP migration out of the EGL (Famulski et al., 2010). Thus, cell adhesion is important for EGL exit as well as radial migration during cerebellar development.

In addition to Pard3, a second PAR protein, Par6α, regulates GCP migration (Solecki et al., 2004). Rather than controlling the surface expression of cell adhesion molecules, Par6α localizes to the centrosome, where it appears to regulate the tubulin cytoskeleton. Accordingly, overexpression of Par6α disrupts perinuclear tubulin cage formation, which is thought to play a role in coordinating movement of the nucleus with the leading process, as well as causes mislocalization of many centrosome-associated proteins (Solecki et al., 2004). Consequently, Par6α overexpression diminishes GCP migration (Solecki et al., 2004). Whether Par3 and Par6 form a complex in migrating GCPs, as they do in epithelial cells, remains to be determined. Like Par6α, the transmembrane Semaphorin Sema6A and its receptor Plexin-A2 control GCP migration by regulating centrosome position (Kerjan et al., 2005; Renaud et al., 2008; Tawarayama et al., 2010). Sema6A and Plexin-A2 act cell autonomously in GCPs, where they coordinate the transition from tangential to radial migration (Renaud et al., 2008). Although parallel fibers form normally in mice lacking Sema6A or Plexin-A2,

radial migration is impaired, leading to an accumulation of GCPs in the molecular layer (Renaud et al., 2008). Together, these studies indicate that centrosome position is tightly regulated in cerebellar GCPs and is critical for proper migration out of the EGL and along Bergmann glia.

In addition to the tubulin-based centrosome and nuclear cage, the actomyosin cytoskeleton controls granule cell migration by pulling the nucleus forward toward the leading process (Solecki et al., 2009). Live imaging of migrating GCPs in vitro demonstrates that active myosin is present ahead of the nucleus, within the leading process, and that actin fibers flow toward the leading process (Solecki et al., 2009). Accordingly, inhibiting actin or myosin disrupts granule cell migration (Solecki et al., 2004) and polarization (Zmuda and Rivas, 2000). Rho GTPases are key regulators of the actin and microtubule cytoskeletons (Govek et al., 2011), and the Rho family member Rac1 has been implicated in regulating GCP migration in the developing cerebellum (Tahirovic et al., 2010; Zhou et al., 2007). Rac1 regulates actin dynamics via the PAK-cofilin pathway and the WAVE-Arp2/3 pathway, and loss of Rac1 in GCPs lead to mislocalization of the WAVE complex in cultured GCPs (Tahirovic et al., 2010), suggesting a role for the Rac1-WAVE-Arp2/3-Actin axis during granule cell migration.

Throughout the developing nervous system, neurotrophins act as growth factors that promote the survival of neurons as well as influence axonogenesis and migration. Loss of the neurotrophin brain-derived neurotrophic factor (BDNF) impairs GCP radial migration, leading to an accumulation of GCPs in the EGL (Borghesani et al., 2002; Schwartz et al., 1997). BDNF is secreted by granule cells in the IGL as well as GCPs in the EGL, and TrkB, the BDNF receptor, is seen in the leading process of migrating GCPs (Zhou et al., 2007). Interestingly, the polarized endocytosis of BDNF by GCPs

requires Rac1 and the guanine nucleotide exchange factor Tiam1 (Zhou et al., 2007), further implicating a role for Rac1 in radial migration. Additionally, the endocytic regulator Numb was shown to regulate TrkB activity and localization to promote BDNF-dependent GCP migration (Zhou et al., 2011).

The importance of Lkb1 in radial migration is somewhat contentious. Whereas one study found that Lkb1 was dispensable for the migration of dorsal telencephalic neurons (Barnes et al., 2007), a subsequent study found that Lkb1 regulates neuronal migration in an APC- and GSK3β-dependent manner, and the contribution of Lkb1 in radial migration remains uncertain (Asada and Sanada, 2010; Asada et al., 2007). *Interestingly, we find that Lkb1 regulates the timely migration of granule cell precursors in vivo during cerebellar development. Lkb1 regulates GCP migration independent of its well-characterized substrate AMPK. Lkb1-deficient GCPs were able to polarize normally in vitro, indicating that loss of polarity unlikely to be responsible for altered migration. Additionally, loss of Lkb1 did not disrupt the distribution of N-Cadherin, an adhesion molecule known to regulate neuronal migration in other regions of the brain.*

Experimental Procedures

Mice. All experiments were performed using young neonatal and adult animals (ages P2-P30), according to regulation of the NIH and VUMC Division of Animal Care. *Lkb1fl/fl* mice (Nakada et al., 2010), and *Sox2-cre* mice (Hayashi et al., 2002) were obtained from Jackson laboratories. *Math1-cre* mice (Schuller et al., 2007) were kindly donated from David Rowitch (UCSF). BrdU (Roche) was dissolved in PBS to a final concentration of 10 mg/ml and administered by intraperitoneal injection.

Immunohistochemistry. Tissue was collected and processed as described previously (Fleming et al., 2013). Paraffin sections underwent antigen-retrieval using Citrate Buffer pH=6.0.

P8 Migration Quantification. Animals were injected with BrdU at P5 (2 injections 1 hour apart) and collected 3 days later at P8. Paraffin sections were co-stained with BrdU and Ki67 and scanned through the Vanderbilt DHSR. Cell Profiler was used to determine the number of cells in each of three regions: the Ki67+ outer EGL, the nuclei-dense IGL, and the region between the oEGL and IGL (iEGL/ML) within the region shown in Figure 3.2. The proportion of cells in each region was determined for n=3 controls and n=5 *Lkb1*^{cko}, and these values were compared using a Student's unpaired t-test in Excel.

Antibodies. The following antibodies were used for immunohistochemistry: p27Kip1 (BD Biosciences, 1:300), Tag1 (Hybridoma Bank, 1:10), γ-tubulin (Sigma, 1:300), BrdU (Hybridoma Bank, 1:100), Ki67 (Thermo Scientific, 1:200), β III-Tubulin (Sigma, 1:500)

EGL Explant Cultures. EGL explant cultures were prepared as described in Kullmann et al. (Kullmann et al., 2012). Briefly, the cerebellum from P3-P6 mice was dissected and meninges were removed. Sagittal sections were made using a razor blade. Core white matter material was dissected away, leaving a ribbon of EGL, which was minced into ~300 μm pieces and plated onto poly-L-lysine and laminin co-coated dishes.

In vitro GCP polarization. GCPs were isolated from control (non-labeled), *Math1-cre; Ai9* and *Lkb1*^{cko}*; Ai9* animals as previously described (Parathath et al., 2008). Briefly,

cerebella were isolated from P4-P6 mice in Hanks buffered saline solution (HBSS) (Gibco) supplemented with glucose. Meninges were removed and cerebella were treated with Trypsin-EDTA. Cerebella were dissociated, large cells were allowed to settle, and GCP-containing supernatants were moved to a fresh tube. Approximately 6000 labeled (that is, using the *Ai9* reporter) were plated on poly-ornithine coated coverslips on a bed of control (non-labeled) control cells. After 1, 2, 3, or 4 days in culture (in absence of Hh pathway stimulation and in the presence of 10% FBS to promote differentiation), coverslips were collected, fixed, and counterstained with Dapi, and imaged using direct fluorescence from the tomato fluorophore.

Results

Granule cell precursor-specific loss of *Lkb1* impairs radial migration *in vivo*

After exiting the cell cycle, differentiating granule cell precursors migrate through the molecular layer along Bergmann glia to eventually reach the internal granule layer (IGL). Upon examining P7 control and $Lkb1^{cko}$ sections stained for p27Kip1, a marker of post-mitotic granule cell precursors, we noted that $Lkb1^{cko}$ had significantly more p27Kip1+ cells in the molecular layer than controls, suggesting that $Lkb1^{cko}$ might have defects in granule cell migration (Figure 3.1). Because p27Kip1 labels not only granule cells but molecular layer-residing interneurons as well, we stained P8 sections with the granule cell specific antibody Neuron Specific Nuclear Protein (NeuN), revealing that the ectopic cells seen with p27Kip1 staining were, indeed, granule cells (Figure 3.1)

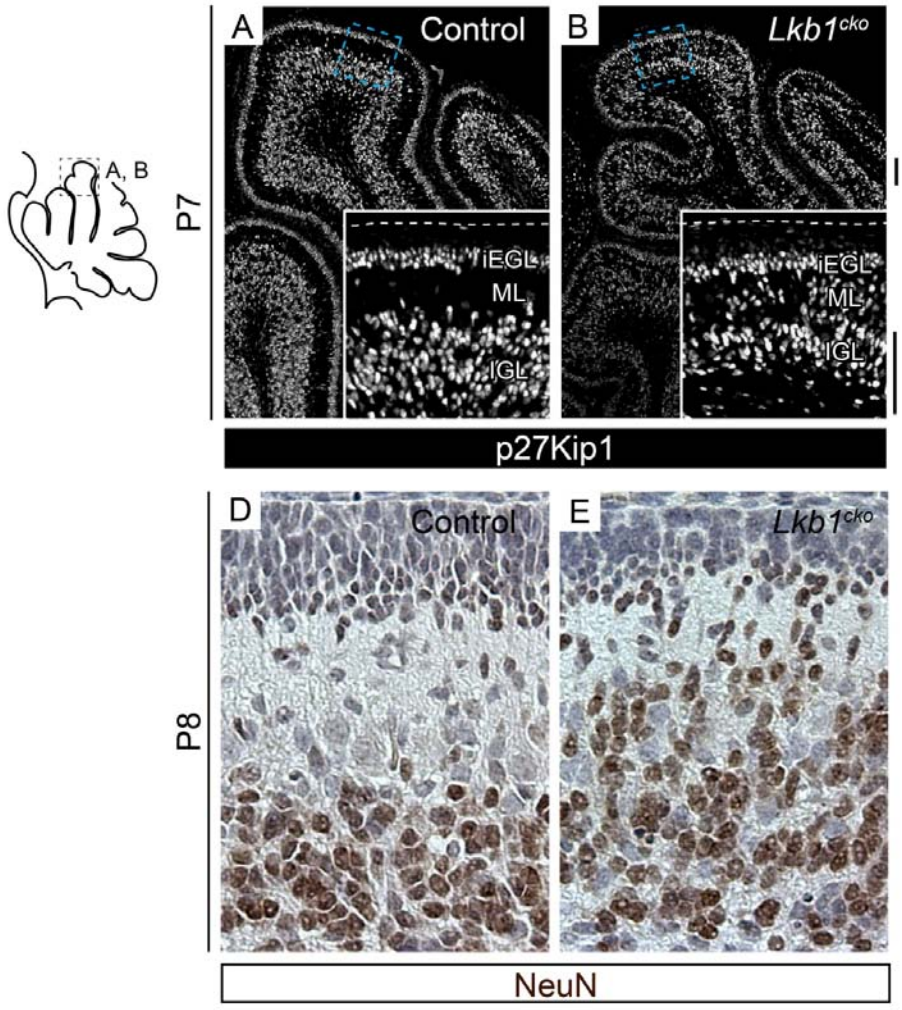

Figure 3.1. *Loss of Lkb1* leads to an accumulation of granule cells in the molecular layer.

A-B. p27Kip1 immunostaining labels post-mitotic GCPs in P7 control (A) and Lkb1^{cko} (B) cerebella. Dashed line in inset denotes cerebellar surface. Note the accumulation of GCPs in the molecular layer of Lkb1^{cko}. D-E. Neuron-specific nuclear protein (NeuN) staining to label postmitotic granule cells. Similar to p27Kip1 staining, Lkb1^{cko} have an increase in the number of NeuN-labeled cells between the EGL and the IGL. Scalebars 50 µm. iEGL = inner external granule layer, ML = molecular layer, IGL = internal granule layer.

A long-term BrdU labeling approach was used to verify that migration was impaired in *Lkb1*^{cko}. Control and *Lkb1*^{cko} pups were injected at P5, when proliferation is at its peak, and tissue was collected three days later at P8 (Figure 3.2). Given that GCPs are continually exiting the cell cycle and undergoing migration, we anticipated that many BrdU-labeled cells would have exited the EGL and begun to migrate to the IGL by this stage. Indeed, BrdU labeled cells formed tight bands corresponding to the outer EGL and IGL in control animals (Figure 3.2). By contrast, BrdU labeled cells in *Lkb1*^{cko} were evenly distributed between all cortical layers (Figure 3.2). Because defects in migration made it difficult to determine the boundaries of the entire EGL, sections were co-stained with Ki67 to define the boundaries of the oEGL, and the proportion of BrdU+ cells in the oEGL, IGL, and region between these two areas (iEGL +ML) was determined. *Lkb1*^{cko} had significantly more BrdU+ cells undergoing migration and significantly fewer BrdU+ cells in the IGL compared to controls, consistent with defects in radial migration (Figure 3.2).

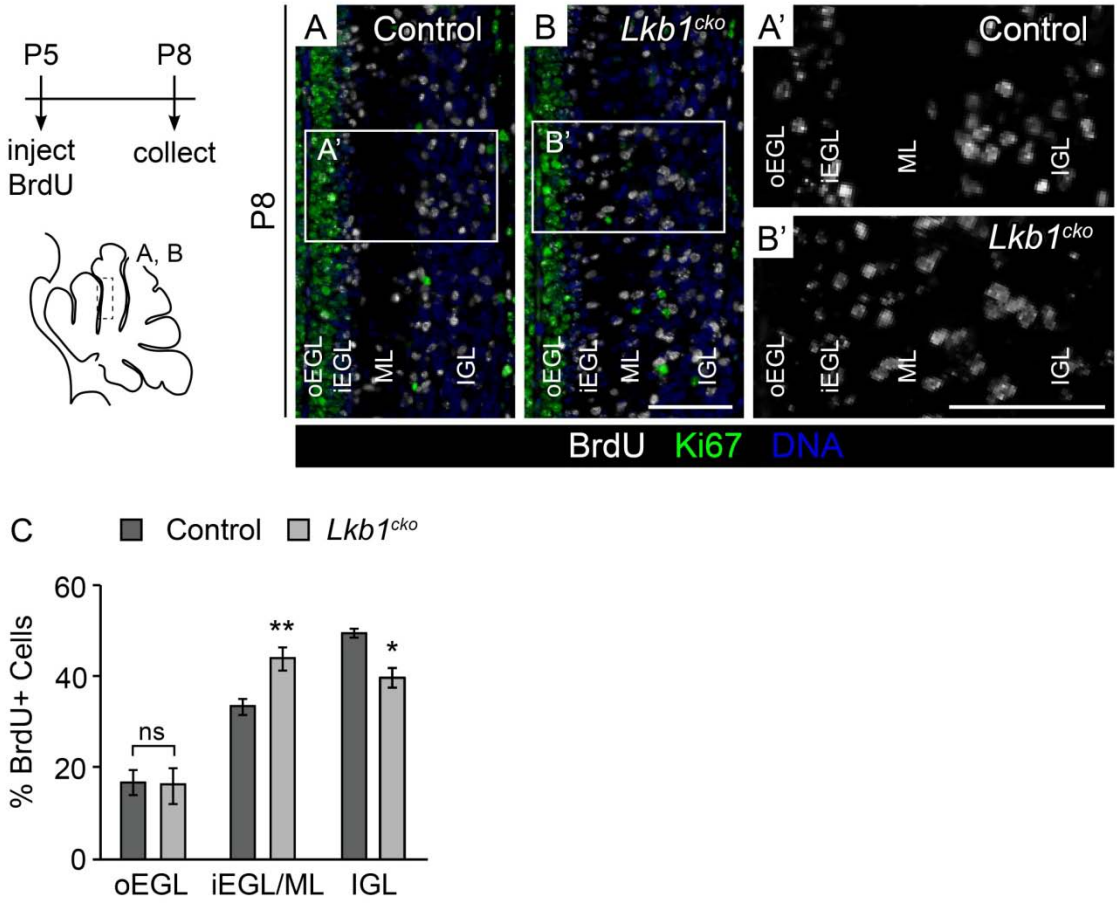

Figure 3.2. *Lkb1^{cko}* cerebella have defects in granule cell migration.
A-B. BrdU/Ki67 co-staining of P8 control (A) and Lkb1^{cko} (B) cerebella three days after BrdU injection. A'-B'. Enlarged images of boxed regions in A and B. C. Quantification of the proportion of BrdU+ cells in each of the specified regions three days after BrdU pulse. N=3 controls, n=5 Lkb1^{cko}. *, $p<0.05$, ** $p<0.005$. Student's unpaired t-test. Scalebar 50 µm. oEGL = outer external granule layer, iEGL = inner external granule layer, ML = molecular layer, IGL = internal granule layer.

Although no reported mouse mutants with defects in GCP migration have been shown to display increased foliation, it is possible that changes in foliation in *Lkb1*^{cko} were due to altered radial migration. To determine if altered radial migration preceded expansion of the cerebellar cortex in *Lkb1*^{cko}, *Lkb1*^{cko} and control sections were stained for p27Kip1 at P2, the first stage where cortical expansion was evident. In contrast to later stages, no discernible difference in the distribution of post-mitotic GCPs was apparent at P2 (Figure 3.3). To determine if defective migration altered adult morphology, adult P30 *Lkb1*^{cko} and control sections were stained with NeuN, a marker of mature neurons commonly used to label granule cells (Figure 3.3). Whereas all NeuN+ cells were located below the Purkinje cell layer, in controls, *Lkb1*^{cko} has a significant number of NeuN+ cells that failed to reach the IGL, forming an indistinct boundary between the IGL and molecular layer. However, no ectopic clusters of GCPs were present in *Lkb1*^{cko}, indicating that *Lkb1*-deficient GCPs properly exited the EGL but failed to reach their final destination.

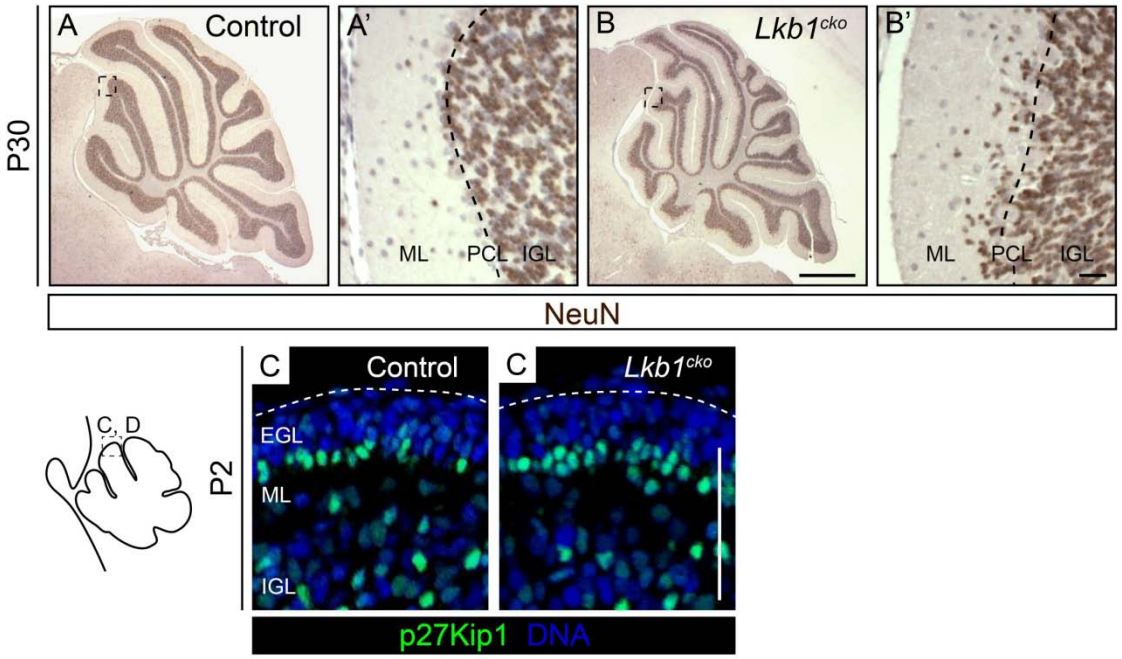

Figure 3.3. Defective migration in *Lkb1*^{cko} is apparent at adult stages but not at P2. A-B. Representative staining for Neuron-specific nuclear protein (NeuN), a marker of mature granule cells, in P30 control (A) and Lkb1^{cko} (B) cerebella. A' and B' are enlargements of the boxed regions in A and B. Dashed lines in A' and A' corresponds to Purkinje cell layer (PCL). Note that a number of granule cells fail to migrate past the Purkinje cell layer in Lkb1^{cko}. Scalebar = 500 µm. C-D. p27Kip1 staining of postnatal day 2 (P2) control (C) and Lkb1^{cko} (D) cerebella indicates that migration is not affected at P2. Dashed line denotes pial surface. Scalebar = 50 µm. EGL = inner external granule layer, ML = molecular layer, IGL = internal granule layer.

Lkb1-deficient neurons have impaired migration in vitro

Although granule cell migration has been traditionally classified as radial, there are in fact three phases of granule cell migration, two of which are glial independent (Komuro et al., 2001). Granule cell precursors first migrate tangentially within the inner EGL before attaching to a Bergmann glial fiber and migrating inward to the Purkinje cell layer, where they detach from glia, elaborate a filopodia, and reach the IGL in a glial-

independent manner (Komuro et al., 2001). Consequently, mutations that disrupt any of these three phases of granule migration (tangential, radial, and filopodia-directed) can result in aberrantly placed granule cells. EGL explant cultures provide one means of studying granule cell migration and maturation in vitro. When small pieces of the EGL are cultured on poly-l-lysine and laminin, GCPs migrate in a glial-independent manner and begin to differentiate; extending parallel fiber-like neurites in the direction of migration (Kawaji et al., 2004). Because migration out of explants is glial-independent, EGL explants are thought to model tangential migration within the inner EGL (Chedotal, 2010). To determine if Lkb1 was important glial-independent GCP migration, EGL explant cultures were established using early postnatal control and *Lkb1*^{cko} mice. After two days, cultures were collected and stained with βIII-tubulin to labels neurites, as well as a nuclear marker. After 2 days in vitro (2 DIV), many control GCPs had migrated out of explants and extended long, relatively straight neurites (Figure 3.4). However, although *Lkb1*^{cko} GCPs were able to migrate out of explants, they did not appear to migrate as far as control cells (Figure 3.4). Interestingly, *Lkb1*^{cko} neurites were not as straight as controls, often crossing one another in a chaotic manner (Figure 3.4). These data indicate that Lkb1 is important for granule cell migration and maturation in vitro.

The nucleus of migrating granule cells is surrounded by a tubulin cage that is thought to play a role in coordinating nuclear migration with that of the cell soma. To determine if nuclear cage formation was impaired the absence of *Lkb1*, control and *Lkb1*^{cko} explants were stained with βIII-tubulin to label neuronal microtubules and Dapi to label DNA. However, nuclear cage formation was normal in both control and *Lkb1*^{cko} migrating GCPs (Figure 3.4), suggesting that *Lkb1* does not regulate migration by controlling nuclear cage formation.

Figure 3.4. *Lkb1*-deficient GCPs have impaired migration and neurite extension in vitro but do not have defects in nuclear cage formation.

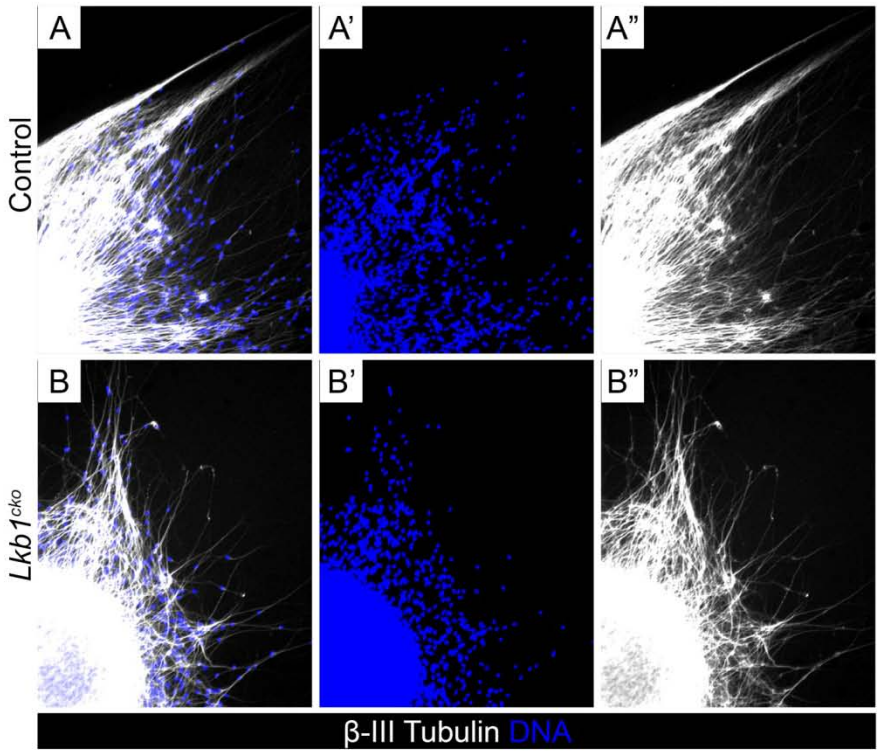

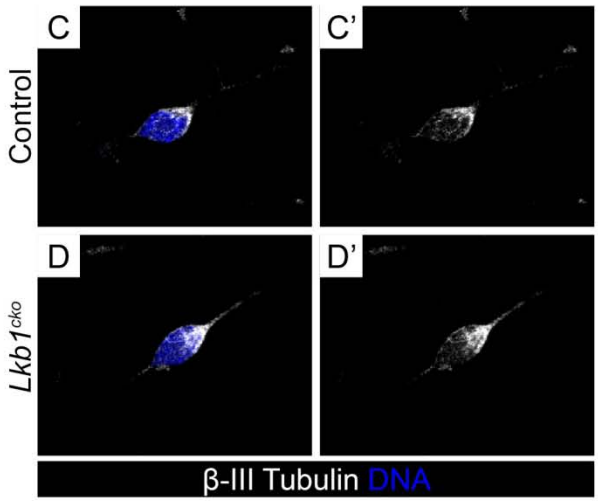

Figure 3.4. Lkb1-deficient GCPs have impaired migration and neurite extension in vitro but do not have defects in nuclear cage formation.
A-B. Low □agnification images of EGL explant cultures derived from control (A-A") and Lkb1^{cko} (B-B") animals and stained for β-III Tubulin, a marker of neuronal processes and Dapi to label DNA. Note that control neurites are relatively straight as they radiate out of explants, whereas neurites in Lkb1^{cko} often cross one another. Note also that the number of Dapi+ nuclei to have migrated out of explants is reduced in Lkb1^{cko}. C-D. High magnification images of individual GCPs migrating out of control © and Lkb1^{cko} (D) EGL explants. The tubulin-based 'cage' surrounding the nucleus forms normally in the absence of Lkb1.

In many migrating cells, including neurons, the centrosome, golgi apparatus, and endocytic recycling machinery are positioned ahead of the nucleus (Cooper, 2013). In migrating granule cells, the centrosome is thought to assist in pulling nucleus forward during migration (Solecki et al., 2004). Indeed, many mutants that disrupt GCP migration alter the position of the centrosome relative to the nucleus (Cooper, 2013; Renaud et al., 2008; Solecki et al., 2004).To determine if centrosome position was altered in GCPs migrating out of explant cultures, explants were stained with γ-tubulin to label the centrosome as well as the nuclear marker p27Kip1 (Figure 3.5). However, the centrosome was located near or in front of the nucleus in both control and *Lkb1*^{cko} explants, indicating that Lkb1 is unlikely to control GCP migration by controlling centrosome position, at least during tangential phases of migration.

Lkb1 has been previously implicated in axonogenesis in forebrain neurons (Barnes et al., 2007; Shelly et al., 2007). In granule cells, axons develop in the form of two parallel fibers within the molecular layer. Impaired axonogenesis could potentially hinder migration by impairing the ability of granule cells to anchor within the molecular layer prior to migration. To determine if *Lkb1*-deficient GCPs were able to elaborate axons, control and *Lkb1*^{cko} GCPs were collected from early postnatal mice and allowed to differentiate in vitro. However, no apparent difference was seen in GCP morphology as polarity progressed between 1 and 4 days in vitro (Figure 3.6). Thus, unlike forebrain neurons, Lkb1 does not regulate GCP polarity in vitro. In support of this finding, no difference in Tag1, a glycoprotein that labels maturing granule cell axons, was seen in *Lkb1*^{cko} cerebella compared to controls (Figure 3.7).

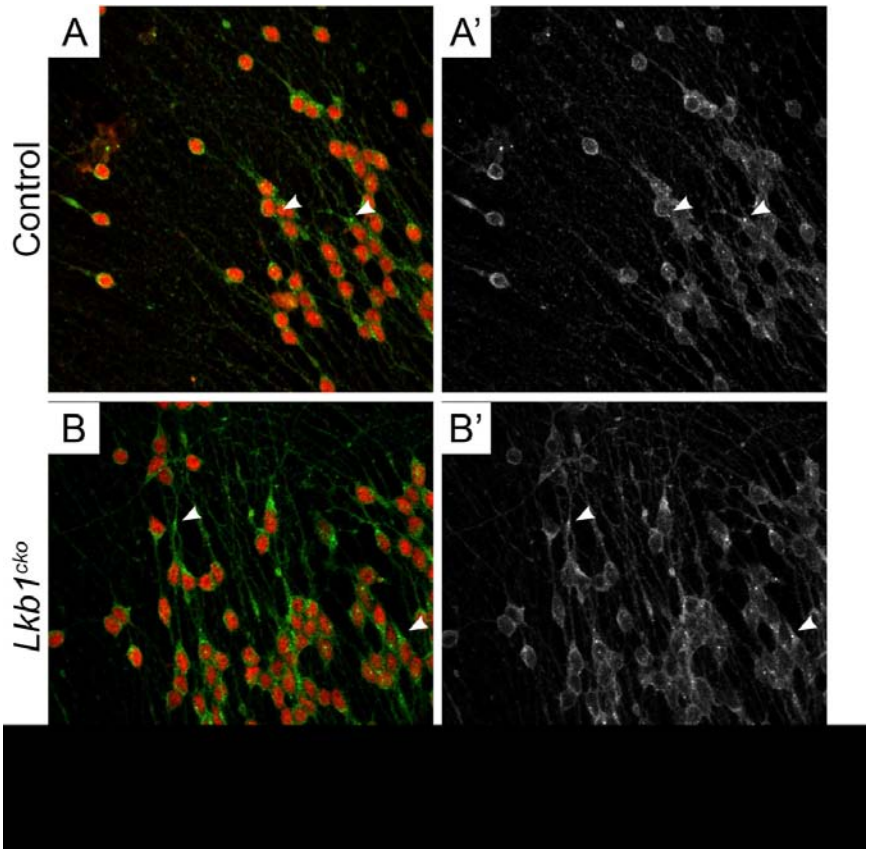

Figure 3.5. Centrosome position is not altered in *Lkb1^{cko}* explants.
A-B. Staining control (A-A') and Lkb1^{cko} explants for p27Kip1 to label granule cell bodies and γ tubulin to label the centrosome. Explant core are located below and to the right. Arrowheads denote the location of the centrosome. Note that the centrosome is located near or ahead of the nucleus in both control and Lkb1-deficient GCPs.

Figure 3.6. *Lkb1*-deficient GCP maturation appears normal in vitro.

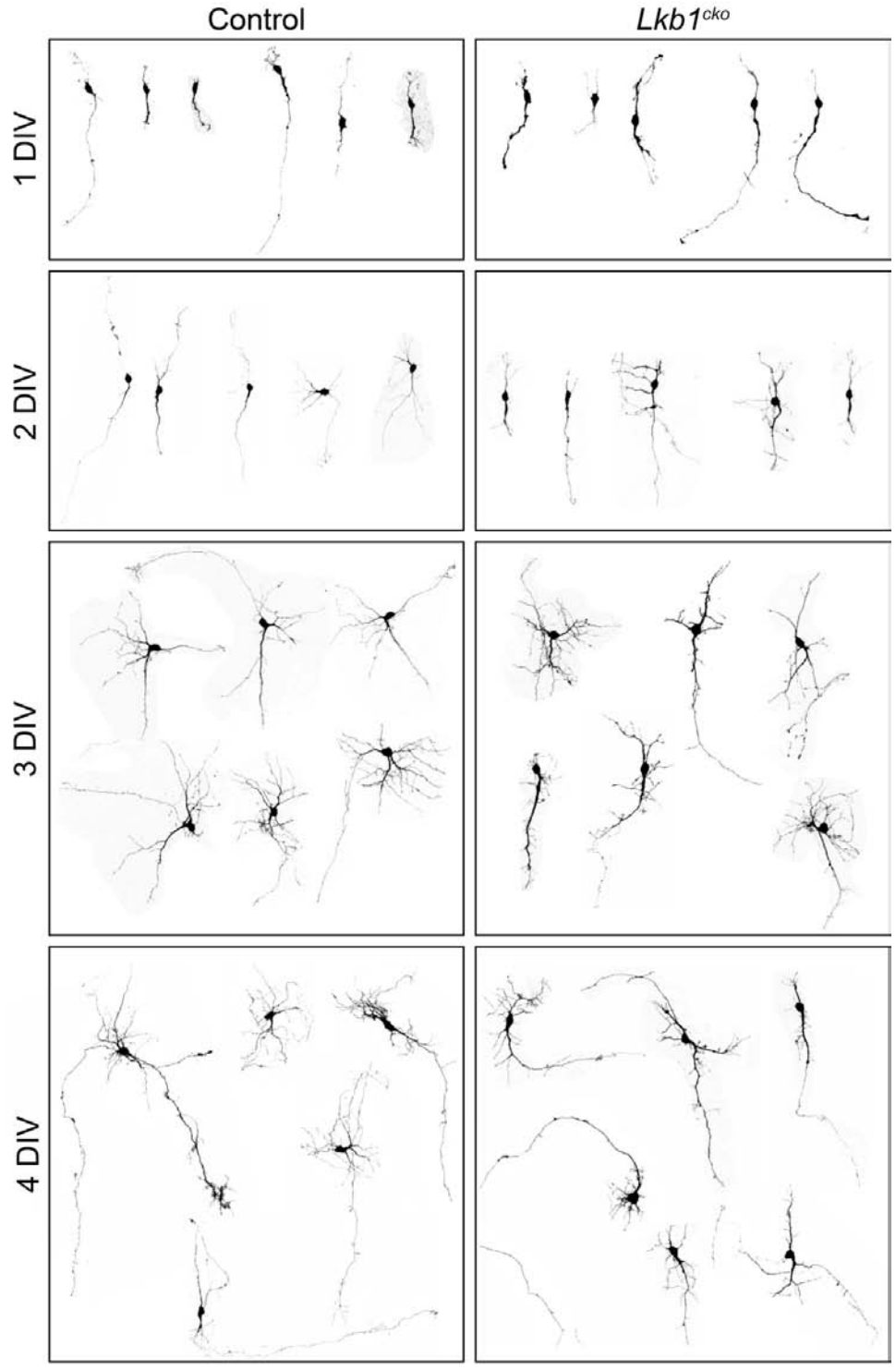

Figure 3.6. Lkb1-deficient GCP maturation appears normal in vitro.
GCPs isolated from Math1-cre; Ai9 controls and Lkb1^{cko}; Ai9 animals were cultured in serum-containing media for 1-4 days to induce differentiation. After 1 day in vitro (1 DIV), two parallel extensions are evident. Parallel fibers continue to extend and begin to branch by 2 DIV. After 3 and 4 DIV many short dendrites have formed around the nucleus. No difference in morphology between Lkb1^{cko} and control cells is evident.

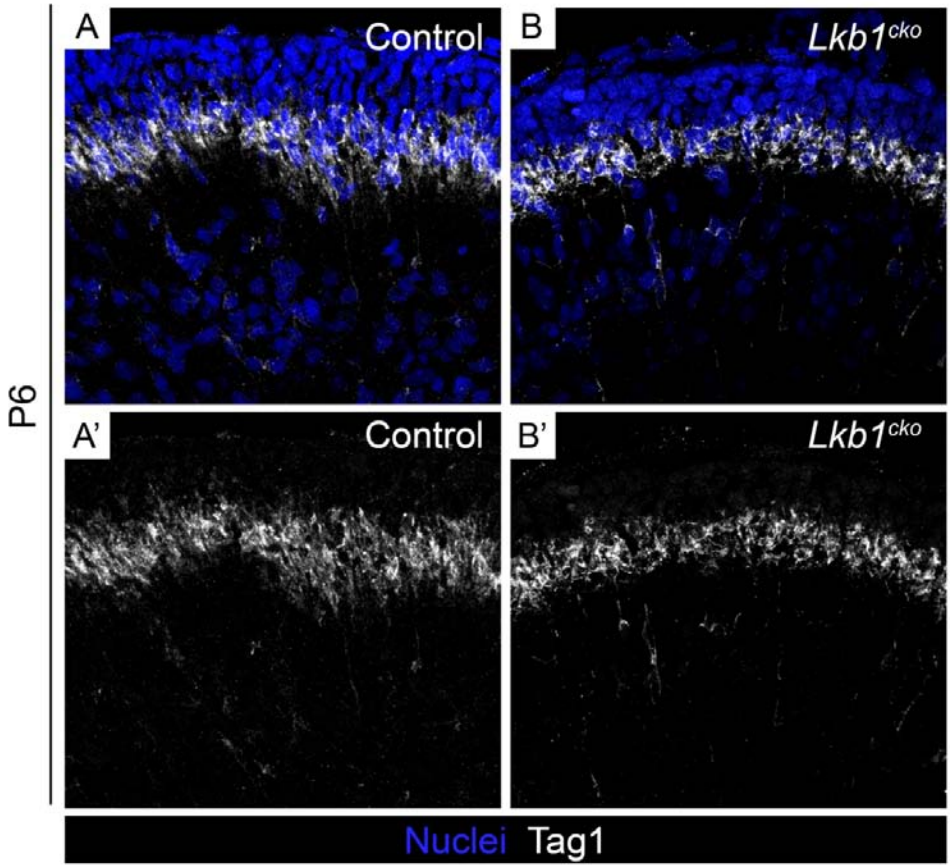

Figure 3.7. Expression of the glycoprotein Tag1, a marker of granule cell axons, is normal in *Lkb1^{cko}*.
A-B. P6 control and Lkb1^{cko} cerebella were stained with Tag1, a marker of developing granule cell axons. Normal Tag1 staining in Lkb1^{cko} suggests axonogenesis is not impaired.

N-Cadherin is expressed normally in *Lkb1^{cko}* cerebella

Cadherins are transmembrane proteins that play an essential role in cell adhesion and migration. N-cadherins are enriched in neuronal tissue and have been shown to play a role in neuronal migration. In the developing zebrafish cerebellum, N-Cadherin is required for chain migration of GCPs (Rieger et al., 2009). In the developing forebrain, surface levels of N-Cadherin are regulated by the endocytic recycling

pathway, including Rab5 and Rab11 (Kawauchi et al., 2010). Consequently, perturbations in Rab activity lead to an accumulation of N-Cadherin on the cell surface, impeding migration by causing the neuron to remain stuck to in one place (Kawauchi et al., 2010). Interestingly, Rab11FIPs (family of interacting proteins) are substrates of the Lkb1 substrate Mark2 (Ducharme et al., 2006). We hypothesized that loss of Lkb1 might impair radial migration via Rab11FIP-mediated recycling of N-Cadherin. To test this, we stained control and *Lkb1*^{cko} cerebella with an N-Cadherin antibody; however, no difference in the distribution of N-Cadherin was apparent (Figure 3.8). Additionally, no difference in surface N-Cadherin level was apparent between control and *Lkb1*^{cko} GCPs cultured in vitro. Thus, impaired migration in *Lkb1*^{cko} is unlikely to be due to defects in N-Cadherin expression or localization.

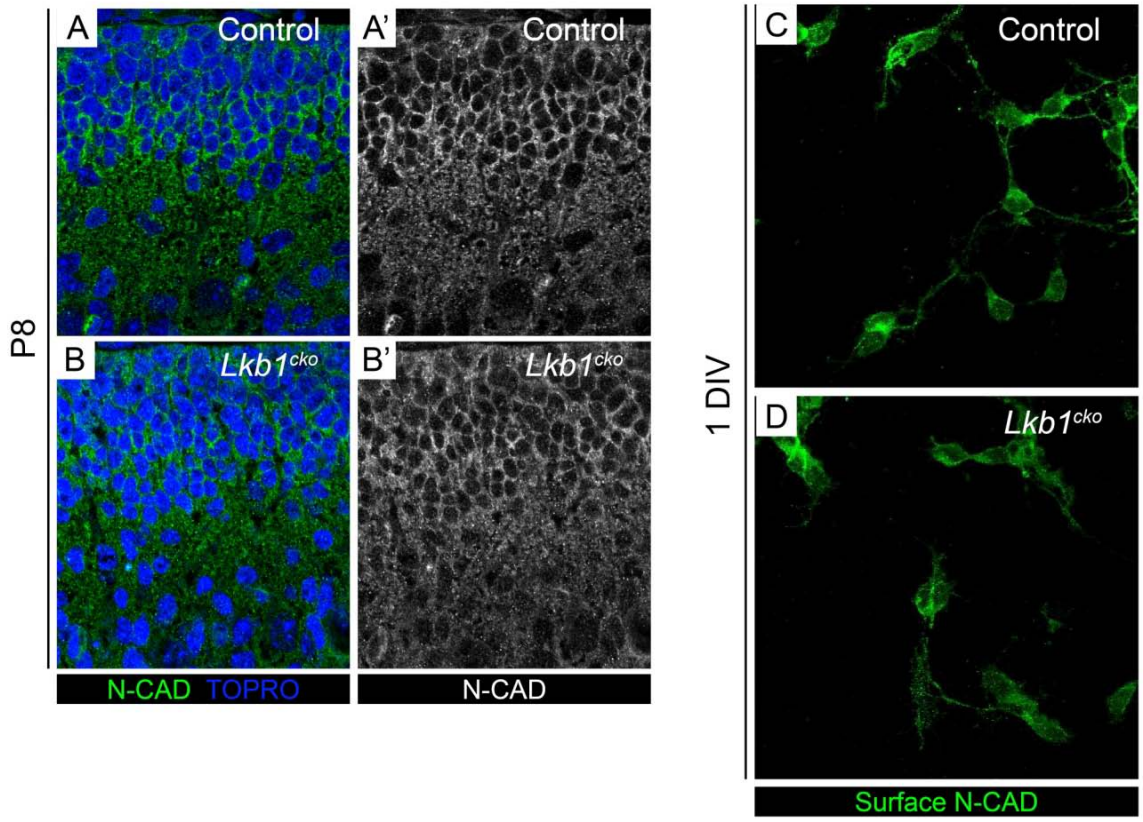

Figure 3.8. N-Cadherin localizes normally in the absence of *Lkb1*.
A-B. Control (A-A') and Lkb1^{cko} (B-B') cerebella were stained for the cell adhesion molecule N-Cadherin at P8. N-Cadherin levels are highest in the innermost region of the EGL, suggesting it may play a role in granule cell migration. However, no difference in N-Cadherin localization or expression levels are evident in Lkb1^{cko}. C-D. Staining of non-permeabilized cultured GCPs derived from control (A) and Lkb1^{cko} animals for N-Cadherin indicates that the subcellular location of N-Cadherin is not altered by loss of Lkb1.

Discussion

During our analysis of differentiation in *Lkb1*^{cko}, we discovered that the distribution of post-mitotic GCPs was altered in *Lkb1*^{cko}. Specifically, loss of *Lkb1*from GCPs resulted in an accumulation of GCPs within the molecular layer of the cerebellum. Immunohistochemical labeling for markers of post-mitotic GCPs, together with long-term BrdU labeling, indicates that *Lkb1*^{cko} have defects in radial migration. Although our investigation of the causes of impaired migration in *Lkb1*^{cko} were abbreviated, we find that Lkb1 does not regulate GCP migration through its well-studied substrate AMPK or by controlling levels of the cell adhesion molecule N-Cadherin.

The role of Lkb1 in neuronal migration in other brain regions has been ambiguous. Initial studies showed that loss of *Lkb1* from dorsal telencephalic progenitors did not lead to dramatic changes in cortical laminae, indicating that *Lkb1* was dispensable for radial migration in the forebrain (Barnes et al., 2007; Shelly et al., 2007). However, subsequently studies of the same region demonstrated that loss of *Lkb1* did impact radial migration by controlling centrosome positioning (Asada and Sanada, 2010; Asada et al., 2007). Our study provides evidence that Lkb1 is important during radial migration of granule cells along Bergmann glia in the developing cerebellum. Interestingly, Lkb1 is not the first PAR protein to be implicated in granule cell migration, as both Pard3 and Par6α have been shown to regulate migration in GCPs by controlling glial adhesion and cytoskeletal remodeling, respectively (Famulski et al., 2010; Solecki et al., 2004).

The mode and speed of GCP migration differs depending on location within the EGL, IGL, and molecular layer (Komuro et al., 2001). Specifically, cells migrate

tangentially within the lower portion of the EGL before beginning to migrate radially (Komuro et al., 2001). Moreover, radial migration is not a smooth and fluid process: migrating cells alternate between phases of movement and periods of stagnation (Komuro et al., 2001). Interestingly, the slowest phase of motion occurs as GCPs leave Bergmann glial processes and cross through the Purkinje cell layer (Komuro et al., 2001). During this phase, the migrating cell changes shape and completely stops before forming filopodia that appear to direct the cell through the Purkinje cell layer to the IGL (Komuro et al., 2001). Interestingly, in the adult *Lkb1*^{cko} cerebellum, granule cells accumulate near the bottom of the molecular layer close to the Purkinje cell layer. One possible interpretation of such accumulation of granule cells near the bottom of the molecular layer is that early phases of GCP migration, including the transition from tangential to radial migration and the procession down glial processes, were normal in *Lkb1*^{cko}, but that the final phase of migration, including passage through the Purkinje cell layer, was disrupted. However, live imaging studies will be required in order to gain further insight into when during maturation GCP migration is perturbed in cells lacking *Lkb1*.

The step-wise progression of GCPs along glia observed in slice cultures (Komuro et al., 2001) is consistent with a “reach-and-pull” model of radial migration wherein the migrating neuron is continuously forming and releasing cell adhesions (Figure 3.9). In this model, the migrating GCP adheres to the glial cell ahead of the nucleus in the leading process using Astrotactin and/or JAM-C and/or additional molecules. Following such adhesion, active myosin in either the distal (He et al., 2010) or proximal (Solecki et al., 2009) leading process causes actin to flow forward, in the direction of migration. The cell then pauses, perhaps to remove the adhesion at the rear of the cell and form new

adhesions further down the glial fiber, before repeating the cycle again. In *C. elegans*, par-4 regulates the distribution of active myosin by regulating the activity of the anillin family of scaffolding proteins (Chartier et al., 2011). Thus, one possible explanation for the migration defects observed in *Lkb1*^{cko} is that Lkb1 normally regulates myosin localization in the leading process, and loss *Lkb1* leads to mislocalization of active myosin in migrating neurons, impairing the ability of GCPs to progress down the glial process. Given that Par6α is important for GCP migration (Solecki et al., 2004), and the fact that *par-4* mutations lead to mislocalization of par-6 in *C. elegans* (Chartier et al., 2011), it would also be of interest to see if Par6α is localized normally in *Lkb1*^{cko}.

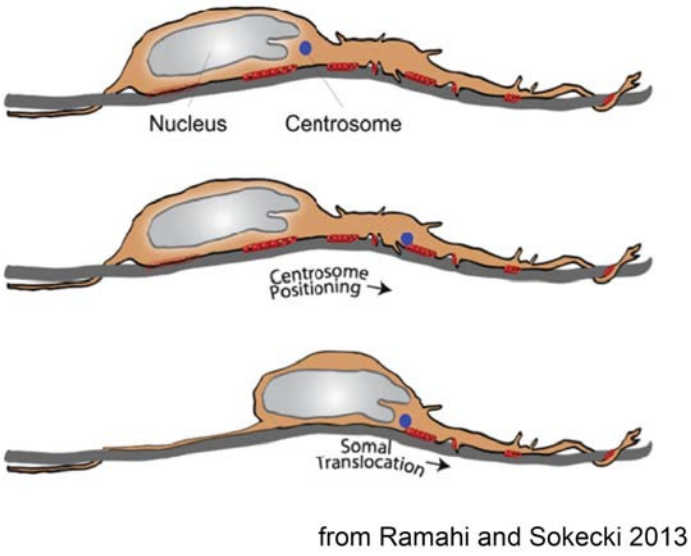

Figure 3.9. Reach-and-pull model of radial neuronal migration.
Illustration of a migrating granule cell along a glial fiber (grey). Top: adhesions (red) form under the leading process (right) and cell soma. Middle: the centrosome (blue) moves forward into the leading process while the cell soma remains stationary. Bottom: release of adhesion molecules below the cell soma allow for the soma to progress along the glial fiber.

The Rho GTPase RhoA regulates myosin II activity in cortical neurons (Govek et al., 2011). Interestingly, introducing Lkb1 into HeLa cells, which do not express Lkb1 endogenously, leads to Rho-dependent reorganization of the actin cytoskeleton (Xu et al., 2010). Moreover, in cultured epithelial cells, Lkb1 regulates cortical actin contractility, and loss of Lkb1 leads to a reduction in GTP-bound RhoA (Rodriguez-Fraticelli et al., 2012). Given that the Rho GTPase Rac1 is required for GCP migration in the developing cerebellum (Tahirovic et al., 2010; Zhou et al., 2007), it is possible that Lkb1 regulates the actin-mediated GCP migration through activation of a Rho GTPase. Thus, it would be of interest to see if F-actin levels are normal in *Lkb1*^{cko} GCPs, as well as to determine if GTP-bound Rac1 levels are altered.

The Lkb1 substrate Par1b/Mark2/EMK1 phosphorylates Rab11FIP1 and Rab11FIP2, members of the Rab11 family of interacting proteins (Rab11FIPs) (Ducharme et al., 2006), which participate in the Rab11 endocytic recycling pathway (Horgan and McCaffrey, 2009). Given the role of Rab11-dependent N-Cadherin recycling in migrating forebrain neurons (Kawauchi et al., 2010), we wondered if perhaps the Lkb1-Par1b-Rab11FIP axis regulated migration in *Lkb1*^{cko} by controlling surface levels of N-Cadherin. The fact that we do not see any difference in N-Cadherin levels in *Lkb1*^{cko} suggests that either N-Cadherin is not important for GCP migration or that endocytic recycling is unaffected by loss of *Lkb1*. To distinguish between these two possibilities, it would be of interest to look at the distribution of other cell adhesion proteins involved in granule cell migration, such as Astrotactin and JAM-C, in *Lkb1*^{cko}. Given that endocytic trafficking likely regulates multiple aspects of granule cell migration, including BDNF reception and internalization by TrkB (Zhou et al., 2011) as well as

adhesion formation and removal, it would also be of interest to stain *Lkb1*^{cko} GCPs with a marker of endocytic vesicles such as α-adaptin.

Interestingly, several of the polarizing functions of Rab11FIP2 do not involve Rab11 or RabVa (Lapierre et al., 2012), suggesting that Rab11FIPs have additional functions outside of endocytic recycling. It is possible that the Lkb1-dependent phosphorylation of Rab11FIP1 or Rab11FIP2 controls GCP migration independent of the endocytic recycling pathway, and would thus be of interest to generate conditional knockouts for either or both of these genes to determine if their loss impairs migration.

It is possible that increased foliation in *Lkb1*^{cko} is due to altered GCP migration. Indeed, in hypothyroid rats, which have increased foliation, radial migration is impaired although GCP proliferation is not (Hosaka et al., 2012). Moreover, the dramatic increase in foliation seen in the human cerebellum has been credited to a prolonged period of proliferation and migration of granule cell precursors (Sillitoe and Joyner, 2007). Whereas all GCPs have migrated to the EGL by postnatal day 21 in the mouse, the window of GCP proliferation and migration extends an entire year in humans. However, mutations that impair radial migration in mice do not consistently lead to an increase in cerebellar folding. More often than not, mutations disrupting GCP migration lead to a reduction in foliation, often due to secondary effects in glial morphology, Purkinje cell development, and/or GCP proliferation (Kokubo et al., 2009; Kullmann et al., 2012; Schwartz et al., 1997; Wang et al., 2007). Consequently, hypothyroid rats are the *only* existing model in which both migration is reduced and foliation is increased. Thus, although it is possible that changes in migration increase foliation in *Lkb1*^{cko}, we feel that this possibility is unlikely. Supportive of this idea is that no defects in migration were apparent at P2, a stage when cortical expansion was already evident. Nonetheless, it

would be of interest to selectively remove *Lkb1* from post-mitotic GCPs in the inner EGL using a *Tag1*- or *NeuN*-driven *cre* to determine if impaired radial migration contributes to increased foliation in *Lkb1*^{cko}; however, such inner-EGL-specific *cre* lines do not currently exist.

CHAPTER IV. GENERAL DISCUSSION

Summary

Aside from neural precursor proliferation, little is known about the cellular and genetic determinants of cortical size and foliation complexity in the cerebellum. My graduate work focused on the role of Lkb1—a polarity protein, tumor suppressor, and kinase—in cerebellar development. We find that GCP-specific deletion of *Lkb1* (that is, in $Lkb1^{cko}$ animals) increases cerebellar cortical area and foliation. Our data suggest that Lkb1 regulates cortical size and folding by controlling the orientation of cell division, and that increased foliation in $Lkb1^{cko}$ is due to an increase in parallel GCP divisions. In addition to alterations in the plane of division, we find that loss of *Lkb1* impairs the timely migration of GCPs to the internal granule layer (IGL). During development, $Lkb1^{cko}$ cerebella show an accumulation of GCPs within the molecular layer. By adult stages, $Lkb1^{cko}$ harbor a number of mature granule cells outside of the IGL in the molecular layer. Though it is possible that reduced migration could increase foliation in $Lkb1^{cko}$, we feel this possibility is unlikely for reasons outlined in the following section. Taken together, this work demonstrates that Lkb1 regulates multiple aspects of granule cell development and uncovers a previously unappreciated role for oriented cell division in cerebellar foliation.

Linking foliation, oriented cell division, and migration

When it comes to science, at least *my* science, I am a skeptic and a pessimist. It took me about six months and at least a dozen mice to believe – really *believe* – that foliation was increased in $Lkb1^{cko}$ animals. It took another six to accept the data I had

collected regarding changes in the plane of division. Consequently, the discovery that granule cell migration was also impaired in the *Lkb1*^{cko} cerebellum, which came less than a year ago was a surprise and put a kink in an otherwise seamless story.

I have spent countless hours attempting to understand the extent to which changes in the plane of division and impaired radial migration contribute to increased foliation in *Lkb1*^{cko}. Perhaps the biggest question I have sought to answer is whether defects in migration could increase foliation in *Lkb1*^{cko}. Put simply, our data and previous work of others do not support a link between impaired migration and increased foliation. For one, we find that cortical expansion in *Lkb1*^{cko} precedes defects in migration. Moreover, of the several dozen mouse mutants with impaired radial migration, none have increased foliation.

Pretending for a moment that impaired migration *could* increase cortical surface area and folding, how would this occur? Perhaps increased numbers of GCPs in the molecular layer of *Lkb1*^{cko} could alter the tension placed on Bergmann glia, causing glial fibers, which stretch to pial surface, to pull inward on the cerebellar surface, increasing surface folds. Indeed, Blbp-labeled Bergmann glial fibers do not appear to be as straight in *Lkb1*^{cko} cerebella as controls, perhaps due to increased numbers of GCPs within the molecular layer (Figure 4.1). However, while changes in Bergmann glial tension might account for increased folding in *Lkb1*^{cko}, they do not account for differences in cerebellar surface area. Moreover, *APC2-/-* mice have an accumulation of GCPs in the molecular layer comparable to *Lkb1*^{cko} animals, but the authors do not report any differences in folia number (Shintani et al., 2012). Nonetheless, it remains a possibility that GCP-specific loss of *Lkb1* increases foliation indirectly through Bergmann glia.

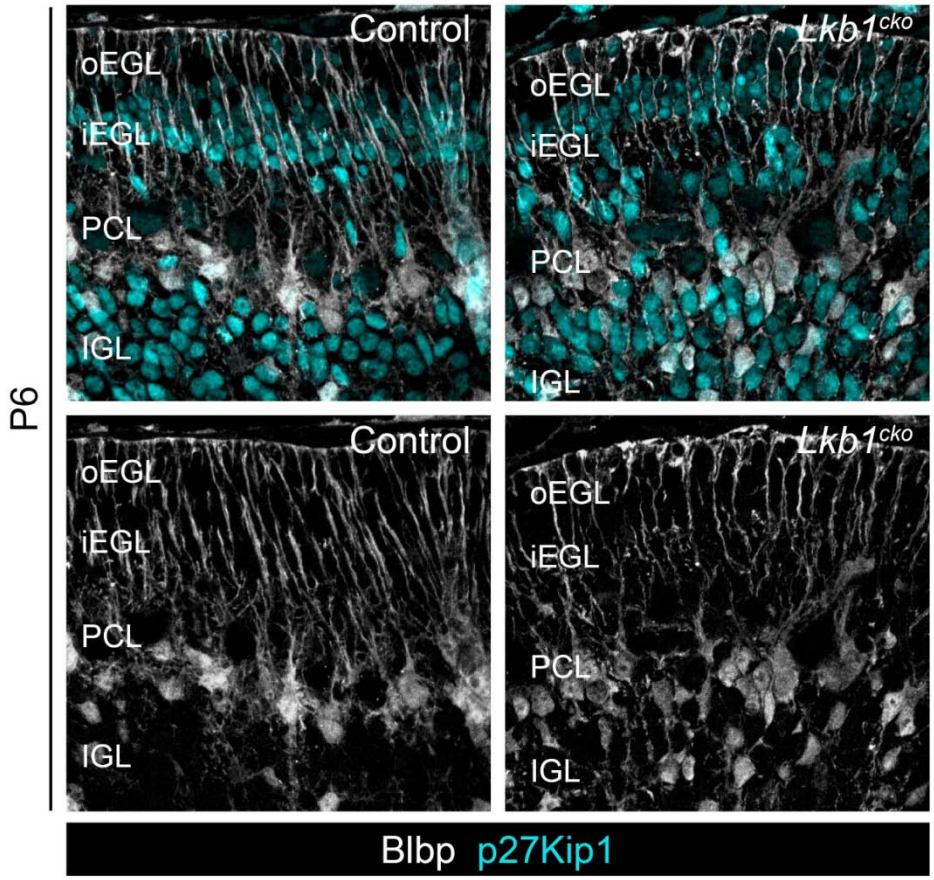

Figure 4.1. GCP-specific loss of *Lkb1* leads to defects in Bergmann glia.
Staining of P6 control (left) and Lkb1^{cko} (right) cerebella for Brain lipid binding protein (Blbp) to label Bergmann glia, and p27Kip1 to label postmitotic granule cells. Note the accumulation of p27Kip1+ cells above the Purkinje cell layer (PCL) in the Lkb1^{cko} cerebellum. Many Bergmann glial cell bodies (white) are ectopically localized below the Purkinje cell layer in Lkb1^{cko}, and Bergmann glial fibers branch more distally in Lkb1^{cko}.

In their seminal 1997 book on the cerebellum, Altman and Bayer speculate that mossy fiber/granule cell synapses may serve as anchoring points for cerebellar folia. Many granule cells fail to reach the IGL in *Lkb1*^{cko} cerebella, even at adult stages, which could hypothetically alter foliation patterns by changing the timing and/or placement of these granule cell/mossy fiber anchoring points. However, that other mouse mutants with ectopically localized granule cells do not have increased foliation makes this possibility somewhat less likely (Kerjan et al., 2005; Kullmann et al., 2012; Shintani et al., 2012).

Could impaired migration increase cortical surface area in *Lkb1*^{cko} cerebella by increasing the number of GCPs near the cerebellar surface? This seems unlikely given that migration appears to be impaired as cells exit the inner EGL, which is some distance from the cerebellar surface. Moreover, previously identified mouse mutants in which GCPs are unable to exit the EGL (eg *BDNF-/-* mice) have reduced, rather than increased, foliation patterns (Borghesani et al., 2002).

Finally, the only other example of a rodent model in which both migration and foliation are altered, hypothyroid rats, display a global impairment in GCP maturation and proliferation. In these animals, radial migration is impaired and GCPs also divide more slowly and less frequently, effectively prolonging cerebellar maturation (Lauder, 1977, 1979). By contrast, *Lkb1*^{cko} have equivalent numbers of mitotic GCPs as do controls and exit the cell cycle similar to control animals. Thus, although it is certainly possible that increased cortical folding in *Lkb1*^{cko} results from impaired migration, this link is difficult to make with any confidence.

Establishing a causative link between the orientation of cell division and organ morphology presents a number of technical challenges in all but the simplest of model

systems. Although spindle orientation can be artificially manipulated in vitro (Lancaster and Baum, 2014), employing such a method in the developing cerebellum, where the spindle orientation of hundreds, if not thousands, of GCPs would need to be manipulated in order to see changes in foliation, would be technically insurmountable. Thus, although we were unable to directly prove causation between randomization of the mitotic spindle orientation and cortical expansion in *Lkb1*^{cko}, several pieces of data support such a model. First, the cerebellar cortex of *Lkb1*^{cko} is larger in the absence of changes in the proportion or total number of proliferating GCPs. Second, the outer EGL, where proliferating GCPs reside, is thinner in *Lkb1*^{cko}, indicating a reorganization of this tissue layer that is consistent with daughter cells being positioned next to one another following mitosis. Third, at stages where increased cortical size and foliation are evident, the proportion of parallel divisions is increased in *Lkb1*^{cko}. Together, these data suggest that, similar to the developing epidermis, increased parallel divisions expand cortical surface area and, subsequently, cortical folding, in the *Lkb1*^{cko} cerebellum.

Future Directions

The majority of my graduate work focused on understanding how changes in the orientation of cell division impacted cerebellar surface area and folding. By contrast, many of the future directions I have proposed center around understanding how Lkb1 regulates granule cell migration. There are several reasons for this focus on migration rather than spindle orientation. For one, only in the final year of my PhD did I discover that migration was also impaired in *Lkb1*^{cko}, and, consequently, I was unable to establish a cellular or molecular mechanism underlying Lkb1's role in migration. Additionally, migration can be studied a number of ways in vitro, including cerebellar slice cultures,

GCP/Glial co-cultures, EGL explant cultures, and migration on laminin-coated dishes. Moreover, because granule cells have historically served as a model for understanding radial migration, a great deal is known about the process, providing a large body of work to draw upon during future investigations. Finally, it is possible that Lkb1 regulates oriented cell division and cell polarity through a common pathway, for example, by controlling cell polarity or cytoskeletal dynamics. Thus, any discoveries made regarding Lkb1-mediated control of migration could be investigated in oriented cell division.

1. Live Imaging

A first step for determining *how* Lkb1 regulates granule cell migration will be to determine *when* migration is impaired. Over a decade ago, Komura et al. used live imaging of cerebellar slice cultures to demonstrate that GCPs migrate at different speeds depending upon their location—eg, outer EGL (oEGL), inner EGL (iEGL), molecular layer (ML), Purkinje cell layer—within the cerebellar cortex (Komuro et al., 2001). Thus, live imaging of early postnatal *Lkb1*^{cko} slice cultures could be used to pinpoint when migration is impaired. These studies would need to be performed using a membrane and/or nuclear marker to label a subset (~10%) of *Lkb1*^{cko} and control GCPs. Confocal imaging for 12-24 hours could then be used to determine the rate of GCP migration within the iEGL, through the molecular layer, and across the Purkinje cell layer. A membrane-directed marker could provide additional insight into whether parallel fibers and leading processes from normally within the iEGL and ML, respectively, as well as whether filopodia form normally as cells breach the Purkinje cell layer.

The results from these experiments could then be used to direct future experiments which could provide insight into the molecular mechanisms underlying

defects in migration. For instance, if the transition from tangential to radial migration is delayed in *Lkb1*^{cko}, one could determine if parallel fibers form normally. If not, perhaps defects in polarity are responsible for impaired migration, similar to *Sema6a* and *Plxn2b* mutants (Kerjan et al., 2005; Renaud et al., 2008). However, if parallel fibers form normally but the transition from tangential to radial migration is impaired, Pard3 signaling or BDNF signaling might be perturbed, as both of these molecules have been previously shown to regulate EGL exit (Borghesani et al., 2002; Famulski et al., 2010). If, alternatively, movement through the molecular layer is altered in *Lkb1*^{cko}, with cells seeming to pause abnormally long between periods of movement, impaired migration could be the result of increased levels of adhesion molecules (eg, astrotactin, JAM-C) on the cell surface. If, however, cells have trouble migrating through the Purkinje cell layer with normally formed filopodia, BDNF signaling, which is highest in the IGL, might be disregulated. Alternatively, if filopodia are defective, actin dynamics may be impaired. A flow chart for interpreting live imaging data is shown in Figure 4.2.

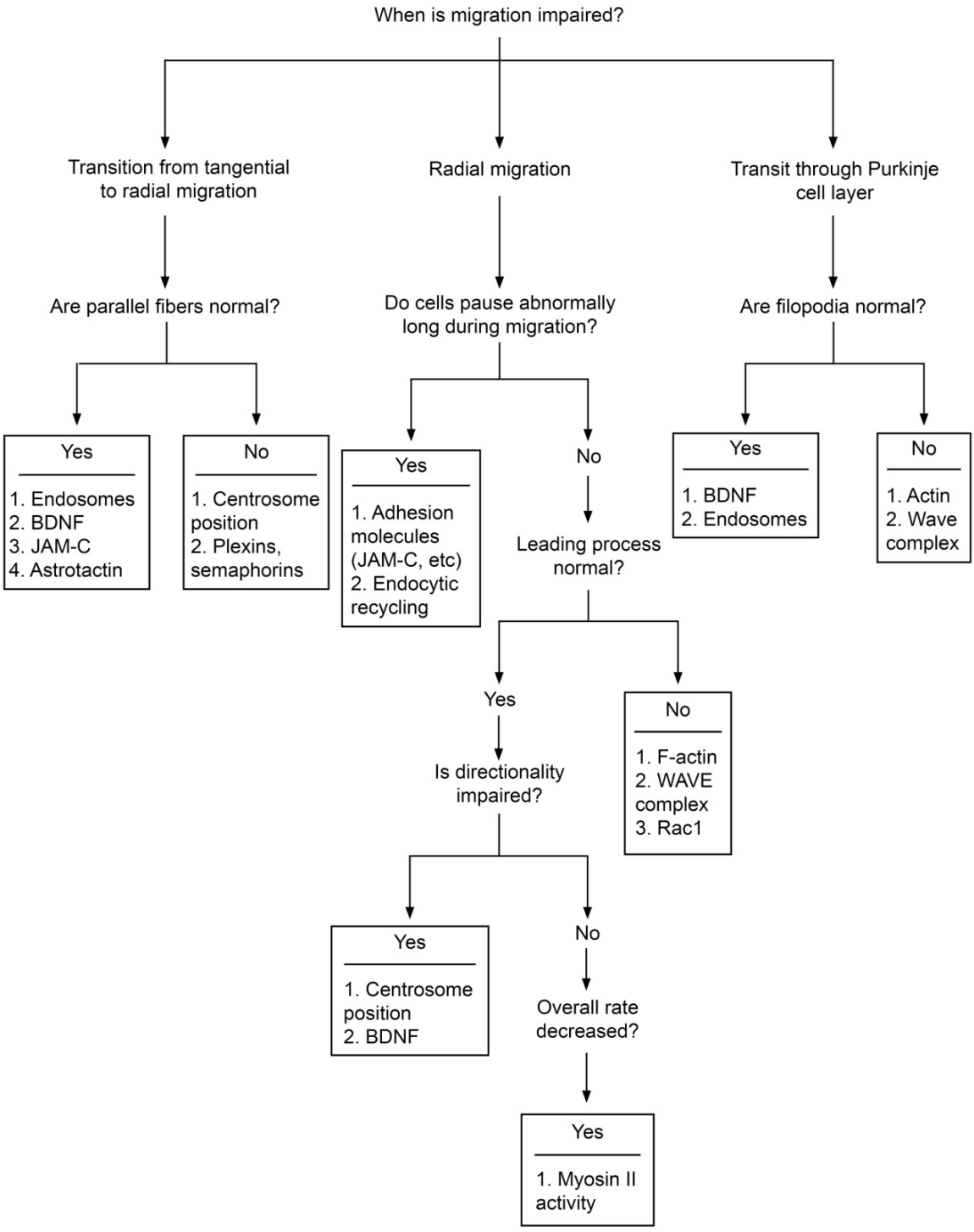

Figure 4.2. Flow chart illustrating potential future experiments based on live imaging.

2. The Actin Cytoskeleton

The actin cytoskeleton plays important roles in both neuronal migration and oriented cell divisions. During granule cell migration myosin II motors directing the forward flow of actin toward the leading process (Solecki et al., 2009). Additionally, cortical F-actin regulates the position of the mitotic spindle in cultured mammalian cell lines (Sandquist et al., 2011). Determining if actin filaments form normally in both mitotic and migrating *Lkb1*^{cko} GCPs could provide insight into whether changes in actin dynamics are responsible for defects in polarity and migration in *Lkb1*^{cko}. Given that Lkb1 has been shown to mobilize a population of myosin in *C. elegans* (Chartier et al., 2011), it would also be of interest to see if myosin II localizes properly in *Lkb1*^{cko} GCPs.

In cultured epithelial cells, loss of *Lkb1* impairs cortical actin contractility due to reduced levels of GTP-bound RhoA (Rodriguez-Fraticelli et al., 2012). Thus, if *Lkb1*^{cko} GCPs have impaired, reduced or mislocalized actin, it would be of interest to see if GTP-Rac1 levels are reduced, particularly because Rac1 has been previously implicated in GCP migration.

3. The role of Rab11FIP1/2

The small GTPase Rab11 is essential for the endocytic recycling pathway, particularly the recycling of endosomes back to the plasma membrane (Maxfield and McGraw, 2004). The Rab11 Family of Interacting Proteins (Rab11FIPs) associate with Rab11 and contribute to endosome recycling (Horgan and McCaffrey, 2009). Rab11FIP2 is a substrate of Par1/Mark2, a substrate of Lkb1 (Ducharme et al., 2006). Interestingly, work in the Goldenring lab suggest that in their phosphorylated form, Rab11FIPs control epithelial polarity in a Rab11-independent manner (Lapierre et al., 2012). We find that

phospho-MARK levels are reduced in *Lkb1*^{cko} GCPs using a pan-phospho-MARK antibody (Figure 4.3). Additionally, we see that p-Rab11FIP1 is expressed in the iEGL of P6 control, but not *Lkb1*^{cko}, cerebella, suggesting that Rab11FIP1 phosphorylation may function downstream of Lkb1 in post-mitotic GCPs preparing to undergo radial migration (Figure 4.3). Future studies are needed to clarify the role of p-Rab11FIP1/2 in GCPs, perhaps using Rab11Fip1/2 floxed alleles available from the Goldenring lab.

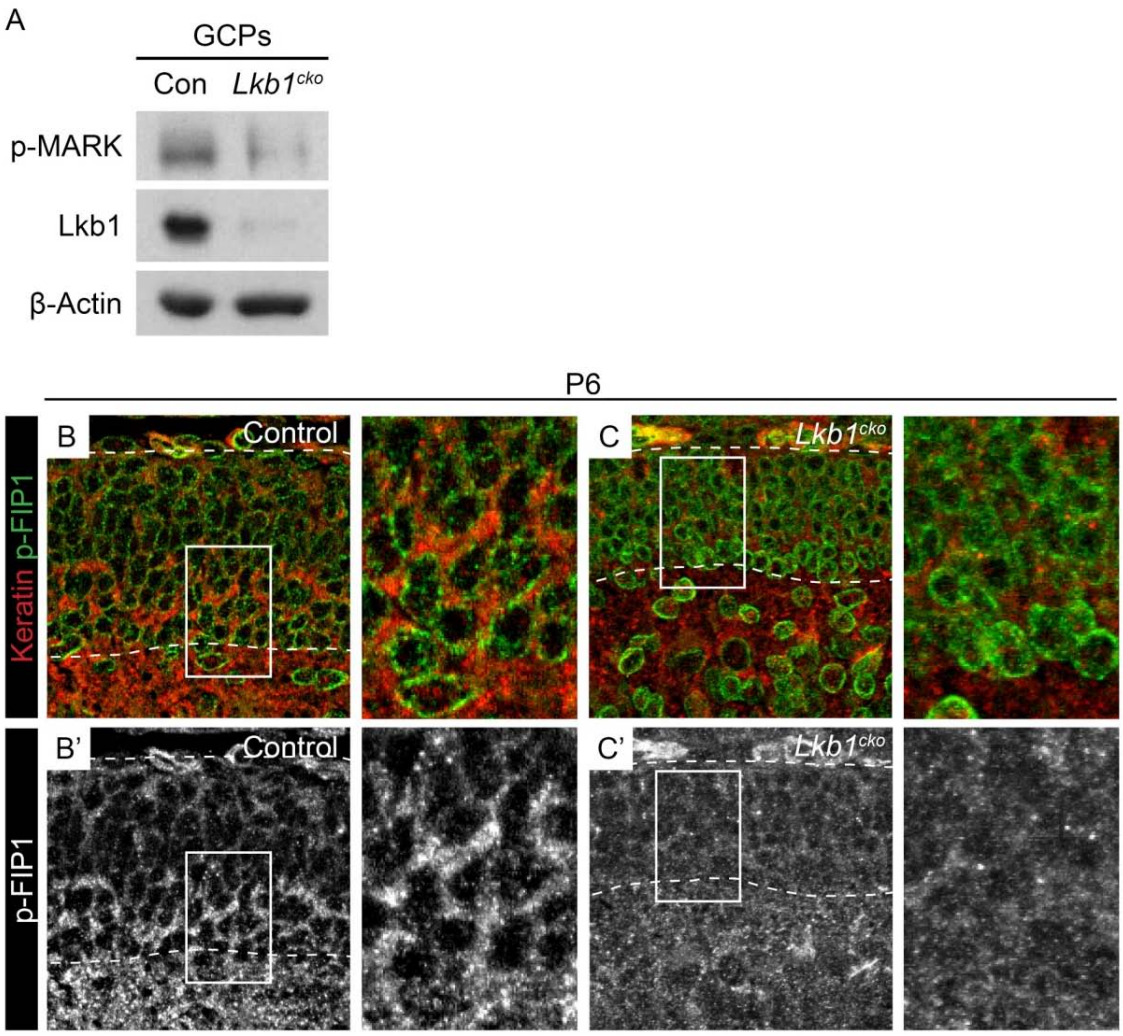

Figure 4.3. Phosphorylation of MARK1-4 and FIP1, a putative target of MARK2, is reduced in *Lkb1^{cko}* GCPs.

A. Western blotting with a pan-phospho-MARK antibody, which detects phosphorylated MARK1-4, reveals that MARK phosphorylation is reduced in Lkb1^{cko}. Actin and Lkb1 serve as controls for loading and knockdown, respectively. B-C. Immunostaining P6 control (B-B') and Lkb1^{cko} (C-C') cerebella with phosphorylated FIP1 and Keratin, which labels the cell cortex. Dashed lines denote the EGL. Boxed regions are enlarged in neighboring panels. Note that p-FIP1 localizes to the inner EGL in the control cerebellum but such inner-EGL staining is absent in Lkb1^{cko}.

4. Miscellaneous experiments

- I am often asked if *Lkb1*^{cko} animals have changes in behavior or motor function. It would be interesting to do **behavioral and motor testing** to see what, if any, effect loss of *Lkb1* has on behavior and/or motor coordination.
- **EGL explant cultures** could be repeated to verify that migration is impaired *in vitro*.
- **Tubulin staining** could be performed on proliferative GCPs in vitro to determine if the mitotic spindle forms normally in *Lkb1*^{cko}. In *Drosophila* neuroblasts and mouse hematopoietic stem cells, loss of *Lkb1* leads to defects in spindle microtubule density (Bonaccorsi et al., 2007; Nakada et al., 2010).
- If/when available, using an **inner EGL specific-cre** to delete *Lkb1* from post-mitotic, pre-migratory neurons would be of interest to determine what, if any, affect altered migration has on foliation.
- **GCP polarity** in *Lkb1*^{cko} could be investigated in vivo using Golgi staining or dye impregnation.

APPENDIX I: HEDGEHOG SECRETION AND SIGNAL TRANSDUCTION IN VERTEBRATES

Summary

Signaling by the Hedgehog (Hh) family of secreted proteins is essential for proper embryonic patterning and development. Dysregulation of Hh signaling is associated with a variety of human diseases ranging from developmental disorders such as holoprosencephaly to certain forms of cancer, including medulloblastoma and basal cell carcinoma. Genetic studies in flies and mice have shaped our understanding of Hh signaling and revealed that nearly all core components of the pathway are highly conserved. While many aspects of the *Drosophila* Hh pathway are conserved in vertebrates, mechanistic differences between the two species have begun to emerge. Perhaps the most striking divergence in vertebrate Hh signaling is its dependence on the primary cilium, a vestigial organelle that is largely absent in flies. This minireview will provide an overview of Hedgehog signaling and present recent insights into vertebrate Hh secretion, receptor binding, and signal transduction.

Introduction

Originally discovered for its role in *Drosophila* embryonic patterning, the Hedgehog (Hh) pathway is among a handful of signaling pathways governing the development of multicellular organisms. Hh signaling is essential for the development of nearly every organ system in vertebrates, from patterning the neural tube and limbs to regulating lung morphogenesis and hair follicle formation (Ingham and McMahon, 2001). While the *Drosophila* genome encodes a single *hh* gene, vertebrates harbor between

three (Sonic hedgehog [*Shh*], Desert hedgehog [*Dhh*] and Indian hedgehog [*Ihh*] in birds and mammals) and six (*Shh*, *Dhh*, and *Ihh* plus Tiggywinkle hedgehog [*Twhh*], Echidna hedgehog [*Ehh*] and Qiqihar hedgehog [*Qhh*] in fish) homologs, differing primarily in tissue distribution (Ingham et al., 2011). In vertebrates, *Shh* is expressed throughout the developing nervous system and in many epithelial tissues, *Ihh* functions primarily in bone development, and *Dhh* expression is limited to the peripheral nervous system and reproductive organs (Ingham and McMahon, 2001). As a result of its widespread expression, much of what is known about vertebrate Hh signaling stems from work on Shh. All Hh ligands undergo a similar series of processing events that result in the covalent attachment of two lipid moieties and are essential for proper signaling activity and tissue distribution (Figure 1). Secreted Hh ligands interact with Patched (Ptc)/co-receptor complexes on the surface of responding cells, relieving Ptc-mediated inhibition of the signal transducer Smoothened (Smo) (Figure 4). Activated Smo prevents the processing of full-length Gli transcription factors (Gli-FL) into transcriptional repressors (Gli-R) so as to allow full-length Gli to activate the transcription of Hh target genes. Thus, the relative abundance of Gli transcriptional activators and inhibitors ultimately regulates the transcription of Hh target genes.

Although many aspects of *Drosophila* Hh signaling are conserved in vertebrates, vertebrate Hh signal transduction differs in its requirement for the primary cilium. Primary cilia are slim, microtubule-based non-motile structures that project from the surface of nearly all vertebrate cells but are conspicuously absent from most *Drosophila* cell types (Goetz and Anderson, 2010). The assembly and maintenance of primary cilia requires intraflagellar transport (IFT) proteins, and several members of the IFT family are essential for proper vertebrate Hh signaling (Goetz and Anderson, 2010; Pedersen and

Rosenbaum, 2008). Mutations in components of the kinesin-driven IFT-B complex, which mediates the anterograde transport of molecules from the base of the cilium to the tip, lead to a complete loss of Hh signaling (Goetz and Anderson, 2010). By contrast, mutations in members of the dynein-driven IFT-A complex, which controls retrograde transport, lead to aberrant Hh pathway activation (Goetz and Anderson, 2010). Nonetheless, it is not currently known whether IFT-A and -B complexes interact directly with Hh pathway components to control their localization and activity or if, instead, these complexes facilitate Hh signaling simply by maintaining proper cilia architecture. Indeed, recent genetic studies suggest that the primary cilium may function primarily as a scaffold for Hh signaling, arguing against a direct role for IFT proteins in regulating the movement of Hh pathway components (Ocbina et al., 2011).

In this minireview, we provide an overview of Hh production and cytosolic signaling in vertebrates (for excellent reviews of *Drosophila* Hh signaling, see references (Ingham et al., 2011; Wilson and Chuang, 2010)). We discuss recent insights into ligand release, receptor binding, and signal transduction and attempt to incorporate these findings into existing models of Hh signaling. Additionally, we present remaining questions regarding Hh secretion and signal transduction that warrant further investigation.

Hedgehog processing and release

The signaling activity of Hedgehog ligands is intimately linked to a complex sequence of post-translational modifications ultimately resulting in the covalent attachment of two lipid moieties, one at each terminus (Figure 1). Following translation, Hh precursor peptide approximately 45 kDa in size translocates into the ER lumen

where it undergoes a cholesterol-dependent autocatalytic cleavage to generate a 19 kDa cholesterol modified N-terminal peptide fragment and a 25 kD C-terminal fragment (Figure 1). This cleavage reaction occurs in two steps. In the first step, the free thiol of Cys198 (human Shh) acts as a nucleophile, attacking the carbonyl carbon of the preceding glycine residue and generating a thioester intermediate (Lee et al., 1994; Porter et al., 1996a; Porter et al., 1995; Porter et al., 1996b). In the second step, this thioester intermediate is subject to nucleophilic attack by the 3β hydroxyl group of cholesterol, generating a cholesterol-modified N-terminal fragment (Hh-N) and displacing the C-terminal fragment (Hh-C). While Cys198 has long been recognized for its role in autocatalytic cleavage, a second conserved cysteine, Cys363, is also required for cleavage, forming a disulfide bond with Cys198 that likely facilitates protein folding and reduction of which generates the reactive thiol required for cleavage (Chen et al., 2011a). As such, mutating either cysteine residue prevents autoproteolysis of Hh precursors (Chen et al., 2011a). Although processing-deficient mutants of Shh are able to illicit juxtacrine signaling in cell-based assays (Tokhunts et al., 2010), the significance of this finding remains enigmatic, as Shh is found exclusively in its cleaved form during embryogenesis (Kawakami et al., 2002). Indeed, mutations disrupting the cleavage of full-length Hh peptides have been linked to developmental disorders such as holoprosencephaly (Maity et al., 2005; Traiffort et al., 2004).

Figure 1. Hedgehog processing and release.

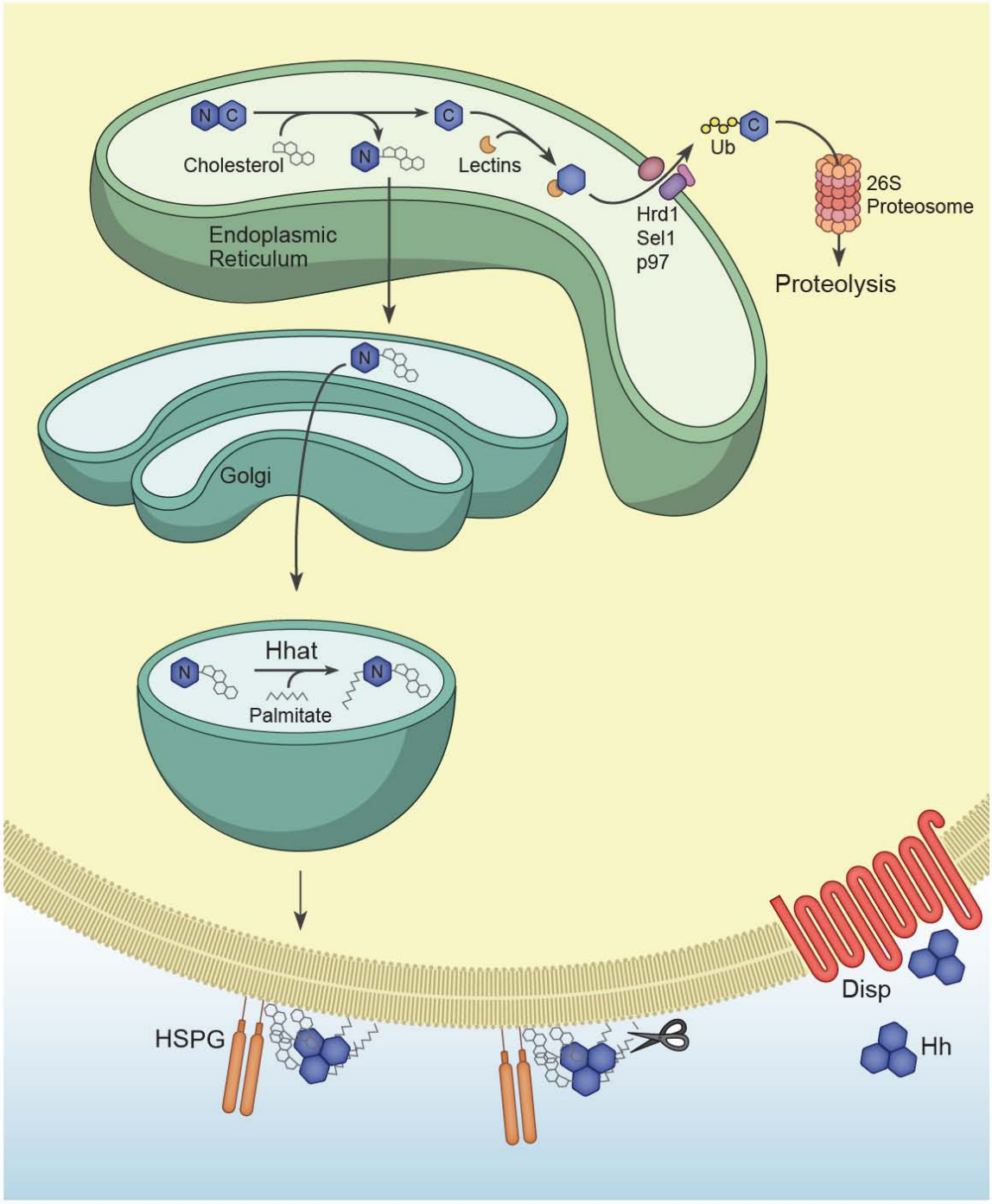

Figure 1. Hedgehog processing and release.
Hedgehog precursor peptides 45 kDa in size undergo a cholesterol-dependent autocatalytic cleavage in the endoplasmic reticulum to generate a cholesterol-modified N-terminal fragment (Hh-N; denoted by N) and a 25 kDa C-terminal fragment (Hh-C, denoted by C). Hh-C is recognized by the lectins OS-9 and XTP3 and ubiquitylated by the ubiquitin ligase Hrd1 and its partner, Sel1. Ubiquitylated Hh-C is moved into the cytosol by the p97 ATPase and subsequently degraded by the proteasome. Cholesterol-modified Hh-N enters the secretory pathway where the acyltransferase Hhat catalyzes the covalent attachment of palmitate to the N-terminal cysteine. Dually lipidated Hh is targeted to the cell membrane, where cholesterol facilitates the assembly of multimeric Hh complexes possibly by tethering Hh to the membrane and promoting interactions with heparin sulfate proteoglycans (HSPGs). Prior to its release, N- and C-terminal peptides may be cleaved by membrane-proximal proteases such as those belonging to the ADAM (A disintegrin and matrix metalloprotease) family, resulting in the removal of both lipid moieties. The twelve-pass transmembrane protein Dispatched (Disp) facilitates the release of Hh multimers into the extracellular environment although the mechanistic details of this process are not well understood.

All of the signaling properties of Hh proteins reside within the N-terminal fragment. The C-terminal fragment undergoes ER-associated degradation (ERAD), a process that requires the lectins OS9 and XTP3, the ubiquitin ligase Hrd1 and its partner Sel1, and the p97 ATPase (Figure 1).The N-terminal fragment (Hh-N) is subject to a second covalent modification by Hh acyltransferase (Hhat)/Skinny Hh (Ski), which catalyzes the attachment of palmitate to the free amino group of the N-terminal cysteine (Buglino and Resh, 2008; Chamoun et al., 2001; Pepinsky et al., 1998). Thus, Hh-N has two covalently attached lipid moieties: cholesterol at its C-terminal end, and palmitate at its N-terminal end.

One unique feature of Hedgehog proteins is their capacity to travel very long distances, up to 300 μm in vertebrate limb, to reach their targets. The release and long-range signaling of the cholesterol- and palmitate-modified Hh-N (hereafter referred to as Hh) requires the activity of Dispatched (Disp), a twelve-pass transmembrane protein belonging to the RND family of bacterial transporters (Burke et al., 1999; Caspary et al., 2002; Kawakami et al., 2002; Ma et al., 2002). While mice and flies deficient in Disp synthesize Hh properly, Hh accumulates in producing cells, able to activate the pathway in neighboring cells but not competent for long-range signaling (Burke et al., 1999; Callejo et al., 2011; Gallet et al., 2003; Li et al., 2006; Ma et al., 2002). While the Hh-distributing function of murine Disp requires two presumptive proton-binding domains in TM4 and TM10, little else is known about how Disp facilitates Hh secretion and long-range signaling (Ma et al., 2002). Recent studies of *Drosophila* imaginal discs indicate that Hh and Disp co-localize within endocytic vesicles and suggest that Disp may traffic Hh to the basolateral membrane where it is released (Callejo et al., 2011). Whether or not the trafficking function of Disp is coupled to its Hh-releasing function, or if these two

activities are distinct, remains to be shown, and additional studies are needed to determine if the trafficking function of Disp is conserved in vertebrates.

Lipid modifications regulate the activity and distribution of Hh

Genetic studies in flies and mice indicate that cholesterol and palmitate are essential for the proper activity and distribution of Hh ligands. The C-terminal cholesterol moiety is required for the formation of multimeric Hh complexes, which are thought to be the biologically relevant form of the morphogen (Eugster et al., 2007; Vyas et al., 2008; Zeng et al., 2001). In cells expressing a truncated form of Hh that cannot be cholesterol modified, Hh proteins are secreted as monomers in a Disp-independent manner (Burke et al., 1999; Huang et al., 2007; Li et al., 2006). While the process by which cholesterol mediates multimerization remains uncertain, one possibility is that by tethering Hh proteins to the membrane, the cholesterol moiety concentrates Hh within specific microdomains, such as lipid rafts, and promotes electrostatic interactions between Hh monomers (Chen et al., 2004a; Dierker et al., 2009a; Dierker et al., 2009b). Cholesterol-mediated clustering may also promote interactions between Hh and other membrane-associated molecules such as heparin sulfate proteoglycans (HSPGs), whose heparin sulfate moieties are known to interact with positively charged residues within a conserved Cardin Weintraub (CW) motif present in all Hh proteins (Figure 2) (Dierker et al., 2009a; Dierker et al., 2009b; Eugster et al., 2007; Vyas et al., 2008). In *Drosophila*, the HS-containing glypicans Dally and Dally-like interact with both Hh and the hemolymph-derived lipoprotein lipophorin, leading to the formation of soluble lipoprotein complexes that mediate patterning in the wing imaginal disc (Eugster et al., 2007; Panakova et al., 2005). Although the addition of HS is sufficient to induce dimerization of

non-cholesterol modified Shh *in vitro*, the composition of vertebrate Hh multimers remains uncharacterized (Dierker et al., 2009b).

In addition to its role in multimerization, cholesterol also regulates the distribution of Hh ligands (Guerrero and Chiang, 2007; Lewis et al., 2001; Li et al., 2006). Although there have been conflicting reports regarding how cholesterol affects Hh distribution, the majority of data are in agreement with a role for cholesterol in restricting the spread of Hh ligands (Callejo et al., 2006; Dawber et al., 2005; Guerrero and Chiang, 2007; Li et al., 2006). Nonetheless, the mechanism by which cholesterol limits the distribution of Hh remains unclear, and the increased range of non-cholesterol modified Hh ligands may be secondary to loss of multimerization or Disp-mediated release. Such an indirect role for cholesterol in regulating Hh distribution is supported by the finding that in *Drosophila*, a cholesterol-modified-form of Hh that cannot multimerize (due to a Lys132Asp mutation) has a restricted distribution and signaling range (Figure 2) (Vyas et al., 2008). Additionally, recent work in vertebrate cell lines suggests that the cholesterol moiety of Shh may be removed by membrane proximal proteases prior to its release (Dierker et al., 2009b). Taken together, these data indicate that the role of cholesterol in determining the range of Hh signaling may not be straightforward and warrants further investigation.

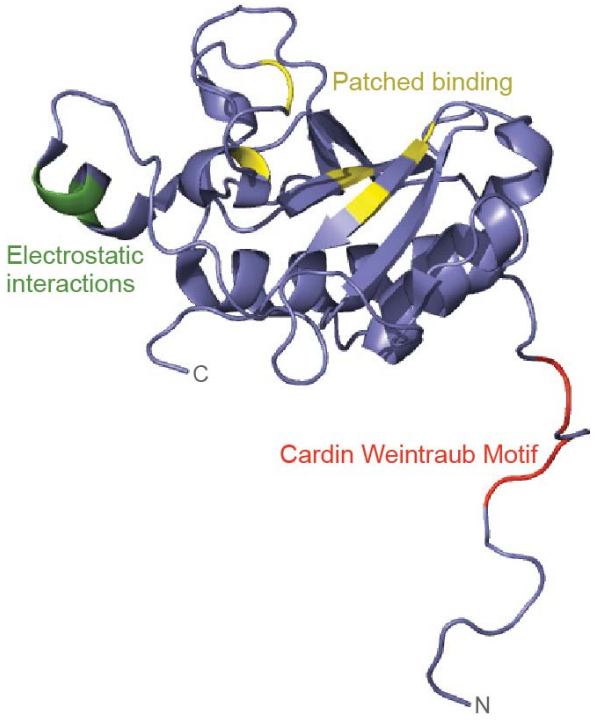

Figure 2. Regions of Shh important for receptor binding and multimerization. Structure of human SHH-N (non-cholesterol-modified N-terminal fragment, PDB: 3M1N (99)). Residues in green (E72, R73 and K75) mediate electrostatic interactions between Hh monomers and are required for multimerization (38). Arg73 is the vertebrate equivalent of Drosophila Lys132, the mutation of which results in decreased long range signaling in the imaginal disc (26). Residues in yellow (H133, H134, H140, H180 and H182) are important for Ptc binding (note that H140 and H182 coordinate with Zinc). Residues in red (K32, R33, R34, K37, K38) form the Cardin Weintraub motif and interact with heparin sulfate. Note how the N-terminus extends away from the globular domain of SHH-N; some of these residues may be cleaved in the formation of active Shh multimers (see text).

Whereas non-cholesterol-modified Hh ligands maintain some of their signaling capacity, loss of palmitoylation abolishes the signaling activity of Hh almost entirely (Chamoun et al., 2001; Chen et al., 2004a; Lee et al., 2001; Pepinsky et al., 1998), indicating that palmitate is absolutely required for Hh signaling. Although the importance of palmitate has long been recognized, only recently have inroads been made in understanding why. Recent work *in vitro* suggests that palmitate facilitates the cleavage of N-terminal amino acids by membrane-proximal proteases such as ADAM (A disintegrin and metalloprotease) family members (Ohlig et al., 2011). Such cleavage is required for the formation of active Shh multimers, as these residues otherwise obstruct the Zn^{2+} coordination site on adjacent molecules, a region that likely interacts with Ptc and is known to regulate Shh stability and activity (Figure 3) (Bishop et al., 2009; Bosanac et al., 2009; Day et al., 1999; Fuse et al., 1999). Thus, in the absence of palmitoylation (due to mutation of the N-terminal Cys), Shh maintains the capacity to multimerize, but these multimers have significantly reduced signaling activity due to their inability to properly interact with Ptc (Ohlig et al., 2011). While these data provide insight into the role of palmitoylation in Hh signaling, they also raise a number of questions regarding the production and secretion of Hh. For instance, how is the cleavage of lipid moieties coupled to Disp-mediated release? Are the lipid moieties of *Drosophila* Hh also cleaved? Future studies are needed to address these questions and to determine if lipid moieties are also cleaved in vivo.

Dual roles of Patched in Hedgehog reception and pathway inhibition

The Hh receptor Patched (Ptc) is a twelve-pass transmembrane protein homology to the RND family of bacterial transporter proteins. Reception of Hh by Ptc is

enhanced by the presence of additional Hh-binding proteins on the cell surface. These presumptive co-receptors include a family of immunoglobulin- and Fibronectin type III (FnIII)-containing integral membrane proteins (Ihog in Boi in *Drosophila*; Cdo and Boc in vertebrates) and the vertebrate-specific cell surface protein Gas1 (Allen et al., 2011; Beachy et al., 2010; Izzi et al., 2011). While removal of a single co-receptor leads to a modest, tissue-specific reduction in Hh pathway activity, removal of two or three co-receptors from *Drosophila* or mice, respectively, leads to a complete loss of signaling, indicating that these co-receptors play an essential role in Hh signaling (Allen et al., 2011; Izzi et al., 2011; Zheng et al., 2010).

In addition to Boc, Cdo, and Gas1, vertebrates harbor a fourth Hh binding protein, Hip, that has no downstream signaling function and likely acts as a decoy receptor by competing with Ptc for Hh binding (Bosanac et al., 2009; Chuang and McMahon, 1999). Analysis of the crystal structure of Hip in complex with Shh reveals that Asp383 of Hip displaces water and completes the tetrahedral coordination of Zn^{2+} in the Shh pseudoactive site (Figure 3) (Bishop et al., 2009; Bosanac et al., 2009). Sequence comparisons of Hip and Ptc reveals that Ptc contains a similar sequence of amino acids capable of binding Shh and competing with Hip for Shh binding, providing novel insight into Hh-receptor interactions (Bosanac et al., 2009). Given that *Drosophila* Hh lacks a Zn^{2+} coordination site and is unable to directly bind Ptc, these data also suggest that Hh-Ptc interactions differs between flies and vertebrates (Beachy et al., 2010). This possible divergence is further supported by the finding that while *Drosophila* Hh binds the second fibronectin III (FnIII) repeat in Ihog, vertebrate Hhs bind a third, non-orthologous FnIII repeat in Cdo (McLellan et al., 2008). Thus, despite the conserved

function of Ptc and co-receptors in Hh signaling, the mode of binding between Hh and these receptor complexes does not appear to be conserved.

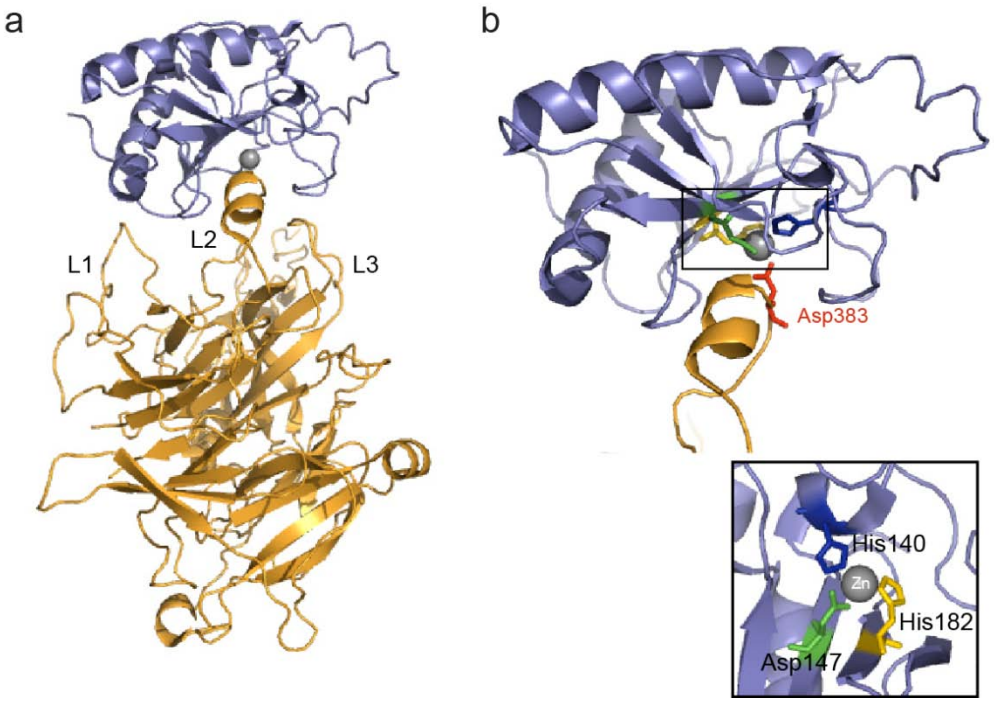

Figure 3. SHH-N receptor binding involves the Zn^{2+} coordination site. a. Structure of human SHH-N in complex with HIP (Hh interacting protein) (PDB: 3HO5 (39)). The L2 loop in the beta-propeller domain of HIP interacts with SHH-N. **b.** HIP binds the pseudoactive site in SHH-N and Asp383 completes the tetrahedral coordination of Zn^{2+} in SHH-N. Inset: His140, His142, and Arg147 of SHH-N coordinate Zn^{2+}. Note that the Zn^{2+} coordination site is also requires for binding to PTC, and PTC likely binds SHH in a manner similar to HIP (see text).

In addition to serving as the Hh receptor, Ptc functions as a potent negative regulator of the Hh pathway by inhibiting the seven-pass transmembrane protein Smoothened (Smo). In the absence of Hh, Ptc localizes to the primary cilium and

maintains Smo in an inactive conformation, preventing Smo from entering the cilium (Rohatgi et al., 2007). While early studies suggested that Ptc could directly bind to and inhibit Smo (Murone et al., 1999), subsequent work revealed that Ptc-mediated inhibition is non-stoichiometric, making direct inhibition unlikely (Taipale et al., 2002). The mechanism by which Ptc inhibits Smo remains enigmatic. Sequence similarities between Ptc and the RND family of bacterial transporter proteins have led many to hypothesize that Ptc may regulate the flux molecules that activate or inhibit Smo, a theory that is supported by the susceptibility of Smo to modulation by small molecules such as the steroidal alkaloid cyclopamine (Chen et al., 2002; Cooper et al., 1998; Taipale et al., 2000). Given that Ptc is enriched around the base of the primary cilium, where vertebrate Hh signaling likely occurs, Ptc might locally control the abundance of Smo inhibitors or activators (Rohatgi et al., 2007). Although a number of Smo agonists and antagonists have been identified, to date none have been shown to be regulated by Ptc. Recent work in *Drosophila* suggests that Ptc may inhibit Hh signaling by regulating the synthesis of phosphotidylinositol 4-phosphate (PI4P), revealing that increased and decreased levels PI4P lead to Hh pathway activation and repression, respectively (Yavari et al., 2010). Importantly, by showing that cells deficient in Ptc have increased PI4P levels, this work provides the first evidence of an endogenous Hh activator that is regulated by Ptc. Nonetheless, future studies are needed to determine how Ptc regulates PI4P synthesis and verify that PI4P activates the pathway at the level of Smo rather than acting further downstream.

Transcriptional repression in the absence of Hh

The zinc finger-containing Gli transcription factors are the principle effectors of canonical Hh signaling. Depending on the availability of Hh ligands, Gli proteins function either as transcriptional activators or repressors. In the absence of Hh, full-length Gli (Gli-FL) is proteolytically processed to yield a truncated N-terminal transcriptional repressor (Gli-R) (Figure 4a). Whereas *Drosophila* harbor a single Gli family member, Cubitus Interruptus (Ci), vertebrates have three, Gli1-Gli3. Of these, Gli2 and Gli3 function as both transcriptional activators and repressors while Gli1 is a target of Hh signaling and exists only as an activator.

Although many aspects of vertebrate Gli-R formation remain enigmatic, processing requires Suppressor of Fused (Sufu), the kinesin Kif7 and the primary cilium (Figure 4a) (Cheung et al., 2009; Endoh-Yamagami et al., 2009; Goetz and Anderson, 2010; Liem et al., 2009; Svard et al., 2006). Sufu stabilizes full-length Gli2 and Gli3 and sequesters both proteins in the cytosol, thus preventing their nuclear translocation and activation (Humke et al., 2010; Tukachinsky et al., 2010; Wang et al., 2010; Wilson and Chuang, 2010). Sufu also promotes the phosphorylation of C-terminal residues in Gli-FL by protein kinase A (PKA), which primes full-length Gli for further phosphorylation by glycogen synthase kinase 3β (GSK3β) and casein kinase 1α (CK1α) (Kise et al., 2009; Tempe et al., 2006). Phosphorylated Gli-FL is recognized by the E3 ubiquitin ligase βTrCP, leading to the ubiquitylation and degradation of C-terminal peptides to generate Gli-R (Bhatia et al., 2006; Kise et al., 2009; Tempe et al., 2006; Wang and Li, 2006). In contrast to its relatively minor role in *Drosophila*, Sufu is absolutely required for proper development and essential for Gli-R formation in vertebrates (Cooper et al., 2005; Svard

et al., 2006). Mice deficient in Sufu die around embryonic day 9.5 with significantly reduced levels of both full-length and repressor forms of Gli and features of aberrant Hedgehog activation that resemble loss of Ptc (Cooper et al., 2005; Svard et al., 2006). In the absence of Sufu, Gli-FL enters the nucleus and is converted into a labile transcriptional activator (Gli-A) that is quickly degraded within the nucleus in a manner that depends upon the cullin3-based ubiquitin ligase adaptor Spop (Chen et al., 2009; Wang et al., 2010; Zhang et al., 2009; Zhang et al., 2006). Indeed, Sufu and Spop have been shown to compete for Gli binding, and loss of Spop from *Sufu*$^{-/-}$ cells leads to a significant recovery in full-length Gli levels (Wang et al., 2010). Together, these data indicate that Sufu regulates Gli-R formation by stabilizing full-length Gli in the cytosol and preventing Spop-dependent degradation in the nucleus. In addition to its role in Gli processing, Sufu may also inhibit the transcription of Hh target genes through its interaction with SAP18, a component of the mSin3-histone deacetylase repressor complex (Cheng and Bishop, 2002). However, this processing-independent role for Sufu was recently challenged (Chen et al., 2009), and additional data are needed to clarify the function of nuclear Sufu in Hh pathway inhibition.

In addition to Sufu, the kinesin 4 family member Kif7 also appears to be required for optimal Gli processing (Cheung et al., 2009; Endoh-Yamagami et al., 2009; Liem et al., 2009; Tay et al., 2005). Mice deficient in Kif7 have increased levels of Gli-FL, decreased levels of Gli-R and exhibit features of pathway de-repression such as polydactyly (Cheung et al., 2009; Endoh-Yamagami et al., 2009; Liem et al., 2009). Although the mechanism by which Kif7 promotes Gli processing remains unclear, one possibility is that, like its *Drosophila* homolog Costal2 (Cos2), Kif7 recruits PKA, GSK3β and CK1α to phosphorylate Gli-FL (Figure 4a). Although Kif7 has been shown to interact

with Gli, additional data are needed to determine if the scaffolding function of Kif7 is conserved in vertebrates.

Studies both in vivo and in vitro indicate that the primary cilium is required for efficient processing of Gli-FL into Gli-R (Goetz and Anderson, 2010). Interestingly, the role of Sufu in Gli-R production appears to be independent of cilia, as cells lacking both primary cilia and Sufu exhibit unkempt Hh pathway activity akin to *Sufu*$^{-/-}$ cells (Chen et al., 2009; Jia et al., 2009). By contrast, the role of Kif7 in Gli processing is cilia-dependent, as mice lacking both cilia and Kif7 resemble cilia mutants (Liem et al., 2009). Although the exact function of the cilium in Gli processing remains enigmatic, the cilium may serve as a platform for Gli processing machinery. Indeed, Kif7, PKA, GSK3β and CK1α are present in the primary cilia and/or basal body in the absence of Hh signaling (Chen et al., 2011b; Cheung et al., 2009; Endoh-Yamagami et al., 2009; Fumoto et al., 2006; Liem et al., 2009; Tuson et al., 2011). Although Sufu cannot localize to the cilium on its own, it is likely recruited there by Gli, as low levels of both Sufu and Gli can be observed in the cilium even in the absence of Hh signaling (Humke et al., 2010; Tukachinsky et al., 2010). Thus, although Gli-Sufu complexes form throughout the cytosol, they may be directed to the cilium by Gli for efficient processing in a Kif7- and kinase-dependent manner.

Although Gli2 and Gli3 both undergo partial proteolytic degradation in the absence of Hh, the processing of Gli3 is significantly more efficient than that of Gli2 (Pan et al., 2006). Consequently, Gli3-R serves as the principle transcriptional repressor of Hh signaling in the absence of ligand, while Gli2-A functions as the predominant transcriptional activator (Hui and Angers, 2011). The increased efficiency of Gli3 processing is due in large part to the sequence of a 200 residue processing determinant

domain (PDD) in its C-terminus (Pan and Wang, 2007). Together with an appropriate degron and the zinc finger domain, the PDD forms a three part signal that is essential for efficient Gli3 processing (Schrader et al., 2011). But what happens to full-length Gli2 in the absence of Hh? Like Gli3, the C-terminus of Gli2 is phosphorylated by PKA in the absence of Hh. Although this phosphorylation leads to a limited amount of processing, it may also destabilize Gli2-FL, leading to complete degradation by the proteosome (Pan et al., 2006; Pan et al., 2009b) . Such a processing-independent role of PKA in Hh pathway inhibition is supported by recent genetic data showing that mice lacking both catalytic subunits of PKA (*Prkaca*$^{-/-}$; *Prkacb*$^{-/-}$) die mid-gestation with a completely ventralized neural tube, a defect that cannot be explained by loss of Gli processing alone and suggests a increase in Gli activation (Huang et al., 2002; Tuson et al., 2011). Given that PKA may also regulate the entry of Sufu-Gli complexes into the cilium, additional studies are required to clarify the mechanism(s) by which PKA inhibits Gli activation and determine to what extent Gli2 phosphorylation inhibits pathway activation (Chen et al., 2011c; Tukachinsky et al., 2010; Tuson et al., 2011).

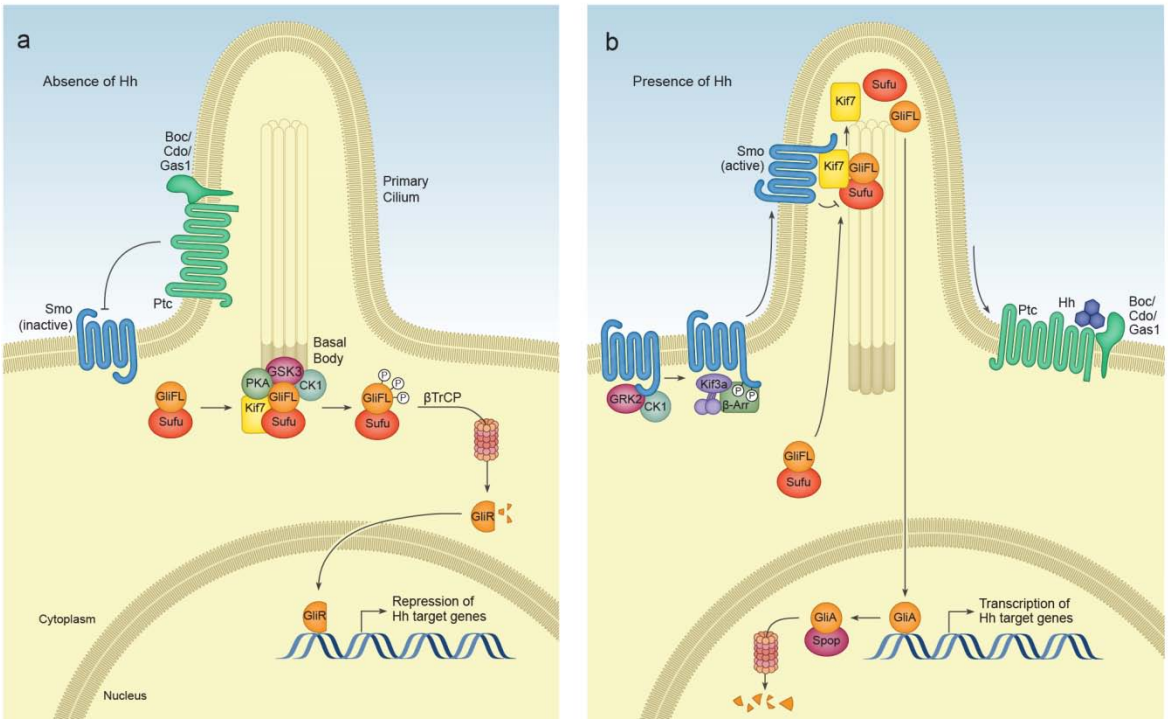

Figure 4. Vertebrate Hedgehog signal transduction. a. In the absence of ligand, the twelve-pass transmembrane protein Patched (Ptc) localizes to the primary cilium base and maintains Smo in an inactive conformation. Full length Gli transcription factors (Gli-FL) complex with Suppressor of Fused (Sufu). Sufu sequesters Gli-FL in the cytosol and stabilizes the protein. Sufu and the kinesin 4 family member Kif7 promote the phosphorylation of C-terminal residues in full length Gli by protein kinase A (PKA), glycogen synthase kinase 3β (GSK3) and casein kinase 1α (CK1), which may occur at the basal body of the primary cilium. Phosphorylated Gli-FL is recognized by the E3 ubiquitin ligase βTrCP, resulting in ubiquitylation and proteosomal degradation of C-terminal residues to generate a truncated N-terminal transcriptional repressor (Gli-R) that inhibits Hh target gene transcription. **b.** In the presence of ligand, Hh binding to Ptc causes Ptc to exit the cilium and relieves its inhibition of Smo. Smo is phosphorylated by CK1α and G-coupled protein receptor kinase 2 (GRK2), inducing a conformational change and enabling β-arrestin- and Kif3a-dependent transport into the cilium. Within the cilium, activated Smo promotes the disassembly of Sufu-Gli complexes. Kif7 also localizes to the cilium in the presence of Hh likely assists Smo in this disassembly. Full-length Gli accumulates in the tip of the cilium and is shuttled into the nucleus, perhaps on cytoplasmic microtubules. Within the nucleus, Gli-FL receives additional modifications that convert it to a labile transcriptional activator (Gli-A) that activates Hh target genes. Gli-A is subsequently degraded in a manner that requires the Cullin3-adaptor Spop.

Smoothened and Gli activation in the presence of Hedgehog

In the presence of Hh, Ptc relieves its inhibition of Smo and allows Smo to become activated. Despite significant sequence differences, many aspects of *Drosophila* Smo activation are conserved in vertebrates. In *Drosophila,* phosphorylation of C-terminal residues by PKA, CK1, and G-coupled protein receptor kinase 2 (GRK2) cause Smo to adopt an open conformation and promote its accumulation on the membrane (Apionishev et al., 2005; Chen et al., 2010; Jia et al., 2004; Lum et al., 2003; Molnar et al., 2007; Su et al., 2011). Although the C-terminus of vertebrate Smo differs significantly from *Drosophila* and lacks PKA phosphorylation sites, recent data indicate that vertebrate Smo is also phosphorylated in response to Hh signaling (Chen et al., 2004b; Chen et al., 2011b; Meloni et al., 2006). CK1α and GRK2 phosphorylate the C-terminal tail of vertebrate Smo, inducing conformational changes and facilitating its lateral translocation into the primary cilium (Figure 4b) (Chen et al., 2011b). The movement of Smo into the cilium is dependent upon β-Arrestins and the kinesin 2 motor subunit Kif3a, both of which are recruited to Smo following its phosphorylation by CK1α and GRK2 (Chen et al., 2004b; Chen et al., 2011b; Kovacs et al., 2008; Milenkovic et al., 2009).

Activated Smo both inhibits Gli processing as well as promotes additional ill-defined modifications that convert full-length Gli proteins into transcriptional activators. Although the details of this process remain somewhat enigmatic, activated Smo likely promotes the disassembly of Sufu-Gli complexes that accumulate in the cilium following pathway activation (Figure 4b) (Humke et al., 2010; Tukachinsky et al., 2010; Wang et al., 2010; Zeng et al., 2010). Kif7 may also promote Sufu-Gli disassembly, as it localizes to the cilium in response to Hh and interacts with overexpressed Smo in tissue culture

cells (Endoh-Yamagami et al., 2009). Indeed, such a positive role of Kif7 in Hh signaling is consistent with the finding that mice deficient in *Kif7* exhibit features of decreased Hh pathway activity, such as reduced *Ptc* expression in the notochord and floor plate (Endoh-Yamagami et al., 2009; Liem et al., 2009). Nonetheless, additional studies are needed to determine if Kif7-Smo interactions are dependent on Smo phosphorylation, as they are for *Drosophila* Cos2 (Jia et al., 2003; Shi et al., 2011). The disassembly of Sufu-Gli complexes allows full-length Gli to enter the nucleus where it is converted to its activator form (Gli-A) (Tukachinsky et al., 2010). The translocation of Gli requires cytoplasmic microtubules, as microtubule de-stabilizing agents such as nocodazole have been shown to inhibit its nuclear accumulation and activity (Humke et al., 2010; Kim et al., 2009). While the details of Gli activation remain nebulous, they may involve phosphorylation, as Gli2 and Gli3 appear to be phosphorylated within the nucleus in response to Hh (Humke et al., 2010). Given that the nucleus is also the site of Spop-mediated degradation, however, it is difficult to ascertain whether this phosphorylation is coupled to Gli activation or degradation (Chen et al., 2009; Wang et al., 2010). Gli proteins might also be deacetylated in response to Hh stimulation, as *HDAC1* overexpression in tissue culture cells leads to Gli1 deacetylation (Canettieri et al., 2010). Activated Gli promotes the transcription of genes involved in differentiation, proliferation, and cell survival as well as several negative regulators of the pathway, such as *Ptc* and *Hip* to downregulate pathway activity.

Conclusions and Perspectives

Over the past two decades, mouse and fly genetics have been instrumental in identifying components of the Hh pathway and elucidating their functions, revealing a

high degree of conservation between the two species. The discovery that vertebrate Hh signaling requires the primary cilium, however, has significantly changed how the pathway is studied and made it somewhat more difficult to draw comparisons between vertebrates and flies. Despite these challenges, significant progress has been made in defining vertebrate Hh signal transduction. Nonetheless, several questions regarding vertebrate Hh secretion and signal transduction remain unanswered. The mechanistic details of Disp-mediated secretion remain elusive, as does the composition of secreted Hh multimers. The mechanism by which Ptc inhibits Smo continues to be a mystery, and a detailed understanding of how activated Smo promotes Gli activation is lacking. Additional studies are needed to examine Kif7's role in Gli processing and activation as well as determine to what extent the motor function of Kif7 is important for Hh signaling. But perhaps most intriguing is the question of how, and why, the primary cilium plays such an essential role in vertebrate Hh signal transduction. As cell and developmental biologists continue to adapt to the challenges inherent in the study of vertebrate Hh signaling, the answers to these and other questions will undoubtedly be revealed.

Acknowledgements

We thank members of the Chiang lab for their support and suggestions, Elizabeth Dong for her help generating Figures 2 and 3, and Bruce Carter and Laura Lee for their assistance revising and organizing the manuscript.

REFERENCES

Allen, B.L., Song, J.Y., Izzi, L., Althaus, I.W., Kang, J.S., Charron, F., Krauss, R.S., and McMahon, A.P. (2011). Overlapping roles and collective requirement for the coreceptors GAS1, CDO, and BOC in SHH pathway function. Dev Cell *20*, 775-787.

Altman, J., and Bayer, S. (1997). Development of the cerebellar system: in relation to its evolution, structure, and functions, 1 edn (New York, CRC Press, Inc).

Anne, S.L., Govek, E.E., Ayrault, O., Kim, J.H., Zhu, X., Murphy, D.A., Van Aelst, L., Roussel, M.F., and Hatten, M.E. (2013). WNT3 inhibits cerebellar granule neuron progenitor proliferation and medulloblastoma formation via MAPK activation. PLoS One *8*, e81769.

Apionishev, S., Katanayeva, N.M., Marks, S.A., Kalderon, D., and Tomlinson, A. (2005). Drosophila Smoothened phosphorylation sites essential for Hedgehog signal transduction. Nat Cell Biol *7*, 86-92.

Asada, N., and Sanada, K. (2010). LKB1-mediated spatial control of GSK3beta and adenomatous polyposis coli contributes to centrosomal forward movement and neuronal migration in the developing neocortex. J Neurosci *30*, 8852-8865.

Asada, N., Sanada, K., and Fukada, Y. (2007). LKB1 regulates neuronal migration and neuronal differentiation in the developing neocortex through centrosomal positioning. J Neurosci *27*, 11769-11775.

Baas, A.F., Boudeau, J., Sapkota, G.P., Smit, L., Medema, R., Morrice, N.A., Alessi, D.R., and Clevers, H.C. (2003). Activation of the tumour suppressor kinase LKB1 by the STE20-like pseudokinase STRAD. EMBO J *22*, 3062-3072.

Baas, A.F., Kuipers, J., van der Wel, N.N., Batlle, E., Koerten, H.K., Peters, P.J., and Clevers, H.C. (2004). Complete polarization of single intestinal epithelial cells upon activation of LKB1 by STRAD. Cell *116*, 457-466.

Balsters, J.H., Cussans, E., Diedrichsen, J., Phillips, K.A., Preuss, T.M., Rilling, J.K., and Ramnani, N. (2010). Evolution of the cerebellar cortex: the selective expansion of prefrontal-projecting cerebellar lobules. Neuroimage *49*, 2045-2052.

Bardeesy, N., Sinha, M., Hezel, A.F., Signoretti, S., Hathaway, N.A., Sharpless, N.E., Loda, M., Carrasco, D.R., and DePinho, R.A. (2002). Loss of the Lkb1 tumour suppressor provokes intestinal polyposis but resistance to transformation. Nature *419*, 162-167.

Barnes, A.P., Lilley, B.N., Pan, Y.A., Plummer, L.J., Powell, A.W., Raines, A.N., Sanes, J.R., and Polleux, F. (2007). LKB1 and SAD kinases define a pathway required for the polarization of cortical neurons. Cell *129*, 549-563.

Beachy, P.A., Hymowitz, S.G., Lazarus, R.A., Leahy, D.J., and Siebold, C. (2010). Interactions between Hedgehog proteins and their binding partners come into view. Genes Dev *24*, 2001-2012.

Bellebaum, C., and Daum, I. (2011). Mechanisms of cerebellar involvement in associative learning. Cortex *47*, 128-136.

Ben-Arie, N., Bellen, H.J., Armstrong, D.L., McCall, A.E., Gordadze, P.R., Guo, Q., Matzuk, M.M., and Zoghbi, H.Y. (1997). Math1 is essential for genesis of cerebellar granule neurons. Nature *390*, 169-172.

Bhatia, B., Northcott, P.A., Hambardzumyan, D., Govindarajan, B., Brat, D.J., Arbiser, J.L., Holland, E.C., Taylor, M.D., and Kenney, A.M. (2009). Tuberous sclerosis complex suppression in cerebellar development and medulloblastoma: separate regulation of mammalian target of rapamycin activity and p27 Kip1 localization. Cancer Res *69*, 7224-7234.

Bhatia, N., Thiyagarajan, S., Elcheva, I., Saleem, M., Dlugosz, A., Mukhtar, H., and Spiegelman, V.S. (2006). Gli2 is targeted for ubiquitination and degradation by beta-TrCP ubiquitin ligase. J Biol Chem *281*, 19320-19326.

Bishop, B., Aricescu, A.R., Harlos, K., O'Callaghan, C.A., Jones, E.Y., and Siebold, C. (2009). Structural insights into hedgehog ligand sequestration by the human hedgehog-interacting protein HHIP. Nat Struct Mol Biol *16*, 698-703.

Bonaccorsi, S., Mottier, V., Giansanti, M.G., Bolkan, B.J., Williams, B., Goldberg, M.L., and Gatti, M. (2007). The Drosophila Lkb1 kinase is required for spindle formation and asymmetric neuroblast division. Development *134*, 2183-2193.

Borghesani, P.R., Peyrin, J.M., Klein, R., Rubin, J., Carter, A.R., Schwartz, P.M., Luster, A., Corfas, G., and Segal, R.A. (2002). BDNF stimulates migration of cerebellar granule cells. Development *129*, 1435-1442.

Borrell, V., and Gotz, M. (2014). Role of radial glial cells in cerebral cortex folding. Curr Opin Neurobiol *27C*, 39-46.

Bosanac, I., Maun, H.R., Scales, S.J., Wen, X., Lingel, A., Bazan, J.F., de Sauvage, F.J., Hymowitz, S.G., and Lazarus, R.A. (2009). The structure of SHH in complex with HHIP reveals a recognition role for the Shh pseudo active site in signaling. Nat Struct Mol Biol *16*, 691-697.

Boudeau, J., Sapkota, G., and Alessi, D.R. (2003). LKB1, a protein kinase regulating cell proliferation and polarity. FEBS Lett *546*, 159-165.

Buglino, J.A., and Resh, M.D. (2008). Hhat is a palmitoylacyltransferase with specificity for N-palmitoylation of Sonic Hedgehog. J Biol Chem *283*, 22076-22088.

Burke, R., Nellen, D., Bellotto, M., Hafen, E., Senti, K.A., Dickson, B.J., and Basler, K. (1999). Dispatched, a novel sterol-sensing domain protein dedicated to the release of cholesterol-modified hedgehog from signaling cells. Cell *99*, 803-815.

Callejo, A., Bilioni, A., Mollica, E., Gorfinkiel, N., Andres, G., Ibanez, C., Torroja, C., Doglio, L., Sierra, J., and Guerrero, I. (2011). Dispatched mediates Hedgehog basolateral release to form the long-range morphogenetic gradient in the Drosophila wing disk epithelium. Proc Natl Acad Sci U S A *108*, 12591-12598.

Callejo, A., Torroja, C., Quijada, L., and Guerrero, I. (2006). Hedgehog lipid modifications are required for Hedgehog stabilization in the extracellular matrix. Development *133*, 471-483.

Canettieri, G., Di Marcotullio, L., Greco, A., Coni, S., Antonucci, L., Infante, P., Pietrosanti, L., De Smaele, E., Ferretti, E., Miele, E.*, et al.* (2010). Histone deacetylase and Cullin3-REN(KCTD11) ubiquitin ligase interplay regulates Hedgehog signalling through Gli acetylation. Nat Cell Biol *12*, 132-142.

Carretero, J., Medina, P.P., Blanco, R., Smit, L., Tang, M., Roncador, G., Maestre, L., Conde, E., Lopez-Rios, F., Clevers, H.C.*, et al.* (2007). Dysfunctional AMPK activity, signalling through mTOR and survival in response to energetic stress in LKB1-deficient lung cancer. Oncogene *26*, 1616-1625.

Carson, R.P., Van Nielen, D.L., Winzenburger, P.A., and Ess, K.C. (2012). Neuronal and glia abnormalities in Tsc1-deficient forebrain and partial rescue by rapamycin. Neurobiol Dis *45*, 369-380.

Caspary, T., Garcia-Garcia, M.J., Huangfu, D., Eggenschwiler, J.T., Wyler, M.R., Rakeman, A.S., Alcorn, H.L., and Anderson, K.V. (2002). Mouse Dispatched homolog1 is required for long-range, but not juxtacrine, Hh signaling. Curr Biol *12*, 1628-1632.

Chamoun, Z., Mann, R.K., Nellen, D., von Kessler, D.P., Bellotto, M., Beachy, P.A., and Basler, K. (2001). Skinny hedgehog, an acyltransferase required for palmitoylation and activity of the hedgehog signal. Science *293*, 2080-2084.

Chartier, N.T., Salazar Ospina, D.P., Benkemoun, L., Mayer, M., Grill, S.W., Maddox, A.S., and Labbe, J.C. (2011). PAR-4/LKB1 mobilizes nonmuscle myosin through anillin to regulate C. elegans embryonic polarization and cytokinesis. Curr Biol *21*, 259-269.

Chedotal, A. (2010). Should I stay or should I go? Becoming a granule cell. Trends Neurosci *33*, 163-172.

Chen, J.K., Taipale, J., Cooper, M.K., and Beachy, P.A. (2002). Inhibition of Hedgehog signaling by direct binding of cyclopamine to Smoothened. Genes Dev *16*, 2743-2748.

Chen, M.H., Li, Y.J., Kawakami, T., Xu, S.M., and Chuang, P.T. (2004a). Palmitoylation is required for the production of a soluble multimeric Hedgehog protein complex and long-range signaling in vertebrates. Genes Dev *18*, 641-659.

Chen, M.H., Wilson, C.W., Li, Y.J., Law, K.K., Lu, C.S., Gacayan, R., Zhang, X., Hui, C.C., and Chuang, P.T. (2009). Cilium-independent regulation of Gli protein function by Sufu in Hedgehog signaling is evolutionarily conserved. Genes Dev *23*, 1910-1928.

Chen, W., Ren, X.R., Nelson, C.D., Barak, L.S., Chen, J.K., Beachy, P.A., de Sauvage, F., and Lefkowitz, R.J. (2004b). Activity-dependent internalization of smoothened mediated by beta-arrestin 2 and GRK2. Science *306*, 2257-2260.

Chen, X., Tukachinsky, H., Huang, C.H., Jao, C., Chu, Y.R., Tang, H.Y., Mueller, B., Schulman, S., Rapoport, T.A., and Salic, A. (2011a). Processing and turnover of the Hedgehog protein in the endoplasmic reticulum. J Cell Biol *192*, 825-838.

Chen, Y., Li, S., Tong, C., Zhao, Y., Wang, B., Liu, Y., Jia, J., and Jiang, J. (2010). G protein-coupled receptor kinase 2 promotes high-level Hedgehog signaling by regulating the active state of Smo through kinase-dependent and kinase-independent mechanisms in Drosophila. Genes Dev *24*, 2054-2067.

Chen, Y., Sasai, N., Ma, G., Yue, T., Jia, J., Briscoe, J., and Jiang, J. (2011b). Sonic Hedgehog dependent phosphorylation by CK1alpha and GRK2 is required for ciliary accumulation and activation of smoothened. PLoS Biol *9*, e1001083.

Chen, Y., Yue, S., Xie, L., Pu, X.H., Jin, T., and Cheng, S.Y. (2011c). Dual Phosphorylation of suppressor of fused (Sufu) by PKA and GSK3beta regulates its stability and localization in the primary cilium. J Biol Chem *286*, 13502-13511.

Cheng, F.Y., Huang, X., Sarangi, A., Ketova, T., Cooper, M.K., Litingtung, Y., and Chiang, C. (2012). Widespread contribution of Gdf7 lineage to cerebellar cell types and implications for hedgehog-driven medulloblastoma formation. PLoS One *7*, e35541.

Cheng, S.Y., and Bishop, J.M. (2002). Suppressor of Fused represses Gli-mediated transcription by recruiting the SAP18-mSin3 corepressor complex. Proc Natl Acad Sci U S A *99*, 5442-5447.

Cheng, Y., Sudarov, A., Szulc, K.U., Sgaier, S.K., Stephen, D., Turnbull, D.H., and Joyner, A.L. (2010). The Engrailed homeobox genes determine the different foliation patterns in the vermis and hemispheres of the mammalian cerebellum. Development *137*, 519-529.

Cheung, H.O., Zhang, X., Ribeiro, A., Mo, R., Makino, S., Puviindran, V., Law, K.K., Briscoe, J., and Hui, C.C. (2009). The kinesin protein Kif7 is a critical regulator of Gli transcription factors in mammalian hedgehog signaling. Sci Signal *2*, ra29.

Chizhikov, V.V., Lindgren, A.G., Currle, D.S., Rose, M.F., Monuki, E.S., and Millen, K.J. (2006). The roof plate regulates cerebellar cell-type specification and proliferation. Development *133*, 2793-2804.

Chizhikov, V.V., Lindgren, A.G., Mishima, Y., Roberts, R.W., Aldinger, K.A., Miesegaes, G.R., Currle, D.S., Monuki, E.S., and Millen, K.J. (2010). Lmx1a regulates fates and location of cells originating from the cerebellar rhombic lip and telencephalic cortical hem. Proc Natl Acad Sci U S A *107*, 10725-10730.

Choi, Y., Borghesani, P.R., Chan, J.A., and Segal, R.A. (2005). Migration from a mitogenic niche promotes cell-cycle exit. J Neurosci *25*, 10437-10445.

Chuang, P.T., and McMahon, A.P. (1999). Vertebrate Hedgehog signalling modulated by induction of a Hedgehog-binding protein. Nature *397*, 617-621.

Clark, D.A., Mitra, P.P., and Wang, S.S. (2001). Scalable architecture in mammalian brains. Nature *411*, 189-193.

Cooper, A.F., Yu, K.P., Brueckner, M., Brailey, L.L., Johnson, L., McGrath, J.M., and Bale, A.E. (2005). Cardiac and CNS defects in a mouse with targeted disruption of suppressor of fused. Development *132*, 4407-4417.

Cooper, J.A. (2013). Cell biology in neuroscience: mechanisms of cell migration in the nervous system. J Cell Biol *202*, 725-734.

Cooper, M.K., Porter, J.A., Young, K.E., and Beachy, P.A. (1998). Teratogen-mediated inhibition of target tissue response to Shh signaling. Science *280*, 1603-1607.

Corrales, J.D., Blaess, S., Mahoney, E.M., and Joyner, A.L. (2006). The level of sonic hedgehog signaling regulates the complexity of cerebellar foliation. Development *133*, 1811-1821.

Corrales, J.D., Rocco, G.L., Blaess, S., Guo, Q., and Joyner, A.L. (2004). Spatial pattern of sonic hedgehog signaling through Gli genes during cerebellum development. Development *131*, 5581-5590.

Courchet, J., Lewis, T.L., Jr., Lee, S., Courchet, V., Liou, D.Y., Aizawa, S., and Polleux, F. (2013). Terminal axon branching is regulated by the LKB1-NUAK1 kinase pathway via presynaptic mitochondrial capture. Cell *153*, 1510-1525.

Dahmane, N., and Ruiz i Altaba, A. (1999). Sonic hedgehog regulates the growth and patterning of the cerebellum. Development *126*, 3089-3100.

Dasgupta, B., and Milbrandt, J. (2009). AMP-activated protein kinase phosphorylates retinoblastoma protein to control mammalian brain development. Dev Cell *16*, 256-270.

Dawber, R.J., Hebbes, S., Herpers, B., Docquier, F., and van den Heuvel, M. (2005). Differential range and activity of various forms of the Hedgehog protein. BMC Dev Biol *5*, 21.

Day, E.S., Wen, D., Garber, E.A., Hong, J., Avedissian, L.S., Rayhorn, P., Shen, W., Zeng, C., Bailey, V.R., Reilly, J.O.*, et al.* (1999). Zinc-dependent structural stability of human Sonic hedgehog. Biochemistry *38*, 14868-14880.

Dey, J., Ditzler, S., Knoblaugh, S.E., Hatton, B.A., Schelter, J.M., Cleary, M.A., Mecham, B., Rorke-Adams, L.B., and Olson, J.M. (2012). A distinct Smoothened mutation causes severe cerebellar developmental defects and medulloblastoma in a novel transgenic mouse model. Mol Cell Biol *32*, 4104-4115.

Dierker, T., Dreier, R., Migone, M., Hamer, S., and Grobe, K. (2009a). Heparan sulfate and transglutaminase activity are required for the formation of covalently cross-linked hedgehog oligomers. J Biol Chem *284*, 32562-32571.

Dierker, T., Dreier, R., Petersen, A., Bordych, C., and Grobe, K. (2009b). Heparan sulfate-modulated, metalloprotease-mediated sonic hedgehog release from producing cells. J Biol Chem *284*, 8013-8022.

Ducharme, N.A., Hales, C.M., Lapierre, L.A., Ham, A.J., Oztan, A., Apodaca, G., and Goldenring, J.R. (2006). MARK2/EMK1/Par-1Balpha phosphorylation of Rab11-family interacting protein 2 is necessary for the timely establishment of polarity in Madin-Darby canine kidney cells. Mol Biol Cell *17*, 3625-3637.

Dzamko, N., van Denderen, B.J., Hevener, A.L., Jorgensen, S.B., Honeyman, J., Galic, S., Chen, Z.P., Watt, M.J., Campbell, D.J., Steinberg, G.R.*, et al.* (2010). AMPK beta1 deletion reduces appetite, preventing obesity and hepatic insulin resistance. J Biol Chem *285*, 115-122.

Edmondson, J.C., Liem, R.K., Kuster, J.E., and Hatten, M.E. (1988). Astrotactin: a novel neuronal cell surface antigen that mediates neuron-astroglial interactions in cerebellar microcultures. J Cell Biol *106*, 505-517.

Endoh-Yamagami, S., Evangelista, M., Wilson, D., Wen, X., Theunissen, J.W., Phamluong, K., Davis, M., Scales, S.J., Solloway, M.J., de Sauvage, F.J.*, et al.* (2009). The mammalian Cos2 homolog Kif7 plays an essential role in modulating Hh signal transduction during development. Curr Biol *19*, 1320-1326.

Eugster, C., Panakova, D., Mahmoud, A., and Eaton, S. (2007). Lipoprotein-heparan sulfate interactions in the Hh pathway. Dev Cell *13*, 57-71.

Famulski, J.K., Trivedi, N., Howell, D., Yang, Y., Tong, Y., Gilbertson, R., and Solecki, D.J. (2010). Siah regulation of Pard3A controls neuronal cell adhesion during germinal zone exit. Science *330*, 1834-1838.

Fatemi, S.H., Aldinger, K.A., Ashwood, P., Bauman, M.L., Blaha, C.D., Blatt, G.J., Chauhan, A., Chauhan, V., Dager, S.R., Dickson, P.E.*, et al.* (2012). Consensus paper: pathological role of the cerebellum in autism. Cerebellum *11*, 777-807.

Fishell, G., and Hatten, M.E. (1991). Astrotactin provides a receptor system for CNS neuronal migration. Development *113*, 755-765.

Fleming, J.T., He, W., Hao, C., Ketova, T., Pan, F.C., Wright, C.C., Litingtung, Y., and Chiang, C. (2013). The Purkinje neuron acts as a central regulator of spatially and functionally distinct cerebellar precursors. Dev Cell *27*, 278-292.

Fumoto, K., Hoogenraad, C.C., and Kikuchi, A. (2006). GSK-3beta-regulated interaction of BICD with dynein is involved in microtubule anchorage at centrosome. EMBO J *25*, 5670-5682.

Fuse, N., Maiti, T., Wang, B., Porter, J.A., Hall, T.M., Leahy, D.J., and Beachy, P.A. (1999). Sonic hedgehog protein signals not as a hydrolytic enzyme but as an apparent ligand for patched. Proc Natl Acad Sci U S A *96*, 10992-10999.

Gallet, A., Rodriguez, R., Ruel, L., and Therond, P.P. (2003). Cholesterol modification of hedgehog is required for trafficking and movement, revealing an asymmetric cellular response to hedgehog. Dev Cell *4*, 191-204.

Goetz, S.C., and Anderson, K.V. (2010). The primary cilium: a signalling centre during vertebrate development. Nat Rev Genet *11*, 331-344.

Goldowitz, D., Cushing, R.C., Laywell, E., D'Arcangelo, G., Sheldon, M., Sweet, H.O., Davisson, M., Steindler, D., and Curran, T. (1997). Cerebellar disorganization characteristic of reeler in scrambler mutant mice despite presence of reelin. J Neurosci *17*, 8767-8777.

Goldstein, B., and Macara, I.G. (2007). The PAR proteins: fundamental players in animal cell polarization. Dev Cell *13*, 609-622.

Govek, E.E., Hatten, M.E., and Van Aelst, L. (2011). The role of Rho GTPase proteins in CNS neuronal migration. Dev Neurobiol *71*, 528-553.

Granot, Z., Swisa, A., Magenheim, J., Stolovich-Rain, M., Fujimoto, W., Manduchi, E., Miki, T., Lennerz, J.K., Stoeckert, C.J., Jr., Meyuhas, O.*, et al.* (2009). LKB1 regulates pancreatic beta cell size, polarity, and function. Cell Metab *10*, 296-308.

Guerrero, I., and Chiang, C. (2007). A conserved mechanism of Hedgehog gradient formation by lipid modifications. Trends Cell Biol *17*, 1-5.

Gurumurthy, S., Hezel, A.F., Sahin, E., Berger, J.H., Bosenberg, M.W., and Bardeesy, N. (2008). LKB1 deficiency sensitizes mice to carcinogen-induced tumorigenesis. Cancer Res *68*, 55-63.

Hall, Z.J., Street, S.E., and Healy, S.D. (2013). The evolution of cerebellum structure correlates with nest complexity. Biol Lett *9*, 20130687.

Hardie, D.G. (2004). The AMP-activated protein kinase pathway--new players upstream and downstream. J Cell Sci *117*, 5479-5487.

Hayashi, S., Lewis, P., Pevny, L., and McMahon, A.P. (2002). Efficient gene modulation in mouse epiblast using a Sox2Cre transgenic mouse strain. Mech Dev *119 Suppl 1*, S97-S101.

He, M., Zhang, Z.H., Guan, C.B., Xia, D., and Yuan, X.B. (2010). Leading tip drives soma translocation via forward F-actin flow during neuronal migration. J Neurosci *30*, 10885-10898.

Horgan, C.P., and McCaffrey, M.W. (2009). The dynamic Rab11-FIPs. Biochem Soc Trans *37*, 1032-1036.

Hosaka, Y.Z., Neki, Y., Hasebe, M., Shinozaki, A., and Uehara, M. (2012). Formation of excess sublobules in the cerebellum of hypothyroid rats. Ann Anat *194*, 329-333.

Hoshino, M., Nakamura, S., Mori, K., Kawauchi, T., Terao, M., Nishimura, Y.V., Fukuda, A., Fuse, T., Matsuo, N., Sone, M.*, et al.* (2005). Ptf1a, a bHLH transcriptional gene, defines GABAergic neuronal fates in cerebellum. Neuron *47*, 201-213.

Huang, J., and Manning, B.D. (2008). The TSC1-TSC2 complex: a molecular switchboard controlling cell growth. Biochem J *412*, 179-190.

Huang, X., Litingtung, Y., and Chiang, C. (2007). Region-specific requirement for cholesterol modification of sonic hedgehog in patterning the telencephalon and spinal cord. Development *134*, 2095-2105.

Huang, X., Liu, J., Ketova, T., Fleming, J.T., Grover, V.K., Cooper, M.K., Litingtung, Y., and Chiang, C. (2010). Transventricular delivery of Sonic hedgehog is essential to cerebellar ventricular zone development. Proc Natl Acad Sci U S A *107*, 8422-8427.

Huang, Y., Roelink, H., and McKnight, G.S. (2002). Protein kinase A deficiency causes axially localized neural tube defects in mice. J Biol Chem *277*, 19889-19896.

Hui, C.C., and Angers, S. (2011). Gli proteins in development and disease. Annu Rev Cell Dev Biol *27*, 513-537.

Humke, E.W., Dorn, K.V., Milenkovic, L., Scott, M.P., and Rohatgi, R. (2010). The output of Hedgehog signaling is controlled by the dynamic association between Suppressor of Fused and the Gli proteins. Genes Dev *24*, 670-682.

Hung, T.J., and Kemphues, K.J. (1999). PAR-6 is a conserved PDZ domain-containing protein that colocalizes with PAR-3 in Caenorhabditis elegans embryos. Development *126*, 127-135.

Ingham, P.W., and McMahon, A.P. (2001). Hedgehog signaling in animal development: paradigms and principles. Genes Dev *15*, 3059-3087.

Ingham, P.W., Nakano, Y., and Seger, C. (2011). Mechanisms and functions of Hedgehog signalling across the metazoa. Nat Rev Genet *12*, 393-406.

Ito, M. (2008). Control of mental activities by internal models in the cerebellum. Nat Rev Neurosci *9*, 304-313.

Izzi, L., Levesque, M., Morin, S., Laniel, D., Wilkes, B.C., Mille, F., Krauss, R.S., McMahon, A.P., Allen, B.L., and Charron, F. (2011). Boc and Gas1 each form distinct Shh receptor complexes with Ptch1 and are required for Shh-mediated cell proliferation. Dev Cell *20*, 788-801.

Jacob, L.S., Wu, X., Dodge, M.E., Fan, C.W., Kulak, O., Chen, B., Tang, W., Wang, B., Amatruda, J.F., and Lum, L. (2011). Genome-wide RNAi screen reveals disease-associated genes that are common to Hedgehog and Wnt signaling. Sci Signal *4*, ra4.

Ji, H., Ramsey, M.R., Hayes, D.N., Fan, C., McNamara, K., Kozlowski, P., Torrice, C., Wu, M.C., Shimamura, T., Perera, S.A*., et al.* (2007). LKB1 modulates lung cancer differentiation and metastasis. Nature *448*, 807-810.

Jia, J., Kolterud, A., Zeng, H., Hoover, A., Teglund, S., Toftgard, R., and Liu, A. (2009). Suppressor of Fused inhibits mammalian Hedgehog signaling in the absence of cilia. Dev Biol *330*, 452-460.

Jia, J., Tong, C., and Jiang, J. (2003). Smoothened transduces Hedgehog signal by physically interacting with Costal2/Fused complex through its C-terminal tail. Genes Dev *17*, 2709-2720.

Jia, J., Tong, C., Wang, B., Luo, L., and Jiang, J. (2004). Hedgehog signalling activity of Smoothened requires phosphorylation by protein kinase A and casein kinase I. Nature *432*, 1045-1050.

Joyner, A.L., Liu, A., and Millet, S. (2000). Otx2, Gbx2 and Fgf8 interact to position and maintain a mid-hindbrain organizer. Curr Opin Cell Biol *12*, 736-741.

Kawaji, K., Umeshima, H., Eiraku, M., Hirano, T., and Kengaku, M. (2004). Dual phases of migration of cerebellar granule cells guided by axonal and dendritic leading processes. Mol Cell Neurosci *25*, 228-240.

Kawakami, T., Kawcak, T., Li, Y.J., Zhang, W., Hu, Y., and Chuang, P.T. (2002). Mouse dispatched mutants fail to distribute hedgehog proteins and are defective in hedgehog signaling. Development *129*, 5753-5765.

Kawauchi, T., Sekine, K., Shikanai, M., Chihama, K., Tomita, K., Kubo, K., Nakajima, K., Nabeshima, Y., and Hoshino, M. (2010). Rab GTPases-dependent endocytic pathways regulate neuronal migration and maturation through N-cadherin trafficking. Neuron *67*, 588-602.

Kemphues, K.J., Priess, J.R., Morton, D.G., and Cheng, N.S. (1988). Identification of genes required for cytoplasmic localization in early C. elegans embryos. Cell *52*, 311-320.

Kerjan, G., Dolan, J., Haumaitre, C., Schneider-Maunoury, S., Fujisawa, H., Mitchell, K.J., and Chedotal, A. (2005). The transmembrane semaphorin Sema6A controls cerebellar granule cell migration. Nat Neurosci *8*, 1516-1524.

Kim, J., Kato, M., and Beachy, P.A. (2009). Gli2 trafficking links Hedgehog-dependent activation of Smoothened in the primary cilium to transcriptional activation in the nucleus. Proc Natl Acad Sci U S A *106*, 21666-21671.

Kise, Y., Morinaka, A., Teglund, S., and Miki, H. (2009). Sufu recruits GSK3beta for efficient processing of Gli3. Biochem Biophys Res Commun *387*, 569-574.

Kokubo, M., Nishio, M., Ribar, T.J., Anderson, K.A., West, A.E., and Means, A.R. (2009). BDNF-mediated cerebellar granule cell development is impaired in mice null for CaMKK2 or CaMKIV. J Neurosci *29*, 8901-8913.

Komuro, H., Yacubova, E., and Rakic, P. (2001). Mode and tempo of tangential cell migration in the cerebellar external granular layer. J Neurosci *21*, 527-540.

Kovacs, J.J., Whalen, E.J., Liu, R., Xiao, K., Kim, J., Chen, M., Wang, J., Chen, W., and Lefkowitz, R.J. (2008). Beta-arrestin-mediated localization of smoothened to the primary cilium. Science *320*, 1777-1781.

Kullmann, J.A., Neumeyer, A., Gurniak, C.B., Friauf, E., Witke, W., and Rust, M.B. (2012). Profilin1 is required for glial cell adhesion and radial migration of cerebellar granule neurons. EMBO Rep *13*, 75-82.

LaMonica, B.E., Lui, J.H., Hansen, D.V., and Kriegstein, A.R. (2013). Mitotic spindle orientation predicts outer radial glial cell generation in human neocortex. Nat Commun *4*, 1665.

Lancaster, M.A., Gopal, D.J., Kim, J., Saleem, S.N., Silhavy, J.L., Louie, C.M., Thacker, B.E., Williams, Y., Zaki, M.S., and Gleeson, J.G. (2011). Defective Wnt-dependent cerebellar midline fusion in a mouse model of Joubert syndrome. Nat Med *17*, 726-731.

Lancaster, O.M., and Baum, B. (2014). Shaping up to divide: Coordinating actin and microtubule cytoskeletal remodelling during mitosis. Semin Cell Dev Biol.

Lapierre, L.A., Avant, K.M., Caldwell, C.M., Oztan, A., Apodaca, G., Knowles, B.C., Roland, J.T., Ducharme, N.A., and Goldenring, J.R. (2012). Phosphorylation of Rab11-FIP2 regulates polarity in MDCK cells. Mol Biol Cell *23*, 2302-2318.

Lauder, J.M. (1977). The effects of early hypo- and hyperthyroidism on the development of rat cerebellar cortex. III. Kinetics of cell proliferation in the external granular layer. Brain Res *126*, 31-51.

Lauder, J.M. (1979). Granule cell migration in developing rat cerebellum. Influence of neonatal hypo- and hyperthyroidism. Dev Biol *70*, 105-115.

Lazaro-Dieguez, F., Cohen, D., Fernandez, D., Hodgson, L., van Ijzendoorn, S.C., and Musch, A. (2013). Par1b links lumen polarity with LGN-NuMA positioning for distinct epithelial cell division phenotypes. J Cell Biol *203*, 251-264.

Lee, J.D., Kraus, P., Gaiano, N., Nery, S., Kohtz, J., Fishell, G., Loomis, C.A., and Treisman, J.E. (2001). An acylatable residue of Hedgehog is differentially required in Drosophila and mouse limb development. Dev Biol *233*, 122-136.

Lee, J.J., Ekker, S.C., von Kessler, D.P., Porter, J.A., Sun, B.I., and Beachy, P.A. (1994). Autoproteolysis in hedgehog protein biogenesis. Science *266*, 1528-1537.

Leiner, H.C., Leiner, A.L., and Dow, R.S. (1993). Cognitive and language functions of the human cerebellum. Trends Neurosci *16*, 444-447.

Lewis, P.M., Dunn, M.P., McMahon, J.A., Logan, M., Martin, J.F., St-Jacques, B., and McMahon, A.P. (2001). Cholesterol modification of sonic hedgehog is required for long-range signaling activity and effective modulation of signaling by Ptc1. Cell *105*, 599-612.

Li, Y., Zhang, H., Litingtung, Y., and Chiang, C. (2006). Cholesterol modification restricts the spread of Shh gradient in the limb bud. Proc Natl Acad Sci U S A *103*, 6548-6553.

Liem, K.F., Jr., He, M., Ocbina, P.J., and Anderson, K.V. (2009). Mouse Kif7/Costal2 is a cilia-associated protein that regulates Sonic hedgehog signaling. Proc Natl Acad Sci U S A *106*, 13377-13382.

Lo, B., Strasser, G., Sagolla, M., Austin, C.D., Junttila, M., and Mellman, I. (2012). Lkb1 regulates organogenesis and early oncogenesis along AMPK-dependent and -independent pathways. J Cell Biol *199*, 1117-1130.

Lu, M.S., and Johnston, C.A. (2013). Molecular pathways regulating mitotic spindle orientation in animal cells. Development *140*, 1843-1856.

Lum, L., Yao, S., Mozer, B., Rovescalli, A., Von Kessler, D., Nirenberg, M., and Beachy, P.A. (2003). Identification of Hedgehog pathway components by RNAi in Drosophila cultured cells. Science *299*, 2039-2045.

Ma, Y., Erkner, A., Gong, R., Yao, S., Taipale, J., Basler, K., and Beachy, P.A. (2002). Hedgehog-mediated patterning of the mammalian embryo requires transporter-like function of dispatched. Cell *111*, 63-75.

Machold, R., and Fishell, G. (2005). Math1 is expressed in temporally discrete pools of cerebellar rhombic-lip neural progenitors. Neuron *48*, 17-24.

MacLeod, C. (2012). The missing link: evolution of the primate cerebellum. Prog Brain Res *195*, 165-187.

Maity, T., Fuse, N., and Beachy, P.A. (2005). Molecular mechanisms of Sonic hedgehog mutant effects in holoprosencephaly. Proc Natl Acad Sci U S A *102*, 17026-17031.

Marcus, A.I., and Zhou, W. (2010). LKB1 regulated pathways in lung cancer invasion and metastasis. J Thorac Oncol *5*, 1883-1886.

Martin-Belmonte, F., and Perez-Moreno, M. (2012). Epithelial cell polarity, stem cells and cancer. Nat Rev Cancer *12*, 23-38.

Matsumoto, S., Iwakawa, R., Takahashi, K., Kohno, T., Nakanishi, Y., Matsuno, Y., Suzuki, K., Nakamoto, M., Shimizu, E., Minna, J.D.*, et al.* (2007). Prevalence and specificity of LKB1 genetic alterations in lung cancers. Oncogene *26*, 5911-5918.

Maxfield, F.R., and McGraw, T.E. (2004). Endocytic recycling. Nat Rev Mol Cell Biol *5*, 121-132.

McLellan, J.S., Zheng, X., Hauk, G., Ghirlando, R., Beachy, P.A., and Leahy, D.J. (2008). The mode of Hedgehog binding to Ihog homologues is not conserved across different phyla. Nature *455*, 979-983.

Meloni, A.R., Fralish, G.B., Kelly, P., Salahpour, A., Chen, J.K., Wechsler-Reya, R.J., Lefkowitz, R.J., and Caron, M.G. (2006). Smoothened signal transduction is promoted by G protein-coupled receptor kinase 2. Mol Cell Biol *26*, 7550-7560.

Milenkovic, L., Scott, M.P., and Rohatgi, R. (2009). Lateral transport of Smoothened from the plasma membrane to the membrane of the cilium. J Cell Biol *187*, 365-374.

Millen, K.J., and Gleeson, J.G. (2008). Cerebellar development and disease. Curr Opin Neurobiol *18*, 12-19.

Miyazawa, K., Himi, T., Garcia, V., Yamagishi, H., Sato, S., and Ishizaki, Y. (2000). A role for p27/Kip1 in the control of cerebellar granule cell precursor proliferation. J Neurosci *20*, 5756-5763.

Molnar, C., Holguin, H., Mayor, F., Jr., Ruiz-Gomez, A., and de Celis, J.F. (2007). The G protein-coupled receptor regulatory kinase GPRK2 participates in Hedgehog signaling in Drosophila. Proc Natl Acad Sci U S A *104*, 7963-7968.

Morales, D., and Hatten, M.E. (2006). Molecular markers of neuronal progenitors in the embryonic cerebellar anlage. J Neurosci *26*, 12226-12236.

Morton, D.G., Roos, J.M., and Kemphues, K.J. (1992). par-4, a gene required for cytoplasmic localization and determination of specific cell types in Caenorhabditis elegans embryogenesis. Genetics *130*, 771-790.

Murone, M., Rosenthal, A., and de Sauvage, F.J. (1999). Sonic hedgehog signaling by the patched-smoothened receptor complex. Curr Biol *9*, 76-84.

Nakada, D., Saunders, T.L., and Morrison, S.J. (2010). Lkb1 regulates cell cycle and energy metabolism in haematopoietic stem cells. Nature *468*, 653-658.

Ocbina, P.J., Eggenschwiler, J.T., Moskowitz, I., and Anderson, K.V. (2011). Complex interactions between genes controlling trafficking in primary cilia. Nat Genet *43*, 547-553.

Ochoa-Espinosa, A., and Affolter, M. (2012). Branching morphogenesis: from cells to organs and back. Cold Spring Harb Perspect Biol *4*.

Ohlig, S., Farshi, P., Pickhinke, U., van den Boom, J., Hoing, S., Jakuschev, S., Hoffmann, D., Dreier, R., Scholer, H.R., Dierker, T.*, et al.* (2011). Sonic hedgehog shedding results in functional activation of the solubilized protein. Dev Cell *20*, 764-774.

Ollila, S., and Makela, T.P. (2011). The tumor suppressor kinase LKB1: lessons from mouse models. J Mol Cell Biol *3*, 330-340.

Pan, N., Jahan, I., Lee, J.E., and Fritzsch, B. (2009a). Defects in the cerebella of conditional Neurod1 null mice correlate with effective Tg(Atoh1-cre) recombination and granule cell requirements for Neurod1 for differentiation. Cell Tissue Res *337*, 407-428.

Pan, Y., Bai, C.B., Joyner, A.L., and Wang, B. (2006). Sonic hedgehog signaling regulates Gli2 transcriptional activity by suppressing its processing and degradation. Mol Cell Biol *26*, 3365-3377.

Pan, Y., and Wang, B. (2007). A novel protein-processing domain in Gli2 and Gli3 differentially blocks complete protein degradation by the proteasome. J Biol Chem *282*, 10846-10852.

Pan, Y., Wang, C., and Wang, B. (2009b). Phosphorylation of Gli2 by protein kinase A is required for Gli2 processing and degradation and the Sonic Hedgehog-regulated mouse development. Dev Biol *326*, 177-189.

Panakova, D., Sprong, H., Marois, E., Thiele, C., and Eaton, S. (2005). Lipoprotein particles are required for Hedgehog and Wingless signalling. Nature *435*, 58-65.

Parathath, S.R., Mainwaring, L.A., Fernandez, L.A., Campbell, D.O., and Kenney, A.M. (2008). Insulin receptor substrate 1 is an effector of sonic hedgehog mitogenic signaling in cerebellar neural precursors. Development *135*, 3291-3300.

Partanen, J.I., Tervonen, T.A., Myllynen, M., Lind, E., Imai, M., Katajisto, P., Dijkgraaf, G.J., Kovanen, P.E., Makela, T.P., Werb, Z.*, et al.* (2012). Tumor suppressor function of Liver kinase B1 (Lkb1) is linked to regulation of epithelial integrity. Proc Natl Acad Sci U S A *109*, E388-397.

Pedersen, L.B., and Rosenbaum, J.L. (2008). Intraflagellar transport (IFT) role in ciliary assembly, resorption and signalling. Curr Top Dev Biol *85*, 23-61.

Pepinsky, R.B., Zeng, C., Wen, D., Rayhorn, P., Baker, D.P., Williams, K.P., Bixler, S.A., Ambrose, C.M., Garber, E.A., Miatkowski, K.*, et al.* (1998). Identification of a palmitic acid-modified form of human Sonic hedgehog. J Biol Chem *273*, 14037-14045.

Porter, J.A., Ekker, S.C., Park, W.J., von Kessler, D.P., Young, K.E., Chen, C.H., Ma, Y., Woods, A.S., Cotter, R.J., Koonin, E.V.*, et al.* (1996a). Hedgehog patterning activity: role of a lipophilic modification mediated by the carboxy-terminal autoprocessing domain. Cell *86*, 21-34.

Porter, J.A., von Kessler, D.P., Ekker, S.C., Young, K.E., Lee, J.J., Moses, K., and Beachy, P.A. (1995). The product of hedgehog autoproteolytic cleavage active in local and long-range signalling. Nature *374*, 363-366.

Porter, J.A., Young, K.E., and Beachy, P.A. (1996b). Cholesterol modification of hedgehog signaling proteins in animal development. Science *274*, 255-259.

Poulson, N.D., and Lechler, T. (2010). Robust control of mitotic spindle orientation in the developing epidermis. J Cell Biol *191*, 915-922.

Ramon y Cajal, S. (1911). Histologie du Systeme Nerveux de l'Home et des Vertebres.

Ray, S., and Lechler, T. (2011). Regulation of asymmetric cell division in the epidermis. Cell Div *6*, 12.

Renaud, J., Kerjan, G., Sumita, I., Zagar, Y., Georget, V., Kim, D., Fouquet, C., Suda, K., Sanbo, M., Suto, F.*, et al.* (2008). Plexin-A2 and its ligand, Sema6A, control nucleus-centrosome coupling in migrating granule cells. Nat Neurosci *11*, 440-449.

Rieger, S., Senghaas, N., Walch, A., and Koster, R.W. (2009). Cadherin-2 controls directional chain migration of cerebellar granule neurons. PLoS Biol *7*, e1000240.

Rochefort, C., Arabo, A., Andre, M., Poucet, B., Save, E., and Rondi-Reig, L. (2011). Cerebellum shapes hippocampal spatial code. Science *334*, 385-389.

Rodriguez-Fraticelli, A.E., Auzan, M., Alonso, M.A., Bornens, M., and Martin-Belmonte, F. (2012). Cell confinement controls centrosome positioning and lumen initiation during epithelial morphogenesis. J Cell Biol *198*, 1011-1023.

Rohatgi, R., Milenkovic, L., and Scott, M.P. (2007). Patched1 regulates hedgehog signaling at the primary cilium. Science *317*, 372-376.

Ryan, K.E., and Chiang, C. (2012). Hedgehog secretion and signal transduction in vertebrates. J Biol Chem *287*, 17905-17913.

Sanchez-Cespedes, M. (2007). A role for LKB1 gene in human cancer beyond the Peutz-Jeghers syndrome. Oncogene *26*, 7825-7832.

Sandquist, J.C., Kita, A.M., and Bement, W.M. (2011). And the dead shall rise: actin and myosin return to the spindle. Dev Cell *21*, 410-419.

Sapir, T., Sapoznik, S., Levy, T., Finkelshtein, D., Shmueli, A., Timm, T., Mandelkow, E.M., and Reiner, O. (2008). Accurate balance of the polarity kinase MARK2/Par-1 is required for proper cortical neuronal migration. J Neurosci *28*, 5710-5720.

Schmahmann, J.D. (2004). Disorders of the cerebellum: ataxia, dysmetria of thought, and the cerebellar cognitive affective syndrome. J Neuropsychiatry Clin Neurosci *16*, 367-378.

Schmahmann, J.D., and Caplan, D. (2006). Cognition, emotion and the cerebellum. Brain *129*, 290-292.

Schmahmann, J.D., and Sherman, J.C. (1998). The cerebellar cognitive affective syndrome. Brain *121 (Pt 4)*, 561-579.

Schrader, E.K., Harstad, K.G., Holmgren, R.A., and Matouschek, A. (2011). A three-part signal governs differential processing of Gli1 and Gli3 proteins by the proteasome. J Biol Chem *286*, 39051-39058.

Schuller, U., Zhao, Q., Godinho, S.A., Heine, V.M., Medema, R.H., Pellman, D., and Rowitch, D.H. (2007). Forkhead transcription factor FoxM1 regulates mitotic entry and prevents spindle defects in cerebellar granule neuron precursors. Mol Cell Biol *27*, 8259-8270.

Schwartz, P.M., Borghesani, P.R., Levy, R.L., Pomeroy, S.L., and Segal, R.A. (1997). Abnormal cerebellar development and foliation in BDNF-/- mice reveals a role for neurotrophins in CNS patterning. Neuron *19*, 269-281.

Sgaier, S.K., Millet, S., Villanueva, M.P., Berenshteyn, F., Song, C., and Joyner, A.L. (2005). Morphogenetic and cellular movements that shape the mouse cerebellum; insights from genetic fate mapping. Neuron *45*, 27-40.

Shackelford, D.B., and Shaw, R.J. (2009). The LKB1-AMPK pathway: metabolism and growth control in tumour suppression. Nat Rev Cancer *9*, 563-575.

Shelly, M., Cancedda, L., Heilshorn, S., Sumbre, G., and Poo, M.M. (2007). LKB1/STRAD promotes axon initiation during neuronal polarization. Cell *129*, 565-577.

Shi, Q., Li, S., Jia, J., and Jiang, J. (2011). The Hedgehog-induced Smoothened conformational switch assembles a signaling complex that activates Fused by promoting its dimerization and phosphorylation. Development *138*, 4219-4231.

Shintani, T., Takeuchi, Y., Fujikawa, A., and Noda, M. (2012). Directional neuronal migration is impaired in mice lacking adenomatous polyposis coli 2. J Neurosci *32*, 6468-6484.

Sillitoe, R.V., and Joyner, A.L. (2007). Morphology, molecular codes, and circuitry produce the three-dimensional complexity of the cerebellum. Annu Rev Cell Dev Biol *23*, 549-577.

Slim, C.L., Lazaro-Dieguez, F., Bijlard, M., Toussaint, M.J., de Bruin, A., Du, Q., Musch, A., and van Ijzendoorn, S.C. (2013). Par1b induces asymmetric inheritance of plasma membrane domains via LGN-dependent mitotic spindle orientation in proliferating hepatocytes. PLoS Biol *11*, e1001739.

Solecki, D.J., Liu, X.L., Tomoda, T., Fang, Y., and Hatten, M.E. (2001). Activated Notch2 signaling inhibits differentiation of cerebellar granule neuron precursors by maintaining proliferation. Neuron *31*, 557-568.

Solecki, D.J., Model, L., Gaetz, J., Kapoor, T.M., and Hatten, M.E. (2004). Par6alpha signaling controls glial-guided neuronal migration. Nat Neurosci *7*, 1195-1203.

Solecki, D.J., Trivedi, N., Govek, E.E., Kerekes, R.A., Gleason, S.S., and Hatten, M.E. (2009). Myosin II motors and F-actin dynamics drive the coordinated movement of the centrosome and soma during CNS glial-guided neuronal migration. Neuron *63*, 63-80.

Stitt, T.N., and Hatten, M.E. (1990). Antibodies that recognize astrotactin block granule neuron binding to astroglia. Neuron *5*, 639-649.

Stoodley, C.J. (2014). Distinct regions of the cerebellum show gray matter decreases in autism, ADHD, and developmental dyslexia. Front Syst Neurosci *8*, 92.

Stoodley, C.J., and Stein, J.F. (2011). The cerebellum and dyslexia. Cortex *47*, 101-116.

Su, Y., Ospina, J.K., Zhang, J., Michelson, A.P., Schoen, A.M., and Zhu, A.J. (2011). Sequential phosphorylation of smoothened transduces graded hedgehog signaling. Sci Signal *4*, ra43.

Sudarov, A., and Joyner, A.L. (2007). Cerebellum morphogenesis: the foliation pattern is orchestrated by multi-cellular anchoring centers. Neural Dev *2*, 26.

Sultan, F. (2002). Analysis of mammalian brain architecture. Nature *415*, 133-134.

Sultan, F. (2005). Why some bird brains are larger than others. Curr Biol *15*, R649-650.

Sun, T., and Hevner, R.F. (2014). Growth and folding of the mammalian cerebral cortex: from molecules to malformations. Nat Rev Neurosci *15*, 217-232.

Svard, J., Heby-Henricson, K., Persson-Lek, M., Rozell, B., Lauth, M., Bergstrom, A., Ericson, J., Toftgard, R., and Teglund, S. (2006). Genetic elimination of Suppressor of fused reveals an essential repressor function in the mammalian Hedgehog signaling pathway. Dev Cell *10*, 187-197.

Tahirovic, S., Hellal, F., Neukirchen, D., Hindges, R., Garvalov, B.K., Flynn, K.C., Stradal, T.E., Chrostek-Grashoff, A., Brakebusch, C., and Bradke, F. (2010). Rac1 regulates neuronal polarization through the WAVE complex. J Neurosci *30*, 6930-6943.

Taipale, J., Chen, J.K., Cooper, M.K., Wang, B., Mann, R.K., Milenkovic, L., Scott, M.P., and Beachy, P.A. (2000). Effects of oncogenic mutations in Smoothened and Patched can be reversed by cyclopamine. Nature *406*, 1005-1009.

Taipale, J., Cooper, M.K., Maiti, T., and Beachy, P.A. (2002). Patched acts catalytically to suppress the activity of Smoothened. Nature *418*, 892-897.

Takeda, H., Miyoshi, H., Kojima, Y., Oshima, M., and Taketo, M.M. (2006). Accelerated onsets of gastric hamartomas and hepatic adenomas/carcinomas in Lkb1+/-p53-/- compound mutant mice. Oncogene *25*, 1816-1820.

Tanori, M., Santone, M., Mancuso, M., Pasquali, E., Leonardi, S., Di Majo, V., Rebessi, S., Saran, A., and Pazzaglia, S. (2010). Developmental and oncogenic effects of insulin-like growth factor-I in Ptc1+/- mouse cerebellum. Mol Cancer *9*, 53.

Tavano, A., and Borgatti, R. (2010). Evidence for a link among cognition, language and emotion in cerebellar malformations. Cortex *46*, 907-918.

Tawarayama, H., Yoshida, Y., Suto, F., Mitchell, K.J., and Fujisawa, H. (2010). Roles of semaphorin-6B and plexin-A2 in lamina-restricted projection of hippocampal mossy fibers. J Neurosci *30*, 7049-7060.

Tay, S.Y., Ingham, P.W., and Roy, S. (2005). A homologue of the Drosophila kinesin-like protein Costal2 regulates Hedgehog signal transduction in the vertebrate embryo. Development *132*, 625-634.

Tempe, D., Casas, M., Karaz, S., Blanchet-Tournier, M.F., and Concordet, J.P. (2006). Multisite protein kinase A and glycogen synthase kinase 3beta phosphorylation leads to Gli3 ubiquitination by SCFbetaTrCP. Mol Cell Biol *26*, 4316-4326.

Tiainen, M., Vaahtomeri, K., Ylikorkala, A., and Makela, T.P. (2002). Growth arrest by the LKB1 tumor suppressor: induction of p21(WAF1/CIP1). Hum Mol Genet *11*, 1497-1504.

Tiainen, M., Ylikorkala, A., and Makela, T.P. (1999). Growth suppression by Lkb1 is mediated by a G(1) cell cycle arrest. Proc Natl Acad Sci U S A *96*, 9248-9251.

Tokhunts, R., Singh, S., Chu, T., D'Angelo, G., Baubet, V., Goetz, J.A., Huang, Z., Yuan, Z., Ascano, M., Zavros, Y.*, et al.* (2010). The full-length unprocessed hedgehog protein is an active signaling molecule. J Biol Chem *285*, 2562-2568.

Traiffort, E., Dubourg, C., Faure, H., Rognan, D., Odent, S., Durou, M.R., David, V., and Ruat, M. (2004). Functional characterization of sonic hedgehog mutations associated with holoprosencephaly. J Biol Chem *279*, 42889-42897.

Tukachinsky, H., Lopez, L.V., and Salic, A. (2010). A mechanism for vertebrate Hedgehog signaling: recruitment to cilia and dissociation of SuFu-Gli protein complexes. J Cell Biol *191*, 415-428.

Tuson, M., He, M., and Anderson, K.V. (2011). Protein kinase A acts at the basal body of the primary cilium to prevent Gli2 activation and ventralization of the mouse neural tube. Development *138*, 4921-4930.

Uhlmann, E.J., Wong, M., Baldwin, R.L., Bajenaru, M.L., Onda, H., Kwiatkowski, D.J., Yamada, K., and Gutmann, D.H. (2002). Astrocyte-specific TSC1 conditional knockout mice exhibit abnormal neuronal organization and seizures. Ann Neurol *52*, 285-296.

Vazquez-Martin, A., Oliveras-Ferraros, C., and Menendez, J.A. (2009). The active form of the metabolic sensor: AMP-activated protein kinase (AMPK) directly binds the mitotic apparatus and travels from centrosomes to the spindle midzone during mitosis and cytokinesis. Cell Cycle *8*, 2385-2398.

Vyas, N., Goswami, D., Manonmani, A., Sharma, P., Ranganath, H.A., VijayRaghavan, K., Shashidhara, L.S., Sowdhamini, R., and Mayor, S. (2008). Nanoscale organization of hedgehog is essential for long-range signaling. Cell *133*, 1214-1227.

Wallace, V.A. (1999). Purkinje-cell-derived Sonic hedgehog regulates granule neuron precursor cell proliferation in the developing mouse cerebellum. Curr Biol *9*, 445-448.

Wang, B., and Li, Y. (2006). Evidence for the direct involvement of {beta}TrCP in Gli3 protein processing. Proc Natl Acad Sci U S A *103*, 33-38.

Wang, C., Pan, Y., and Wang, B. (2010). Suppressor of fused and Spop regulate the stability, processing and function of Gli2 and Gli3 full-length activators but not their repressors. Development *137*, 2001-2009.

Wang, V.Y., Rose, M.F., and Zoghbi, H.Y. (2005). Math1 expression redefines the rhombic lip derivatives and reveals novel lineages within the brainstem and cerebellum. Neuron *48*, 31-43.

Wang, V.Y., and Zoghbi, H.Y. (2001). Genetic regulation of cerebellar development. Nat Rev Neurosci *2*, 484-491.

Wang, W., Mullikin-Kilpatrick, D., Crandall, J.E., Gronostajski, R.M., Litwack, E.D., and Kilpatrick, D.L. (2007). Nuclear factor I coordinates multiple phases of cerebellar granule cell development via regulation of cell adhesion molecules. J Neurosci *27*, 6115-6127.

Watts, J.L., Morton, D.G., Bestman, J., and Kemphues, K.J. (2000). The C. elegans par-4 gene encodes a putative serine-threonine kinase required for establishing embryonic asymmetry. Development *127*, 1467-1475.

Wechsler-Reya, R.J., and Scott, M.P. (1999). Control of neuronal precursor proliferation in the cerebellum by Sonic Hedgehog. Neuron *22*, 103-114.

Wei, C., Bhattaram, V.K., Igwe, J.C., Fleming, E., and Tirnauer, J.S. (2012). The LKB1 tumor suppressor controls spindle orientation and localization of activated AMPK in mitotic epithelial cells. PLoS One *7*, e41118.

Williams, T., Courchet, J., Viollet, B., Brenman, J.E., and Polleux, F. (2011). AMP-activated protein kinase (AMPK) activity is not required for neuronal development but regulates axogenesis during metabolic stress. Proc Natl Acad Sci U S A *108*, 5849-5854.

Wilson, C.W., and Chuang, P.T. (2010). Mechanism and evolution of cytosolic Hedgehog signal transduction. Development *137*, 2079-2094.

Wilson, P.M., Fryer, R.H., Fang, Y., and Hatten, M.E. (2010). Astn2, a novel member of the astrotactin gene family, regulates the trafficking of ASTN1 during glial-guided neuronal migration. J Neurosci *30*, 8529-8540.

Xenaki, D., Martin, I.B., Yoshida, L., Ohyama, K., Gennarini, G., Grumet, M., Sakurai, T., and Furley, A.J. (2011). F3/contactin and TAG1 play antagonistic roles in the regulation of sonic hedgehog-induced cerebellar granule neuron progenitor proliferation. Development *138*, 519-529.

Xu, X., Omelchenko, T., and Hall, A. (2010). LKB1 tumor suppressor protein regulates actin filament assembly through Rho and its exchange factor Dbl independently of kinase activity. BMC Cell Biol *11*, 77.

Yavari, A., Nagaraj, R., Owusu-Ansah, E., Folick, A., Ngo, K., Hillman, T., Call, G., Rohatgi, R., Scott, M.P., and Banerjee, U. (2010). Role of lipid metabolism in smoothened derepression in hedgehog signaling. Dev Cell *19*, 54-65.

Yeo, C.H. (2004). Memory and the cerebellum. Curr Neurol Neurosci Rep *4*, 87-89.

Zeng, H., Jia, J., and Liu, A. (2010). Coordinated translocation of mammalian Gli proteins and suppressor of fused to the primary cilium. PLoS One *5*, e15900.

Zeng, X., Goetz, J.A., Suber, L.M., Scott, W.J., Jr., Schreiner, C.M., and Robbins, D.J. (2001). A freely diffusible form of Sonic hedgehog mediates long-range signalling. Nature *411*, 716-720.

Zhang, Q., Shi, Q., Chen, Y., Yue, T., Li, S., Wang, B., and Jiang, J. (2009). Multiple Ser/Thr-rich degrons mediate the degradation of Ci/Gli by the Cul3-HIB/SPOP E3 ubiquitin ligase. Proc Natl Acad Sci U S A *106*, 21191-21196.

Zhang, Q., Zhang, L., Wang, B., Ou, C.Y., Chien, C.T., and Jiang, J. (2006). A hedgehog-induced BTB protein modulates hedgehog signaling by degrading Ci/Gli transcription factor. Dev Cell *10*, 719-729.

Zhang, S., Schafer-Hales, K., Khuri, F.R., Zhou, W., Vertino, P.M., and Marcus, A.I. (2008). The tumor suppressor LKB1 regulates lung cancer cell polarity by mediating cdc42 recruitment and activity. Cancer Res *68*, 740-748.

Zhang, W., Wang, Q., Wu, Y., Moriasi, C., Liu, Z., Dai, X., Liu, W., Yuan, Z.Y., and Zou, M.H. (2014). Endothelial cell-specific liver kinase B1 deletion causes endothelial dysfunction and hypertension in mice in vivo. Circulation *129*, 1428-1439.

Zheng, B., and Cantley, L.C. (2007). Regulation of epithelial tight junction assembly and disassembly by AMP-activated protein kinase. Proc Natl Acad Sci U S A *104*, 819-822.

Zheng, X., Mann, R.K., Sever, N., and Beachy, P.A. (2010). Genetic and biochemical definition of the Hedgehog receptor. Genes Dev *24*, 57-71.

Zhou, P., Alfaro, J., Chang, E.H., Zhao, X., Porcionatto, M., and Segal, R.A. (2011). Numb links extracellular cues to intracellular polarity machinery to promote chemotaxis. Dev Cell *20*, 610-622.

Zhou, P., Porcionatto, M., Pilapil, M., Chen, Y., Choi, Y., Tolias, K.F., Bikoff, J.B., Hong, E.J., Greenberg, M.E., and Segal, R.A. (2007). Polarized signaling endosomes coordinate BDNF-induced chemotaxis of cerebellar precursors. Neuron *55*, 53-68.

Zmuda, J.F., and Rivas, R.J. (2000). Actin filament disruption blocks cerebellar granule neurons at the unipolar stage of differentiation in vitro. J Neurobiol *43*, 313-328.